BEHAVIORAL CORRELATES OF UNILATERAL DOPAMINE DEPLETION
IN THE MPP+ RAT MODEL OF PARKINSON'S DISEASE

JARED C. HARDY
B.Sc., Brigham Young University, 2004

A Thesis
Submitted to the School of Graduate Studies
Of the University of Lethbridge
In Partial Fulfillment of the
Requirements for the Degree

MASTER OF SCIENCE

Department of Neuroscience
University of Lethbridge
LETHBRIDGE, ALBERTA, CANADA

BEHAVIORAL CORRELATES OF UNILATERAL DOPAMINE DEPLETION IN THE MPP+ RAT MODEL OF PARKINSON'S DISEASE

JARED C. HARDY

Approved: Date:

_____

Dr. Ian Q. Whishaw, Supervisor, Neuroscience

_____

Dr. Bryan Kolb, Thesis Committee Member, Neuroscience

_____

Dr. Robert McDonald, Thesis Committee Member, Neuroscience

_____

Dr. Peter Dibble, Thesis Committee Member, Chemistry

_____

Dr. Timothy Schallert, External Examiner, University of Texas at Austin, Psychology

_____

Dr. Dayna Daniels, Thesis Examination Chair, Kinesiology and Physical Education

ABSTRACT

Conventional cylinder test measures have limited sensitivity in determining hemiparkinson rat forelimb use asymmetry and approximating substantia nigra (SN) dopaminergic neuron loss. This thesis investigates which cylinder test measures of hemiparkinson rat forelimb use asymmetry best predict methamphetamine-induced rotation and extent of dopaminergic neuron loss. Long-Evans rats were cylinder-tested after unilateral 1-methyl-4-phenylpyridinium (MPP+)-induced SN dopamine depletion. Time and count of numerous forepaw wall contact patterns were documented for MPP+ hemiparkinson rats and sham-operated controls using frame-by-frame video analysis, then regressed against methamphetamine-induced rotation and tyrosine hydroxylase-positive neuron depletion. Severely dopamine-asymmetric rats initiated movements slower and less often with the contralateral-to-lesion forepaw, indicating that the cylinder test may be used to assess Parkinson Disease motor impairments of bradykinesia and akinesia. Several new time and count asymmetry measures may improve cylinder test sensitivity to hemiparkinson-specific forelimb use asymmetries.

ACKNOWLEDGEMENTS

TABLE OF CONTENTS

LIST OF TABLES

LIST OF FIGURES

LIST OF ABBREVIATIONS

6-OHDA = 6-hydroxydopamine
ac = anterior commissure
CC = corpus callosum
CPu = caudate-putamen
DA = dopamine
DAT = dopamine transporter
e.g. = for example [Latin: *exempli gratia*]
EP = entopeduncular nucleus
et al. = and others [Latin: *et alii, et alia*, etc.]
etc. = and so on [Latin: *et cetera*]
GP = globus pallidus
GPe = globus pallidus pars externa
GPi = globus pallidus pars interna
i.e. = that is to say [Latin: *id est*]
ic = internal capsule
ip = intraperitoneal
JNK = c-Jun N-terminal kinase
LV = lateral ventricle
ml = medial lemniscus
MPP+ = 1-methyl-4-phenylpyridinium
MPPP = 1-methyl 4-phenyl 4-propionoxypiperidine
MPTP = 1-methyl-4-phenyl-1,2,3,6-tetrahydropyridine
NADH = nicotinamide dehydrogenase
OT = optic tract
PD = Parkinson's disease
Pu = putamen
RRF = retrorubral field
sc = sub-cutaneous
SN = substantia nigra
SNc = substantia nigra pars compacta
SNr = substantia nigra pars reticulata
STN = subthalamic nucleus
Th = thalamus
TH = tyrosine hydroxylase
TH+ = tyrosine hydroxylase-positive
ZI = zona incerta

INTRODUCTION

Neurological Disorders

Neurological disorders include all conditions that disrupt normal function of the central or peripheral nervous system. Approximately one in five people suffer from nervous system damage in the form of more than 600 neurological conditions. Some major categories and examples of neurological disorders include the following:

Table 1. Categories and examples of neurological disorders

Category	Common Example(s)
cerebrovascular diseases	stroke
convulsive disorders	epilepsy
developmental disorders	cerebral palsy; spina bifida
infectious diseases	meningitis; shingles
neurodegenerative diseases	Parkinson's disease; Alzheimer's disease
neurogenetic conditions	Huntington's disease; muscular dystrophy
trauma	spinal cord injury; head injury
tumors	pituitary tumors

Mental illnesses such as schizophrenia and bipolar disorder have traditionally been classified separately from neurological disorders. However, accumulating evidence indicates that mental illnesses have underlying neurochemical mechanisms. Based on this evidence, mental illnesses could also be classified as neurological disorders (Martin, 2002).

Parkinson's Disease

Parkinson's disease (PD) is a human neurodegenerative disease characterized by muscle rigidity, resting tremor, bradykinesia (slow movement), and postural instability. PD was first documented as a distinct disorder in 1817 by the British physician James Parkinson (2002), and was later shown to result from extensive dopaminergic neuron loss in the substantia nigra pars compacta (SNc), which reduces dopamine delivery the caudate nucleus and putamen (striatum). Without modulatory input from the substantia nigra pars compacta, putamen output is altered, leading to abnormal inhibition of thalamic output to the premotor cortex (see Figure 3, page 5) and subsequent poverty of movement. Clinical signs of PD are not evident until approximately 80% of striatal dopamine (DA) and 50% of nigral neurons are lost (Fearnley & Lees, 1991; Marsden, 1994).

Figure 1 (page 3) and Figure 2 (page 4) show major dopaminergic pathways in the human and in the rat. Figure 3 (page 5) contrasts the basal ganglia motor circuit of normal brains with Parkinson's Disease brains. Figure 4 (page 6) shows the projection of a single rat DA neuron from the substantia nigra to the striatum.

In addition to nigrostriatal dopaminergic degeneration, other dopaminergic and non-dopaminergic pathways are also affected, contributing to mood, cognition, sensation, and sleep disturbances, as well as autonomic nervous system dysfunction.
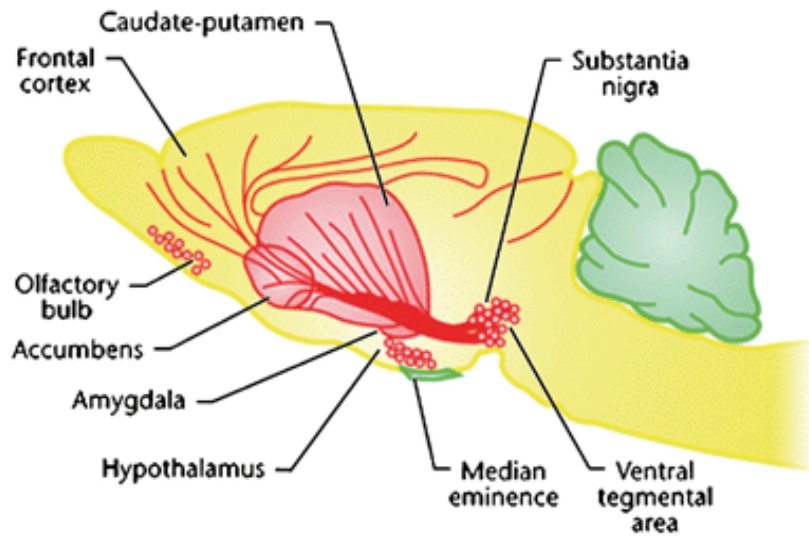
Figure 1. Major dopaminergic pathways in the rat brain.
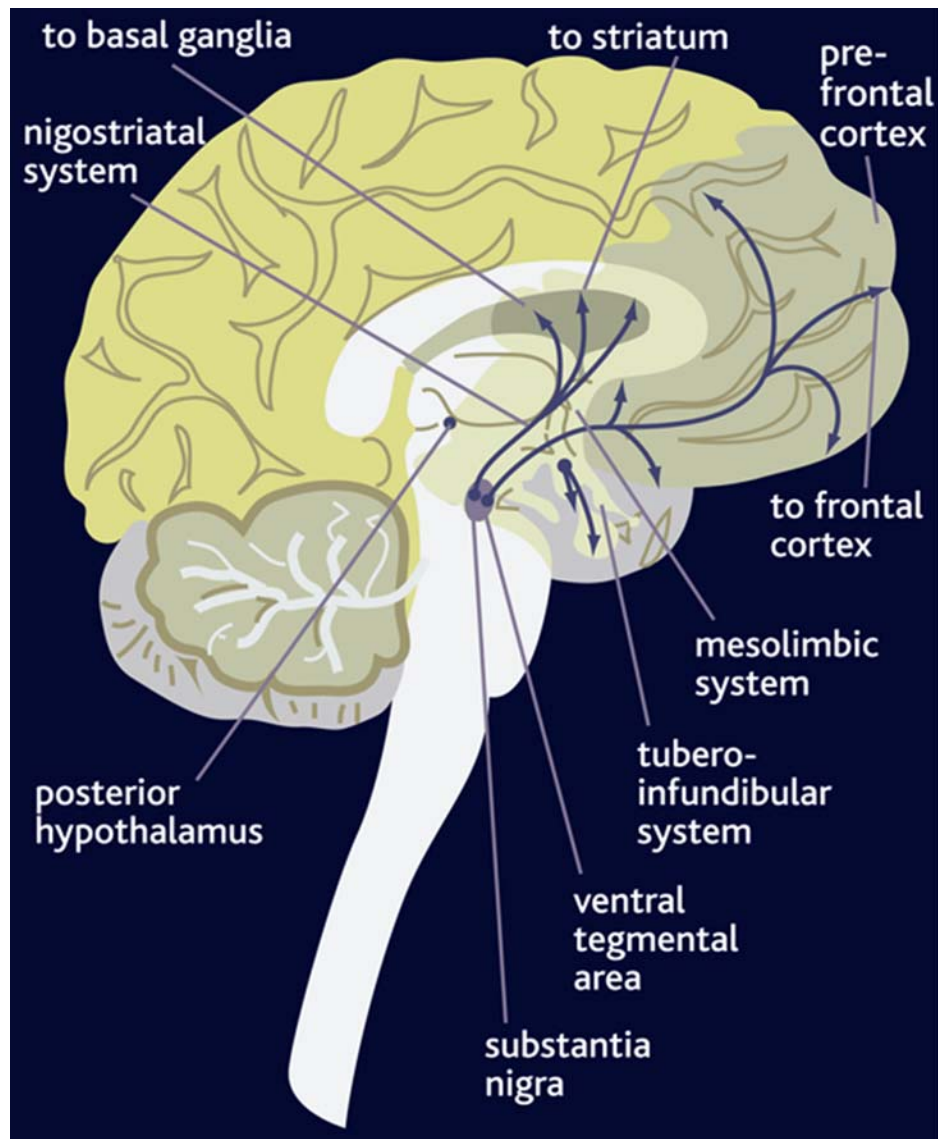
Figure 2. Major dopaminergic pathways in the human brain.

Normal Brain

GPe = globus pallidus pars externa
GPi = globus pallidus pars interna
Pu = putamen
SNc = substantia nigra pars compacta
SNr = substantia nigra pars reticulata
STN = subthalamic nucleus
Th = thalamus

Parkinson's Disease Brain
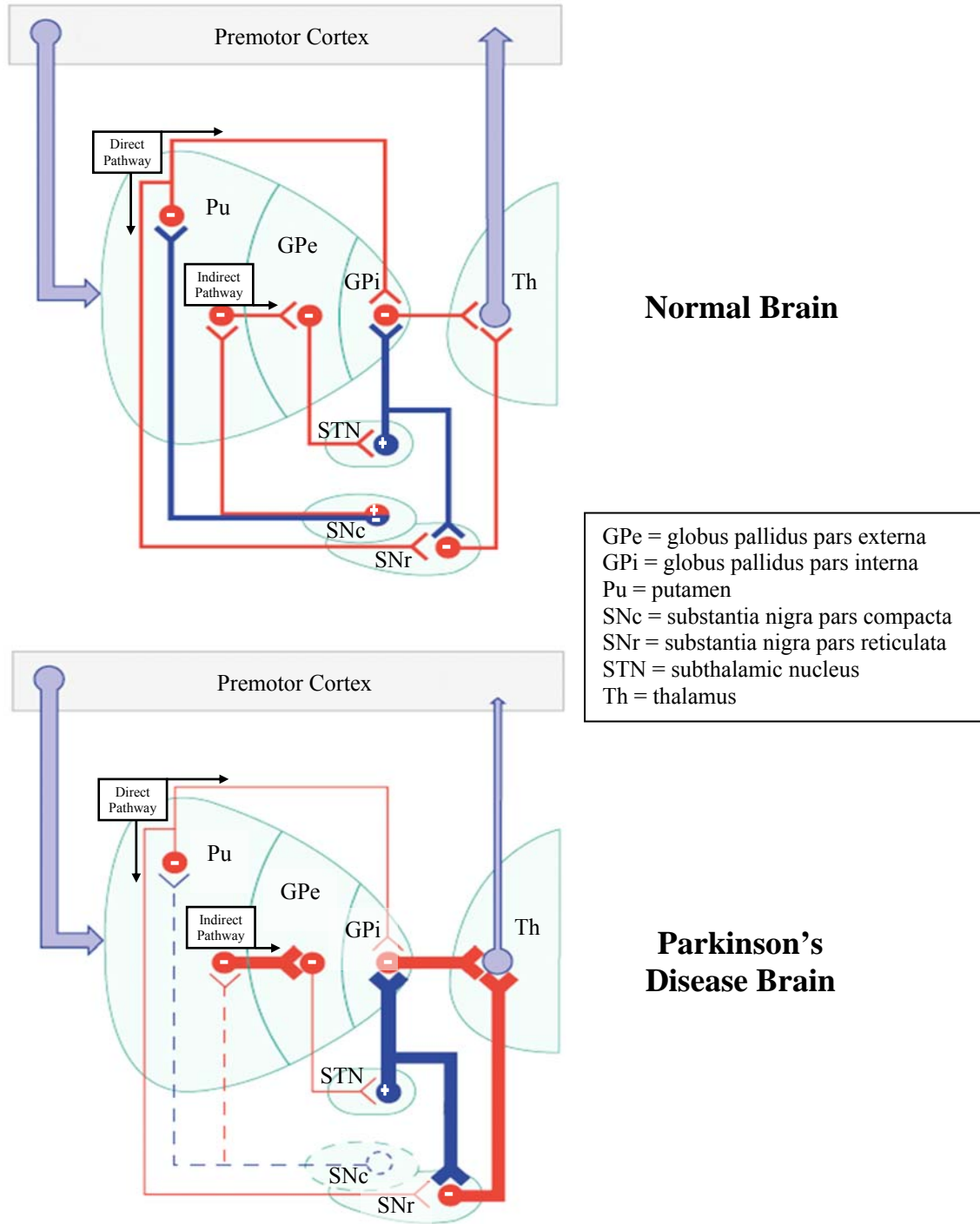
Figure 3. Simplified basal ganglia motor circuit in the normal brain and in Parkinson's Disease. Inhibitory pathways (-) are shown as red lines, and excitatory pathways (+) as blue lines. Thicker lines indicate increased neuronal activity, thinner lines indicate decreased activity, and dashed lines represent degenerated nigrostriatal dopamine neurons. (Adapted from Hornykiewicz, 2001).
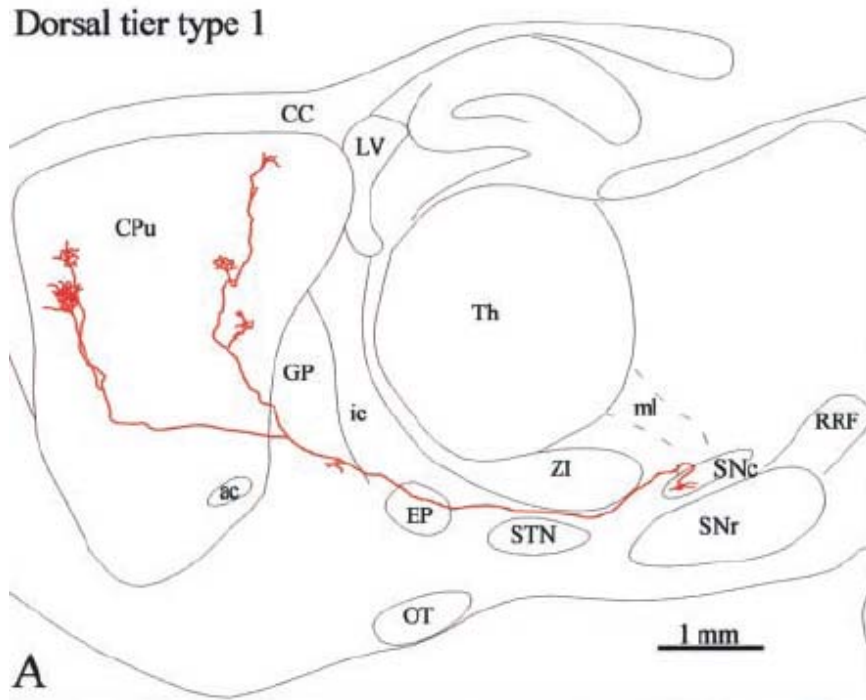
Figure 4. Projections of a single rat SNc dorsal tier type I dopaminergic neuron into the striatum. (Extracted from Prensa & Parent, 2001).

ac = anterior commissure
CC = corpus callosum
CPu = caudate-putamen
EP = entopeduncular nucleus
GP = globus pallidus
ic = internal capsule
LV = lateral ventricle
ml = medial lemniscus
OT = optic tract
RRF = retrorubral field
SNc = substantia nigra pars compacta
SNr = substantia nigra pars reticulata
STN = subthalamic nucleus
Th = thalamus
ZI = zona incerta

A key pathological feature of PD is the presence of abnormal cytoplasmic inclusions called Lewy bodies. Lewy bodies contain various forms of protein, including α-synuclein, ubiquitin-protein conjugates, phosphorylated proteins, and oxidatively damaged proteins (McNaught & Olanow, 2006). They are found not only in the SN, but also in the cortex, amygdala, locus coeruleus, vagal nucleus, and the peripheral autonomic nervous system (Braak et al., 2003; Wakabayashi & Takahashi, 1997).

The role of Lewy bodies in the pathogenesis of PD is unknown. Formation of Lewy bodies may be associated with a compromised ubiquitin-proteasome system (Betarbet, Sherer, & Greenamyre, 2005). Inhibition of proteasomes has been shown to produce Lewy bodies in rats (McNaught, Perl, Brownell, & Olanow, 2004; Sherman & Goldberg, 2001).

Certain rare forms of PD are known to be genetic in origin (Gasser, 2001; Huang, Cheung, Rowe, & Halliday, 2004; Marder et al., 1996). The results of a large twin study showed that incidence of early-onset (<50 years) PD was higher in monozygotic twins; however, incidence of later-onset PD was no higher in monozygotic twins than dizygotic twins, indicating that sporadic cases of PD do not have a strong genetic basis (Tanner et al., 1999).

The majority of PD cases are sporadically occurring, meaning that the cause of dopaminergic neuron loss is not known. Sporadic forms of PD may be associated with environmental factors such as rural living, farming, exposure to pesticides, and drinking well water (Priyadarshi, Khuder, Schaub, & Priyadarshi, 2001).

Animal Models of Parkinson's Disease

6-OHDA

The first animal model of PD to achieve dopaminergic cell death in the SNc involved use of the neurotoxin 6-hydroxydopamine (6-OHDA) in rats (Ungerstedt, 1968). 6-OHDA is a structural analog of dopamine (see Figure 5). It is uptaken by dopaminergic and noradrenergic transporters (Luthman, Fredriksson, Sundstrom, Jonsson, & Archer, 1989) and leads to cell death by non-apoptotic mechanisms (Jeon, Jackson-Lewis, & Burke, 1995). Oxidative stress has long been recognized as a mechanism of 6-OHDA-induced cell death (Sachs & Jonsson, 1975). 6-OHDA is toxic to mitochondrial complex I and promotes formation of superoxide free radicals and quinones (Bove, Prou, Perier, & Przedborski, 2005).

| 6-hydroxydopamine (6-OHDA) | Dopamine (DA) |
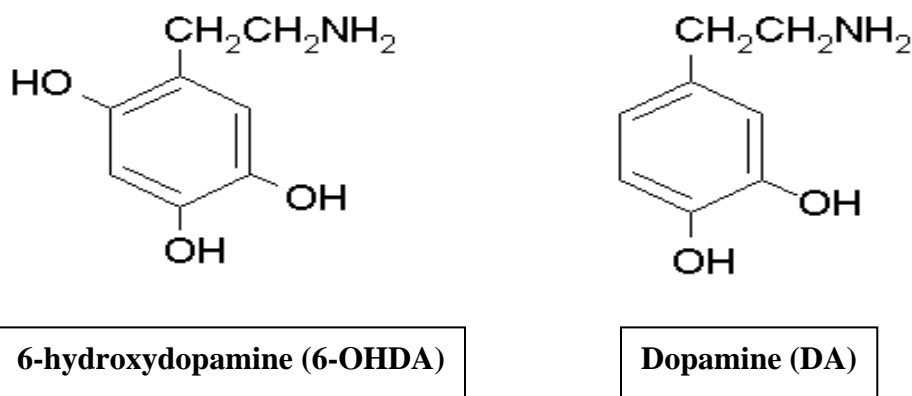
Figure 5. Similarity in the chemical structure of 6-hydroxydopamine (6-OHDA) and dopamine (DA).

Because 6-OHDA does not cross the blood-brain barrier, researchers have infused it stereotaxically into the brain in several ways, including intraventricular, intracisternal, and intracerebral.

Both intraventricular and intracisternal injection of 6-OHDA causes a bilateral catecholaminergic lesion that is apparent within several hours (Bove et al., 2005). Animals given severe bilateral lesions often display aphagia, adipsia, and seizures (Bourn, Chin, & Picchioni, 1972; Ungerstedt, 1971), which limits the usefulness of bilateral lesions of 6-OHDA for PD model research.

Animals given unilateral intracerebral injections, on the other hand, care for themselves adequately and are widely used for research. Common sites of intracerebral injection include the SN, medial forebrain bundle, and striatum (Schober, 2004).

MPTP and MPP+

The discovery of the neurotoxic effects of 1-methyl-4-phenyl-1,2,3,6-tetrahydropyridine (MPTP) provided compelling evidence that environmental agents contribute to PD. Drug users who injected (Davis et al., 1979; Langston, Ballard, Tetrud, & Irwin, 1983) or inhaled (Wright, Wall, Perry, & Paty, 1984) 1-methyl-4-phenyl-4-propionoxypiperidine (MPPP), a synthetic opiate analog of meperidine (Demerol®) that was contaminated with MPTP, subsequently developed a syndrome clinically similar to PD. These patients initially responded well to L-dopa therapy and later experienced dyskinesias and on-off fluctuations similar to idiopathic PD patients (Ballard, Tetrud, & Langston, 1985).

MPTP is highly lipophilic and readily crosses the blood-brain barrier (Shimohama, Sawada, Kitamura, & Taniguchi, 2003). It is converted to 1-methyl-4-phenylpyridinium (MPP+) by monoamine oxidase B (MAO-B) in astrocytes and serotonergic neurons (Ransom, Kunis, Irwin, & Langston, 1987), and transported into dopaminergic neurons by the dopamine transporter (DAT). Inside dopaminergic neurons, MPP+ inhibits mitochondrial complex I (Nicklas, Youngster, Kindt, & Heikkila, 1987), interrupting the flow of electrons in the mitochondrial electron transport chain and promoting production of reactive oxygen species, which trigger the process of apoptosis (Fiskum, Starkov, Polster, & Chinopoulos, 2003). Figure 6 and Figure 7 (page 11) illustrate conversion to MPP+, uptake by DAT, and mitochondrial complex I inhibition.

In aged non-human primates, MPTP produces inclusions that resemble immature Lewy bodies (Forno, Langston, DeLanney, & Irwin, 1988; Kowall et al., 2000). Similar inclusion bodies have been reported in transgenic mice (Song, Shults, Sisk, Rockenstein, & Masliah, 2004), although others have reported no inclusion bodies (Shimoji, Zhang, Mandir, Dawson, & Dawson, 2005).

The MPP+ rat model of PD involves unilateral infusion of MPP+ into the nigrostriatal bundle, striatum, or substantia nigra. Because MPP+ is a charged particle that has not been shown to cross the blood-brain barrier, whereas MPTP is known to readily cross the blood-brain barrier, the unilateral MPP+ model is considered to be distinctly safer than MPTP models (Przedborski et al., 2001).
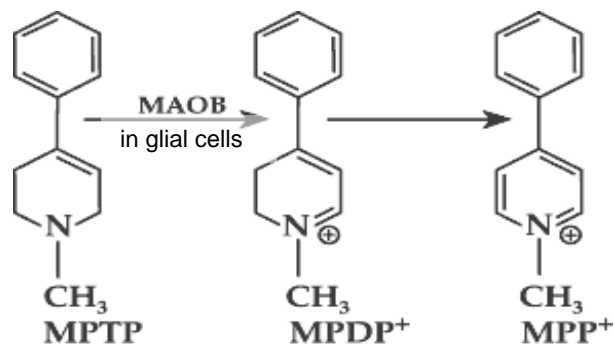
Figure 6. Conversion of MPTP to MPP+ in glial cells.
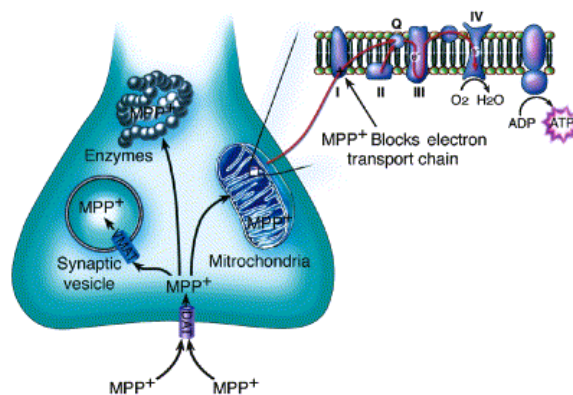
Figure 7. Mechanism of MPP+ induced cell death.

Paraquat

Paraquat (N,N′-dimethyl-4-4′-bipiridinium), a pesticide that is structurally very

similar to MPP+, has been shown in mice to cross the blood-brain barrier, despite its

charge (Brooks, Chadwick, Gelbard, Cory-Slechta, & Federoff, 1999). Paraquat appears

to cross the blood-brain barrier via L-neutral amino acid transporters, because

pretreatment with L-valine or L-phenylalanine completely blocks neurodegeneration

(McCormack et al., 2002). Mice that are chronically exposed to paraquat develop SNc

dopaminergic neuron degeneration and α-synuclein-containing inclusions (Manning-Bog

et al., 2002).
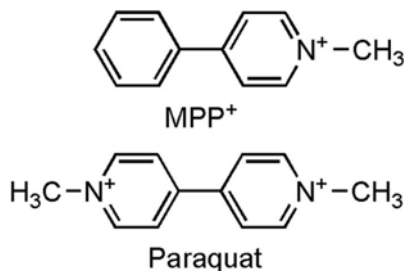
Figure 8. Similarity in the chemical structure of MPP+ and paraquat.

The mechanism of paraquat-induced cell death involves reactive oxygen species

(ROS) produced by reduction-oxidation cycling (Przedborski & Ischiropoulos, 2005).

Paraquat can also trigger apoptosis by activating the c-Jun N-terminal kinase (JNK)

pathway (Peng, Mao, Stevenson, Hsu, & Andersen, 2004).

Rotenone

Chronic systemic administration of rotenone has been shown to reproduce many features of PD in rats, including nigrostriatal dopaminergic degeneration, hypokinesia, rigidity, and cytoplasmic inclusions that contain ubiquitin and α-synuclein (Betarbet et al., 2000). However, high variability has been observed in the severity of dopaminergic cell damage caused by chronic rotenone injection (Zhu et al., 2004).

Rotenone is highly lipophilic and thus quickly passes the blood-brain barrier, where it inhibits NADH-ubiquinone reductase in mitochondrial complex I, leading to cell death (Schuler & Casida, 2001).
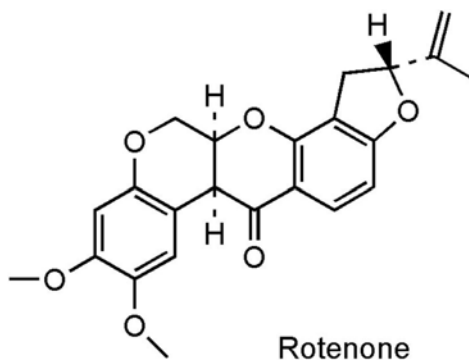
Rotenone

Figure 9. Chemical structure of rotenone.

Proteasome Inhibitors.

Rats systemically administered the proteasome inhibitor epoxomicin apparently
exhibit progressive signs of bradykinesia, rigidity, tremor, and abnormal posture
(McNaught et al., 2004), although these results have not yet been replicated.

Figure 10. Chemical structure of epoxomicin.

Mechanisms of dopaminergic cell death as a result of proteasome inhibitors show
parallels with known human mechanisms of neuronal death, including inflammation and
apoptosis.

Genetic models

Although familial PD is rare, genetic PD models have revealed mechanisms of
dopaminergic cell death and provided clues to the development of sporadic PD. For
example, α-synuclein knockout mice have been shown to be resistant to the neurotoxic
effects of MPP+ and MPTP on dopaminergic neurons (Dauer et al., 2002), suggesting a
common mechanism between mitochondrial complex I inhibition and α-synuclein
abnormalities. In addition, mutant forms of *Drosophila* that over-express the α-synuclein
gene develop progressive locomotor dysfunction (Feany & Bender, 2000).

Drug-induced Rotation

Spontaneous rotation behavior occurs in rats that are depleted of DA-producing neurons in the nigrostriatal pathway of only one brain hemisphere. These animals lack DA to elicit a motor response in the contralateral limbs. This causes an ipsilateral-to-lesion rotation behavior that occurs without administration of drugs.

Several pre-synaptic and post-synaptic DA agonist drugs can be used to quickly approximate degree of rat DA depletion; amphetamines and apomorphine and have predominantly been used by researchers during the past several decades.

Amphetamine acts primarily by blocking reuptake of DA into synaptic terminals. Because it uses dopamine already present in dopaminergic neurons to produce its effect, it simply amplifies the existing dopamine asymmetry and speeds ipsilateral-to-lesion rotation.

Apomorphine acts on both pre- and post-synaptic DA receptors. In hemiparkinson-lesioned rats, post-synaptic DA receptors are up-regulated in the DA-depleted hemisphere. Because apomorphine mimics the effect of dopamine by stimulating these receptors, apomorphine administration results in an exaggerated DA response corresponding to the degree of post-synaptic DA receptor up-regulation in the lesioned hemisphere. Whereas hemiparkinson rats normally turn in an ipsilateral direction, rats that are severely unilaterally DA-depleted rotate in the contralateral-to-lesion direction when given apomorphine.

Cylinder Test

The cylinder test has been used to test functional outcome for rat models of Huntington's Disease (McBride et al., 2004), Parkinson's Disease (Lundblad et al., 2002; Shi et al., 2004), spinal cord injury (Jin, Fischer, Tessler, & Houle, 2002) and various stroke models (Karhunen et al., 2003; Schallert, 2006; Windle et al., 2006).

Because the cylinder test assesses spontaneous forelimb use, it has important advantages over conventional measures of DA asymmetry. Drug-induced rotation with drugs such as apomorphine and amphetamine has limitations, and may not adequately assess functional recovery (Pinna, Pontis, & Morelli, 2006; Robinson et al., 1994; Lane, Cheetham, & Jenner, 2006). In addition, administering these drugs may interfere with brain recovery and interact negatively with experimental treatments.

Severely DA-depleted hemiparkinson rats have been shown to prefer use of their ipsilateral-to-lesion forepaw when first supporting their weight against a transparent cylinder wall during an exploratory rear and upon landing after a rear (Schallert et al., 2000). The cylinder exploration behavior of hemiparkinson rats has not been systematically analyzed, however, to determine whether it includes unique characteristics that could be used as hemiparkinson-specific cylinder test measures to shed light on motor impairments such as bradykinesia, akinesia, and difficulty initiating movement.

Some potentially useful characteristics that have not been studied in hemiparkinson rats include asymmetry in the total number of touches with the ipsilateral-to-lesion verses contralateral-to-lesion forepaw on the cylinder wall, sequence and grouping of wall contacts with ipsilateral-to-lesion verses contralateral-to-lesion forepaw,

and duration of contact on the cylinder wall with ipsilateral-to-lesion verses contralateral-to-lesion forepaw.

This thesis was undertaken mainly to investigate these characteristics and evaluate their usefulness as hemiparkinson-specific measures for the cylinder test by asking the question, "how do rats with various degrees of unilateral DA depletion differ from each other and from normal rats in forepaw placement behavior on the cylinder wall?"

METHODS

Animals

Female Long Evans rats (n=36), raised and maintained at the University of Lethbridge vivarium, were used in the experiment. They were housed in groups of 2-3 in hanging plastic cages in a room with a temperature of 21°C, relative humidity of 35%, and a 12 hour light-dark cycle with lights on at 08:00. Food and water were available *ad libitum*. The experiment was conducted in accordance with guidelines set by the Canadian Council of Animal Care. Rats were cared for by an animal care technician who was responsible for feeding, watering, grooming, and monitoring general health of the animals.

Nigrostriatal Dopamine Depletion

Surgery was performed when the rats were approximately 60 days old (225-300 g). Prior to surgery, rats' heads were shaved to prevent infection during surgery. The rats were then anesthetized with isoflurane (4% for initiation, 1.75% for maintenance) and placed in a Kopf stereotax. Six rats received a single 2 μl injection of sterile 0.9% saline, and 30 rats received a single 2 μl infusion of 1-methyl-4-phenylpyridinium iodide (MPP+) dissolved in 0.9% saline. One of the rats receiving a saline injection died unexpectedly during surgery. Of the 30 rats receiving MPP+ solution, 22 were infused with a solution containing 2 μg MPP+/μl 0.9% saline, and 8 were infused with a solution

containing 1 μg MPP+/μl 0.9% saline. All infusions were done in the right hemisphere at the following coordinates: 4.0 mm posterior to bregma, 1.5 mm lateral to the midline, and 8.5 mm ventral to the skull surface, with the skull flat between lambda and bregma (taken from Paxinos and Watson, 1998). Infusion took place over 6 minutes, with 6 minutes for diffusion. Rats received an analgesic (Buprenorphine, 0.05 mg/kg, sc) post-surgery.

Drug-Induced Rotation

To measure d-methamphetamine-induced turning bias, each rat was injected with d-methamphetamine HCl (2.5 mg/kg, ip, dissolved in 0.9% saline) 28 days after surgery and placed into a cylindrical rotometer bowl (30 cm diameter). A cuff was placed around the trunk of the rat, with its dorsal side attached by a wire lead to a microswitch connected to a computer. A customized computer program recorded the total number of rotations ipsilateral and contralateral to the lesion during the 60 minute period after injection.

To measure apomorphine-induced turning bias, each rat was injected with apomorphine HCl (0.05 mg/kg, sc, dissolved in 0.9% saline and 0.02% ascorbic acid) 35 days after surgery and placed into rotometer bowls as described above. Total number of rotations ipsilateral and contralateral to the lesion were recorded for the 40 minute period after injection.

Cylinder Test

All rats were placed in a transparent cylinder for 5 minutes on day 14 and 42 after surgery. Half of the rats (n=18) were also tested in the cylinder on day 70 and 98 after surgery to assess behavioral changes during additional repeated testing.

The cylinder was high enough (30 cm) so that rats could not reach the top edge by rearing. The diameter of the cylinder (20 cm) allowed rats to freely turn while scanning the horizontal surface. The cylinder was sufficiently heavy that it did not move when the animal supported its weight against the wall. The cylinder was placed on a glass table, beneath which was an inclined mirror. Animals were video recorded from a ventral perspective through the mirror. A Canon ZR 80 MC camcorder (shutter speed set at 1/1000 second) and a cold light source were used for illumination. A Sony DSR-11 digital videocassette recorder was used for subsequent frame-by-frame analysis at 30 frames per second.

To document forelimb wall contact during each 5-minute cylinder test session, the timer display for each video frame (00:00:00-04:59:29) was recorded on a separate row of a Microsoft Excel spreadsheet. A code was inserted in the cell adjacent to each video frame during which one or both rat forepaws were contacting the cylinder wall, (L for exclusive left forepaw contact, R for exclusive right forepaw contact, and B for both forepaws contacting the cylinder wall). If neither forepaw was contacting the cylinder wall during a given frame, the spreadsheet cell adjacent to that timer reading was left blank. For a graphic representation of this forelimb wall contact documenting method, see Figure 11 (page 22).

Formulas in cells adjacent to the L/R/B codes counted the occurrence of various patterns of forepaw contact with the cylinder wall, including number of touches made with each forepaw, wall contact time with each forepaw, and forepaw-wall touch sequences during "sets", defined as periods of continuous wall contact comprised of one or more forepaw-cylinder wall contact combinations. "Simple sets" are comprised of only one wall contact combination (right forepaw only, left forepaw only, or both forepaws simultaneously contacting the cylinder wall), whereas "complex sets" include two or more wall contact combinations, with either the right, left, or both forepaws contacting the wall at any given time during the "set". For a graphic example of simple and complex sets, see Figure 11 (page 22).

Raw counts of touches and wall contact time with each forepaw were used to calculate other scores, such as average time per touch with the left and right forepaws. These scores, as well as the most commonly-used conventional cylinder test scores of forelimb use asymmetry (Schallert et al., 2000; Shallert & Woodlee, 2005), were regressed against both d-methamphetamine rotation and right hemisphere TH+ neuron depletion.

MIN	SEC	FRM				
1	16	25		R		✋
1	16	26		R		✋
1	16	27		R		✋
1	16	28				
1	16	29		R		✋
1	17	0		R		✋
1	17	1		L	✋	
1	17	2		L	✋	
1	17	3		L	✋	
1	17	4				
1	17	5		R		✋
1	17	6		R		✋
1	17	7		B	✋	✋
1	17	8		B	✋	✋
1	17	9		B	✋	✋
1	17	10		R		✋
1	17	11		R		✋

RIGHT forepaw contacting the cylinder wall during a "simple set"

LEFT forepaw contacting the cylinder wall during a "complex set"

BOTH forepaws contacting the cylinder wall during a "complex set"

Figure 11. Method of representing forepaw contact with the cylinder wall. "Wall contact" with the left and right forepaw is represented as ✋ and ✋, respectively. "Touches" on the wall with the left and right forepaw are shown as ✋ and ✋, respectively. A "set" is a period of continuous wall contact comprised of one or more forepaw-cylinder wall contact combinations. This figure depicts one "simple set" and two "complex sets", each delineated by a left curved bracket, "(".

22

Histology

After finishing all behavioral tests, animals were deeply anesthetized with sodium pentobarbital and perfused through the heart with a 0.9% sodium chloride solution and 4% paraformaldehyde. The brains were extracted and post-fixed for 24-48 hours, then cryoprotected in 30% sucrose and 4% paraformaldehyde at 4°C for coronal sectioning (40 μm thickness) and TH immunostaining.

The right hemisphere was marked for later identification by inserting a syringe needle through an area dorsal to nuclei A8-A10, leaving all TH+ neurons intact. Brains were then cut into 40-μm sections on a freezing microtome. For tyrosine hydroxylase (TH) immunocytochemistry, the sections were washed in 1 M phosphate buffer and incubated overnight at room temperature with anti TH monoclonal antiserum (1:10,000, Sigma). The sections were then processed by the ABC method (Vector, Vectastain, Burlingame, CA, USA) with anti-mouse antiserum IgG and horse serum and reacted with 3,3′-diaminobenzidine tetrahydrochloride (0.6%), hydrogen peroxide (0.3%) and nickel solution.

For quantification of TH-positive (TH+) neuron depletion, four representative sections through the mesencephalon were chosen, corresponding to four TH-stained sections of nuclei A8-A10 given by German and Manaye (1993). Optimally focused digital images of each hemisphere of these sections were made using a 5X objective lens on a Carl Zeiss AxioVision microscope camera and Carl Zeiss Vision AxioVision software (release 4.3, Nov 2004). The number of TH+ cell bodies was counted in each of these images using a counting feature of ImageJ (Rasband, 1997). The difference in TH+

neuron count for the lesion and intact hemispheres was divided by TH+ neuron count of the intact hemisphere to estimate percentage of TH+ neurons depleted in the lesion hemisphere.

Statistical Analysis

Numerous rat wall contact patterns were linearly regressed against both right hemisphere TH+ neuron depletion and d-methamphetamine rotation to determine which cylinder test measures best approximate DA depletion.

Statistical analysis for behavior and histology was performed using Number Cruncher Statistical Systems 2001 (Kaysville, UT).

RESULTS

Histology

The TH stain revealed a wide range of TH+ neuron loss among MPP+ lesioned rats, whereas saline-infused rats had no detectable TH+ neuron loss. The difference between TH-labeled cells in the MPP+ infused hemisphere compared with the intact hemisphere was obvious to the unaided eye in the sample sections of many rats, as in Figure 12 (page 26). In the sample sections of other MPP+ rats, the difference between the MPP+ lesioned hemisphere and the intact hemisphere was indistinguishable to the unaided eye, similar to the sample sections of sham rats.

Complete TH+ neuron count data are shown in Table 2 (page 27). For each rat, estimated right hemisphere TH+ neuron depletion was calculated by dividing the difference between right and left hemisphere TH+ neuron count by left (intact) hemisphere TH+ neuron count.

As shown in Figure 13 (page 28), the saline and MPP+ groups clearly differed in right hemisphere TH+ neuron depletion. A two-tailed t-test for TH+ neuron count in each region (A-D) between saline and MPP+ groups, using both the Mann-Whitney U (Wilcoxon rank-sum) test for difference in medians and the Kolmogorov-Smirnov test for different distributions, yielded $p < 0.01$.

Linear regression of right hemisphere TH+ neuron depletion against amphetamine and apomorphine-induced rotation is on page 29. Amphetamine rotation is linearly correlated with TH+ neuron counts ($p < 0.0001$), whereas apomorphine rotation is not.

	Left hemisphere	**Right hemisphere**
Region A		
Region B		
Region C		
Region D		
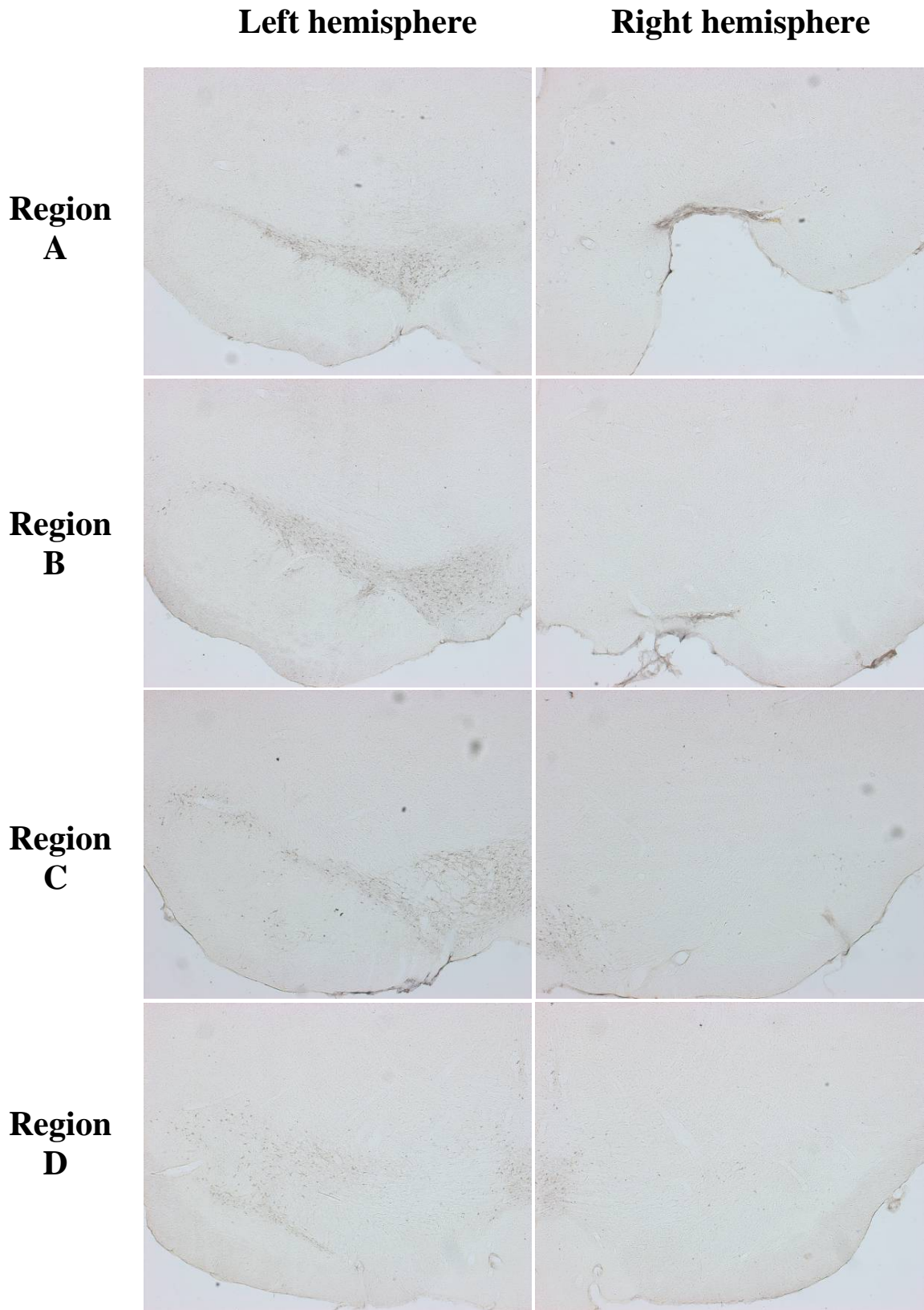
Figure 12. Unilateral right hemisphere MPP+ lesion.

Table 2. TH+ neuron count by region

Rat	Group	All Regions Combined			Region A		Region B		Region C		Region D	
		L	R	% Depl	L	R	L	R	L	R	L	R
A01	MPP+	1116	921	17.5%	396	350	260	209	339	288	121	74
A02	MPP+	1398	360	74.2%	462	30	338	128	293	114	305	88
A03	MPP+	1488	143	90.4%	563	59	362	8	324	22	239	54
A04	MPP+	1755	302	82.8%	450	62	330	67	491	71	484	102
A05	MPP+	1532	361	76.4%	486	51	318	84	431	113	297	113
A06	MPP+	1778	204	88.5%	564	54	348	40	336	45	530	65
A11	MPP+	1345	550	59.1%	565	245	241	198	311	69	228	38
A12	MPP+	1191	179	85.0%	312	32	161	14	276	16	442	117
A13	MPP+	1256	171	86.4%	371	18	226	16	327	46	332	91
A14	MPP+	1043	165	84.2%	233	39	102	9	363	65	345	52
A15	MPP+	1805	1273	29.5%	517	607	379	223	482	270	427	173
A16	MPP+	1743	185	89.4%	444	15	434	28	448	43	417	99
A21	MPP+	1444	298	79.4%	573	51	208	25	313	41	350	181
A22	MPP+	1327	112	91.6%	328	30	246	11	373	25	380	46
A23	MPP+	1848	639	65.4%	632	161	338	205	488	88	390	185
A24	MPP+	1744	380	78.2%	600	68	282	48	395	62	467	202
A25	MPP+	2107	697	66.9%	685	43	355	89	397	263	670	302
A26	MPP+	1604	913	43.1%	675	359	361	233	251	129	317	192
B01	MPP+	1108	782	29.4%	473	268	174	104	236	164	225	246
B02	Saline	952	922	3.2%	458	418	186	204	195	121	113	179
B03	MPP+	1445	287	80.1%	645	160	239	38	256	28	305	61
B04	MPP+	827	622	24.8%	333	254	182	103	243	198	69	67
B06	MPP+	1412	790	44.1%	481	387	248	140	243	117	440	146
B11	MPP+	1021	643	37.0%	408	312	205	151	234	108	174	72
B12	Saline	1087	1031	5.2%	330	285	215	185	249	275	293	286
B13	MPP+	1353	263	80.6%	363	25	229	45	350	89	411	104
B14	Saline	932	941	-1.0%	345	369	106	144	257	208	224	220
B15	MPP+	1450	1100	24.1%	609	462	203	163	306	216	332	259
B16	MPP+	1371	1114	18.7%	379	334	286	170	253	246	453	364
B21	MPP+	1211	505	58.3%	475	154	186	71	187	96	363	184
B22	MPP+	991	610	38.4%	292	39	185	103	347	238	167	230
B23	Saline	834	716	14.1%	135	122	174	157	167	155	358	282
B24	Saline	1082	1011	6.6%	382	372	244	239	267	204	189	196
B25	MPP+	1204	964	19.9%	496	363	258	182	303	241	147	178
B26	MPP+	1029	258	74.9%	276	18	253	27	208	75	292	138

L = left hemisphere
R = right hemisphere
% Depl = estimated percent right hemisphere TH+ neuron depletion. % Depl = (L-R)/L

Percent TH+ Neuron Depletion
in the Right Hemisphere by Region
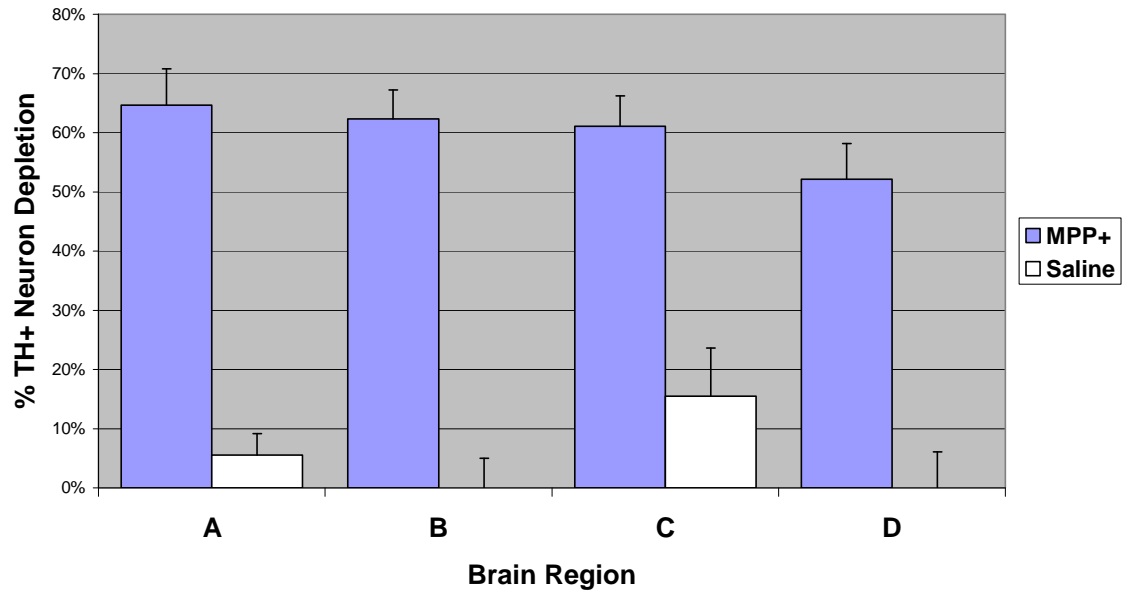
Figure 13. Percentage right hemisphere TH+ neuron depletion (compared to left hemisphere TH+ neuron counts) in four different brain regions.
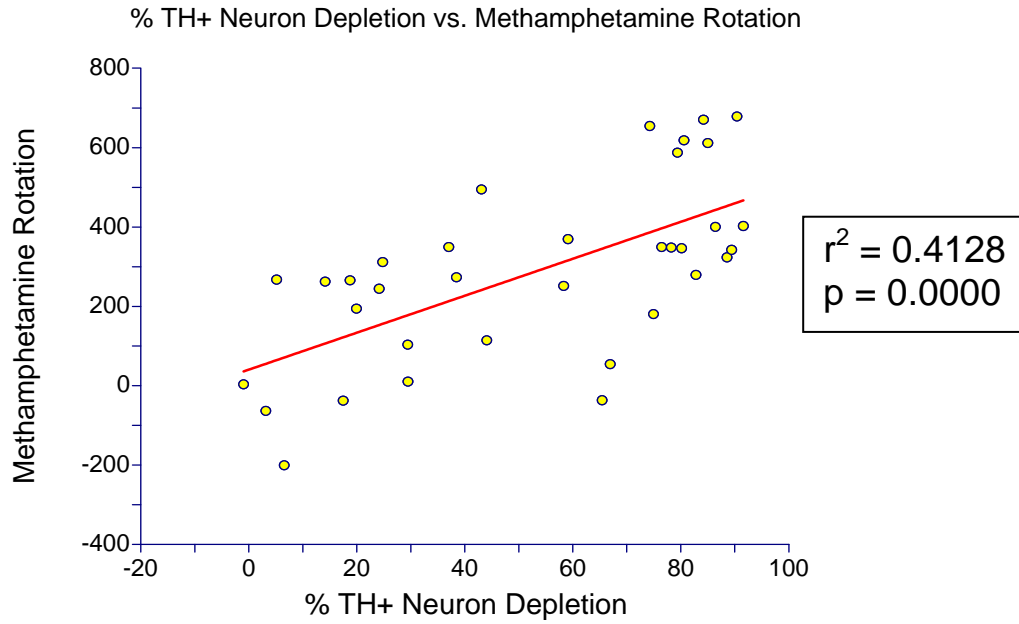
Figure 14. Linear regression of right hemisphere TH+ neuron depletion against d-methamphetamine rotation.
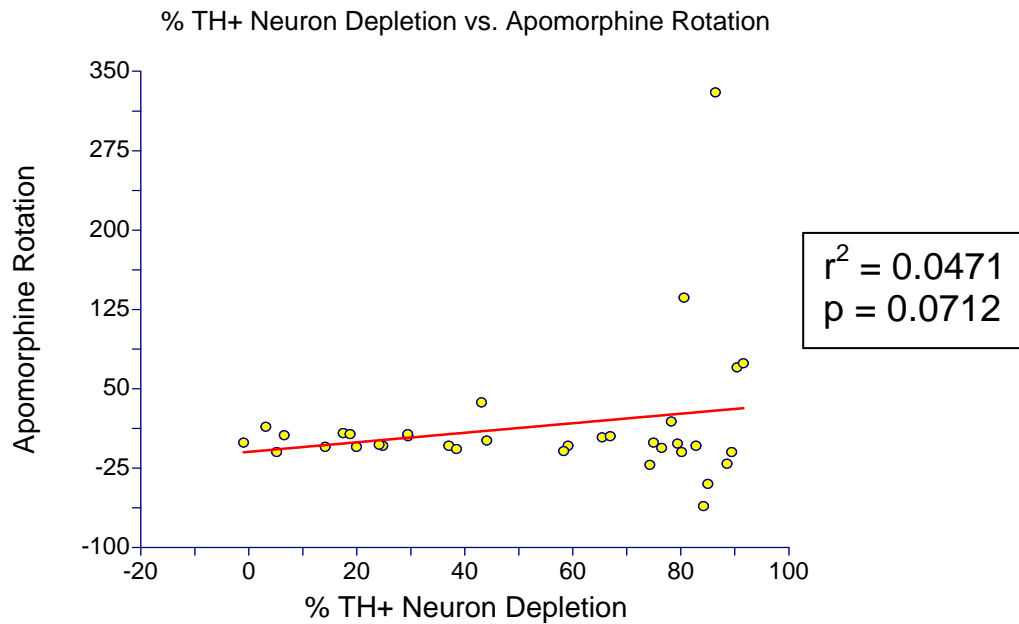
Figure 15. Linear regression of right hemisphere TH+ neuron depletion against apomorphine rotation.

Drug-Induced Rotation

Complete d-methamphetamine and apomorphine rotation results are shown in Table 3 (page 31), and are summarized in graph form in Figure 16 (page 30). A two-tailed t-test between MPP+ and saline groups showed a significant difference ($p<0.001$) for net methamphetamine rotation, but not for net apomorphine rotation ($p>0.05$).

Linear regression of TH+ neuron count with d-methamphetamine- and apomorphine-induced rotation is shown on page 29. Amphetamine rotation was highly correlated with TH+ neuron counts ($p<0.0001$), whereas apomorphine rotation was not linearly correlated, perhaps because the dose used was inadequate to elicit rotation across the full spectrum of dopamine depletion.
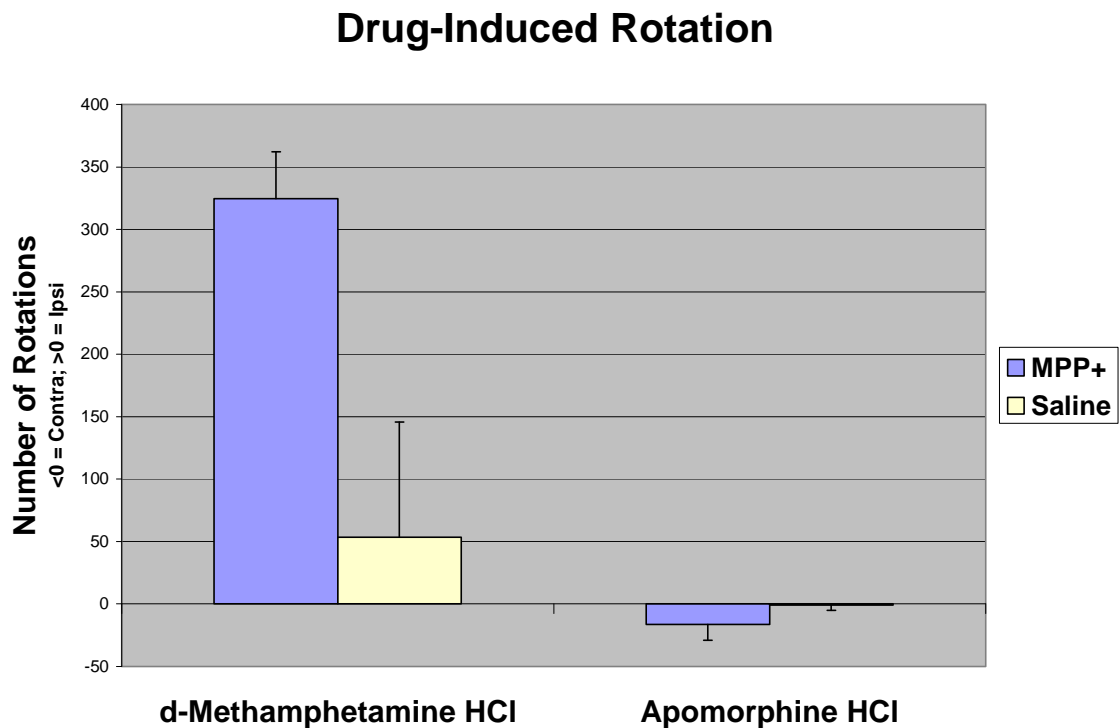
Figure 16. Drug-induced rotation results.

Table 3. Drug-induced rotation results

Rat	Group	d-Methamphetamine HCl			Apomorphine HCl		
		Contra	Ipsi	NET	Contra	Ipsi	NET
A01	MPP+	66	28	-38	10	2	-8
A02	MPP+	2	656	654	0	22	22
A03	MPP+	1	679	678	72	2	-70
A04	MPP+	34	313	279	3	7	4
A05	MPP+	10	359	349	0	6	6
A06	MPP+	1	324	323	1	22	21
A11	MPP+	0	369	369	2	6	4
A12	MPP+	1	612	611	4	44	40
A13	MPP+	6	406	400	346	16	-330
A14	MPP+	0	670	670	1	62	61
A15	MPP+	48	58	10	9	4	-5
A16	MPP+	3	345	342	1	11	10
A21	MPP+	5	592	587	6	8	2
A22	MPP+	6	408	402	88	14	-74
A23	MPP+	74	37	-37	4	0	-4
A24	MPP+	0	348	348	27	8	-19
A25	MPP+	39	93	54	6	1	-5
A26	MPP+	0	494	494	41	4	-37
B01	MPP+	21	124	103	12	5	-7
B02	Saline	114	50	-64	19	5	-14
B03	MPP+	1	347	346	1	11	10
B04	MPP+	4	315	311	4	8	4
B06	MPP+	4	118	114	4	3	-1
B11	MPP+	8	357	349	1	5	4
B12	Saline	0	267	267	0	10	10
B13	MPP+	0	618	618	144	8	-136
B14	Saline	63	66	3	3	4	1
B15	MPP+	15	259	244	8	11	3
B16	MPP+	42	307	265	9	2	-7
B21	MPP+	1	252	251	0	9	9
B22	MPP+	1	274	273	2	9	7
B23	Saline	4	266	262	4	9	5
B24	Saline	253	52	-201	8	2	-6
B25	MPP+	1	195	194	1	6	5
B26	MPP+	24	204	180	4	5	1

Contra = contraversive rotations
Ipsi = ipsiversive rotations
NET = net rotations (Ipsi – Contra). NET values were used for linear regressions.

Cylinder **Behavior**

Cylinder behavior was extensively analyzed, including both count and duration of specific behaviors. For all measures presented, a two-tailed t-test showed no significant difference (p>0.05) between the cylinder behavior data of day 14 and day 42, using both the Mann-Whitney U (Wilcoxon rank-sum) test for difference in medians and the Kolmogorov-Smirnov test for different distributions; therefore, these two days' results were combined for linear regressions.

In the cylinder behavior result sections that follow, count, time, and average time of all behaviors measured are presented first, followed by count asymmetry, time asymmetry, and average time asymmetry. The sections that report count, time, and average time include *"General Forelimb Use"* results (page 33, pooling together ipsilateral and contralateral forelimb use), *"Right and Left Forelimb Use"* (page 39: forelimb-specific results; ipsilateral and contralateral forelimb use measured separately), and *"Wall Contact Sequences"* (page 48: order and duration of ipsilateral and contralateral forelimb placements); the sections that report count asymmetry, time asymmetry, and average time asymmetry include *"Right Verses Left Forelimb Use Asymmetries"* (page 54)*,* and *"Wall Contact Sequence Asymmetries"* (page 66). The section entitled *"Previously-used Cylinder Test Asymmetries"* (page 75) reports both count and count asymmetry results for the standard cylinder test scores (Schallert et al., 2000; Schallert & Woodlee, 2005), plus a few additional related measures inspired by the standard asymmetry scores.

General Forelimb Use

The most severely DA-depleted rats appear to be slightly less active in the cylinder test than normal rats, as measured by the occurrence and duration of wall contact (right and left forepaw use pooled together). This section gives additional information about these observations.

General forelimb use was measured as count [#], time [^], and average time [^/] of the following behaviors: 1) simple and complex sets, 2) wall touches, and 3) wall contact. "Sets" are defined as periods of continuous wall contact comprised of one or more forepaw-cylinder wall contact combinations. "Simple sets" are comprised of only one wall contact combination (right forepaw only, left forepaw only, or both forepaws simultaneously contacting the cylinder wall), whereas "complex sets" include two or more wall contact combinations, with either the right, left, or both forepaws contacting the wall at any given time during the "set". For a graphic example of the difference between simple and complex sets, as well wall touches and wall contact time, see Figure 11 (page 21).

General forelimb use results are shown in Table 4 on page 35. (Behavior codes given in this section [in square brackets] correspond to those in Table 4. For a detailed explanation of these codes, refer to the "Codes" key under Table 4). The p-values given for each measure apply to linear regressions of *both* d-methamphetamine rotation and TH+ neuron depletion (e.g. linear regression of d-methamphetamine rotation against time of simple sets [^(1)] gave p=0.0143, whereas linear regression of right hemisphere TH+

neuron depletion against time of simple sets [^(1)] gave p=0.0004; thus, time of simple

sets [^(1)] is reported as significant at p<0.05).

Severely right hemisphere DA-depleted rats tended to have fewer complex sets

[#(>1)] (p<0.05; see graphs on page 36) and spend less total time contacting the cylinder

wall [^A] (p<0.05; see graphs on page 38) than more normal rats. DA-depleted rats also

tended to spend more time during the first touch of sets [^(A] (p<0.01; see graphs on page

37), which consist of simple sets [^(1)] (p<0.05) and the first touch of complex sets [^(A*]

(p<0.05). They also showed less total time in simple sets [^(1)] (p<0.05) than more

normal rats. Average time spent in simple sets [^/(1)] approached significance (p<0.06).

Table 4. Linear regression results of both d-methamphetamine rotation and right hemisphere TH+ neuron depletion against general forelimb use.

Count			Total Time			Average Time		
Codes	Trends		Codes	Trends		Codes	Trends	
#(1)			^(1)	*	\	^/(1)		
#(>1)	*	\	^(>1)			^/(>1)		
#(A)			^(A	**	\	^/(A		
See #(>1), above.			^(A*	*	\	^/(A*		
#*A*			^*A*			^/*A*		
See #(>1), above.			^*A)			^/*A)		
#A			^A	*	\	^/A		
#At			^At			^/At		
#*At			^*At			^/At		

"Codes" Key:

\# = number of occurrences.
^ = total time spent on a behavior.
^/ = average time spent on a behavior.
( ) = designates a set [i.e. a period of continuous forepaw contact with the cylinder wall].

NOTE: "L", "B", and "R" in the following signify cylinder wall contact with Left, Both, and Right forepaws, respectively:

(1) = (L)+(B)+(R); sum of all simple sets.
(>1) = (L*+(B*+(R*; sum of all complex or non-simple sets.
A = "All"; sum of Left, Both, and Right [e.g. #A = #L+#B+#R].
At = All touches [e.g. #At = #Lt+#Rt].
(= beginning of a set [e.g. "(L" means any simple or complex set beginning with a left forepaw touch; (L = (L)+(L*].
) = ending of a set [e.g. "L)" means the left forepaw is the last touching the cylinder wall in a set].
* = a "wildcard"; signifies one or more distinct forepaw contacts during a period of continuous wall contact [e.g. #*At means all *non-initial* touches in all complex sets. #*At = #*Lt+#*Rt].

"Trends" Key:

Linear regression against **both** d-methamphetamine rotation and right hemisphere TH+ neuron depletion showed these results:

* = $p < 0.05$ for both regressions.
** = $p < 0.01$ for both regressions.
☐ (blank cells) = $p > 0.05$ for one or both regressions.
\ = negatively-sloped linear regression lines (i.e. severely right hemisphere DA-depleted rats tended to have lower numbers, as in the graphs on page 36).

% TH+ Neuron Depletion vs. #(>1)

$r^2 = 0.1446$
$p = 0.0012$
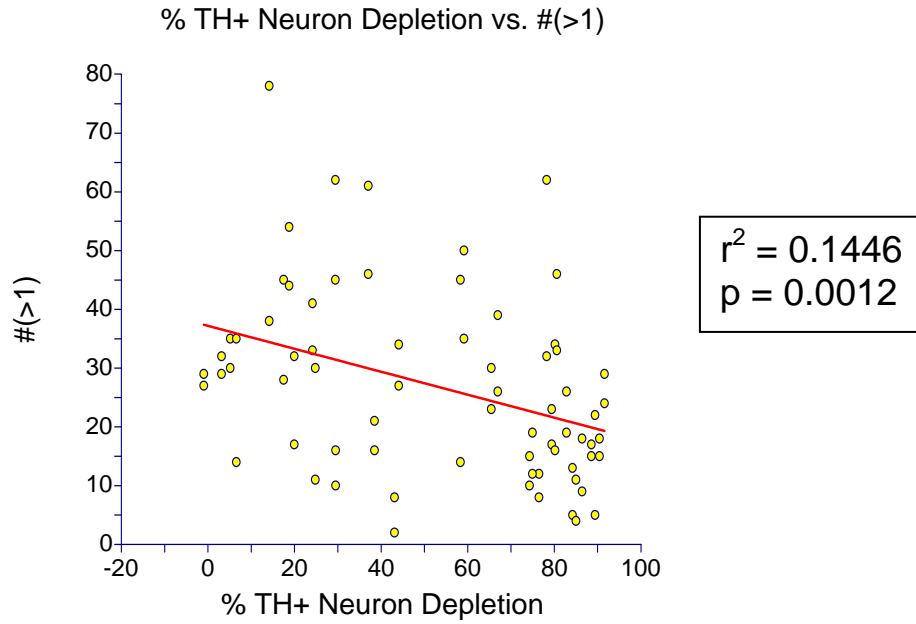
Figure 17. Linear regression of right hemisphere TH+ neuron depletion against number of complex sets [#(>1)].

Methamphetamine Rotation vs. #(>1)

$r^2 = 0.0677$
$p = 0.0296$
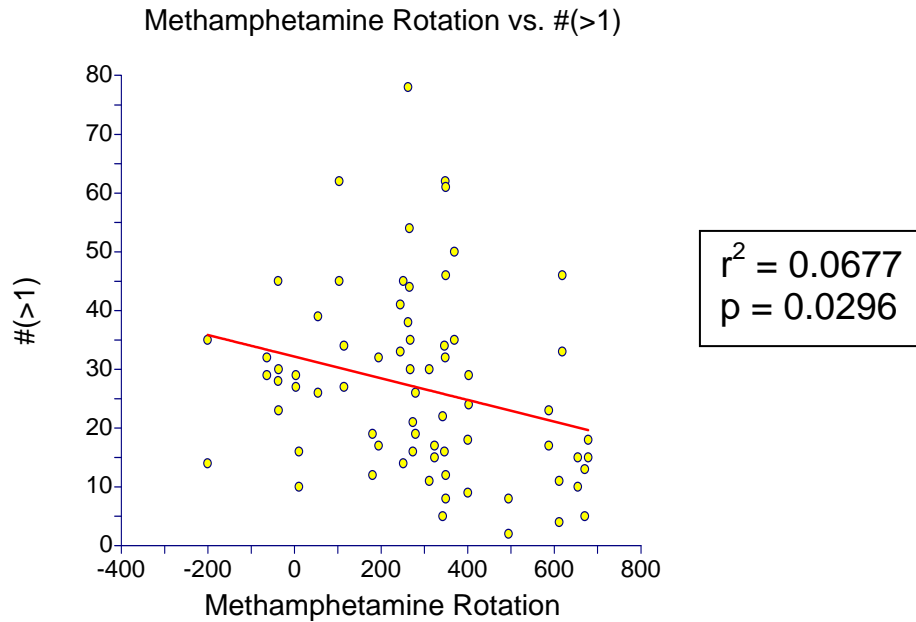
Figure 18. Linear regression of d-methamphetamine rotation against number of complex sets [#(>1)].
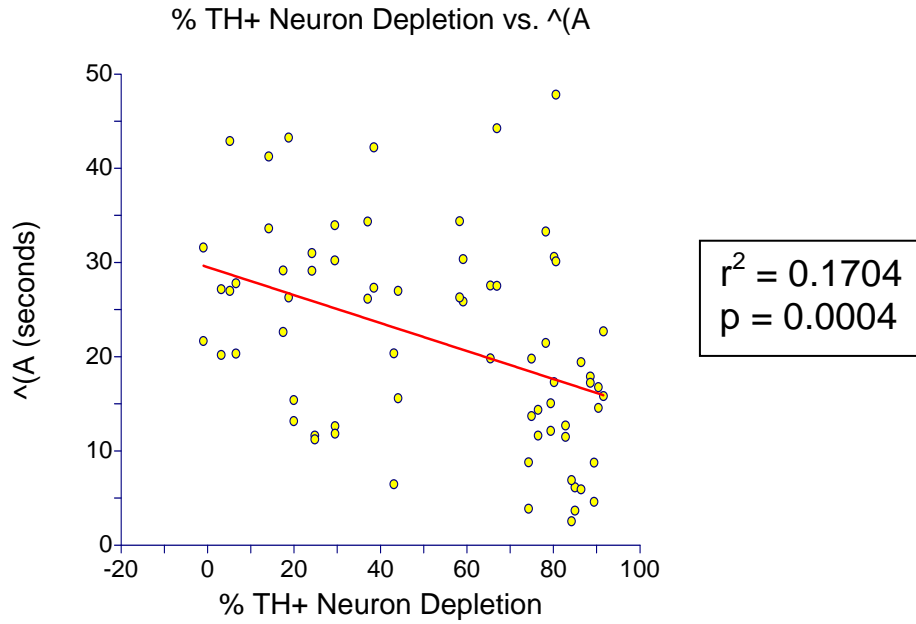
Figure 19. Linear regression of right hemisphere TH+ neuron depletion against total time spent in the first touch of all sets [^(A].
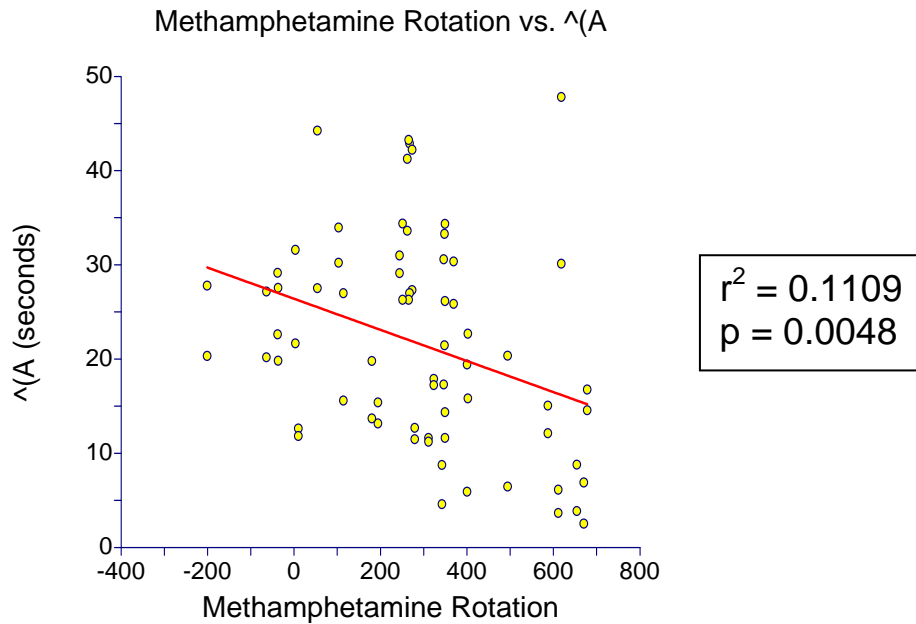
Figure 20. Linear regression of d-methamphetamine rotation against total time spent in the first touch of all sets [^(A].

% TH+ Neuron Depletion vs. ^A

$r^2 = 0.0600$
$p = 0.0410$
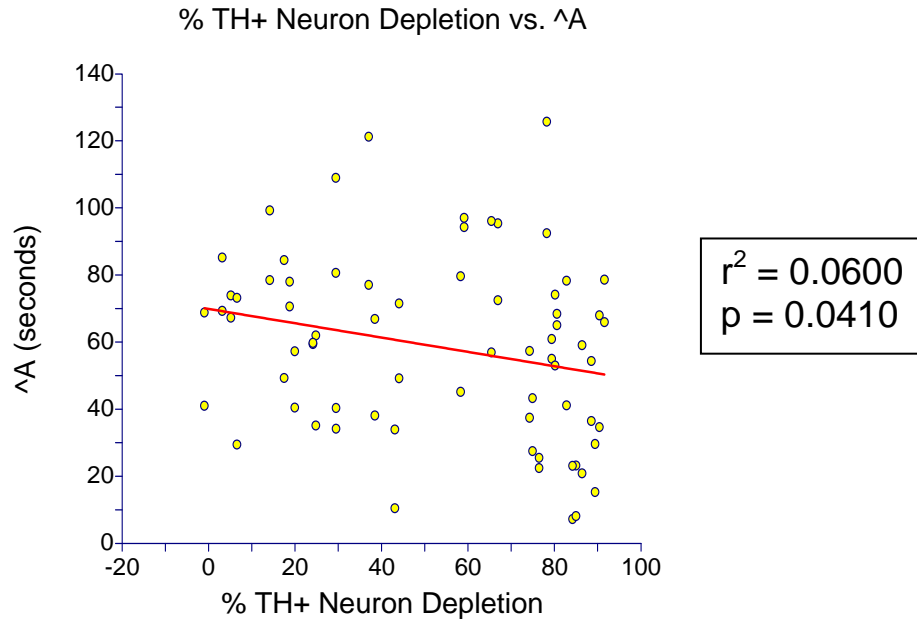
Figure 21. Linear regression of right hemisphere TH+ neuron depletion against total time spent contacting the cylinder wall [^A].

Methamphetamine Rotation vs. ^A

$r^2 = 0.0704$
$p = 0.0264$
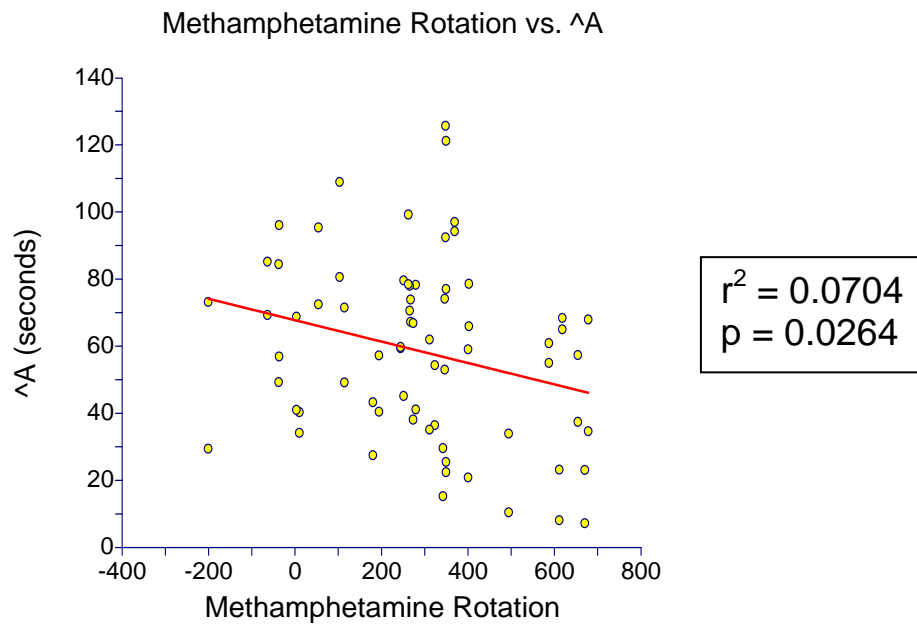
Figure 22. Linear regression of d-methamphetamine rotation against total time spent contacting the cylinder wall [^A].

Right and Left Forelimb Use

Severely DA-depleted rats made fewer left (contralateral-to-lesion) forepaw placements on the cylinder wall and spent less total time touching the cylinder wall with the left (contralateral-to-lesion) forepaw than rats with less DA depletion. In addition, severely DA-depleted rats spent longer on average during right (ipsilateral-to-lesion) forepaw placements at the beginning of complex sets. This section gives additional information about these observations.

Right verses left forelimb use was measured as count [#], time [^], and average time [^/] of wall touches and wall contact during simple and complex sets. (Figure 11 on page 22 illustrates the difference between simple and complex sets, as well as the difference between wall touches and wall contact time).

Right verses left forelimb use results are shown in Table 5 on page 41. (Behavior codes given in this section [in square brackets] correspond to those given in Table 5. For a detailed explanation of these codes, refer to the "Codes" key under Table 5). The p-values given for each measure apply to linear regressions of *both* d-methamphetamine rotation and TH+ neuron depletion (e.g. linear regression of d-methamphetamine rotation against number of left forepaw wall contact periods [#L] gave p= 0.0126, whereas linear regression of right hemisphere TH+ neuron depletion against this measure gave p=0.0065; thus, number of left forepaw wall contact periods [#L] is reported as significant at p<0.05).

The measures given on the first three rows of Table 5 under "Count" [#(L, #(B, and #(R] are purposely redundant with the following six rows. They are used to calculate

39

the conventional cylinder test asymmetry score (Schallert et al., 2000; Schallert & Woodlee, 2005); thus, results for #(L (row 1) match those of #(L) (row 4) and #(L* (row 7) closely, because #(L = #(L)+#(L*.

Count of left-forepaw wall contact was generally lower in severely right hemisphere DA-depleted rats, particularly number of exclusive left sets [#(L)] (p<0.001; see graphs on page 42) and complex sets beginning or ending with the left forepaw ([#(L*] (p<0.001; see graphs on page 43) and [#*L)] (p<0.001; see graphs on page 44), respectively). This is reflected in fewer total left touches on the cylinder wall [#Lt] (p<0.01; see graphs on page 45). They did not make fewer non-initial left touches [#*Lt], however, compared to normal rats.

Total wall contact time followed the pattern of wall contact count: rats that contacted the wall less frequently with the left (contralateral-to-lesion) forepaw tended to have less total wall contact time with that forepaw [^L] (p<0.001; see graphs on page 46). Severely right hemisphere DA-depleted rats spent less total time contacting the cylinder wall with the left forepaw, particularly during exclusive left sets [^(L)] (p<0.0001) and beginning and ending touches with the left forepaw during complex sets ([^(L*] (p<0.01) and [^*L)] (p<0.01), respectively).

Average wall contact time showed fewer differences. Severely right hemisphere DA-depleted rats appeared to spend less time on average for periods of exclusive left (contralateral-to-lesion) forepaw wall contact [^/L] (p<0.05) than more normal rats. On the other hand, they tended to spend less time during right (ipsilateral-to-lesion) forepaw first touches of complex sets [^/(R*] (p<0.01; see graphs on page 47) than more normal rats.

Table 5. Linear regression results of both d-methamphetamine rotation and right hemisphere TH+ neuron depletion against forelimb-specific cylinder wall activity.

Count		Total Time		Average Time	
Codes	Trends	Codes	Trends	Codes	Trends
#(L	*** \	^(L	**** \	^/(L	
#(B		^(B	* \	^/(B	
#(R		^(R		^/(R	
#(L)	*** \	^(L)	**** \	^/(L)	
#(B)		^(B)		^/(B)	
#(R)		^(R)		^/(R)	
#(L*	*** \	^(L*	** \	^/(L*	
#(B*		^(B*	* \	^/(B*	
#(R*		^(R*		^/(R*	** /
#*L*		^*L*		^/*L*	
#*B*		^*B*		^/*B*	
#*R*		^*R*		^/*R*	
#*L)	*** \	^*L)	** \	^/*L)	
#*B)		^*B)		^/*B)	
#*R)		^*R)		^/*R)	
#L	* \	^L	*** \	^/L	* \
#B		^B		^/B	
#R		^R		^/R	
#Lt	** \	^Lt		^/Lt	
#Rt		^Rt		^/Rt	
#*Lt		^*Lt		^/*Lt	
#*Rt		^*Rt		^/*Rt	

"Codes" Key:

\# = number of occurrences.
^ = time spent contacting the cylinder wall.
^/ = average time spent contacting the cylinder wall.
L = Left (contralateral-to-lesion) forepaw contacting the cylinder wall exclusively.
B = Both forepaws contacting the cylinder wall simultaneously.
R = Right (ipsilateral-to-lesion) forepaw contacting the cylinder wall exclusively.
t = touch [e.g. "Lt" means a left forepaw touch on the cylinder wall.].
(= beginning of a set [e.g. "(L" means any simple or complex set beginning with a left forepaw touch; (L = (L)+(L*].
) = ending of a set [e.g. "L)" means the left forepaw is the last touching the cylinder wall in a set].
Shaded cells contain key components of conventional cylinder test measures.
* = a "wildcard"; signifies one or more distinct forepaw contacts during a set [e.g. "(L*" might represent "(LR)", "(LBLR)", etc.].

"Trends" Key:

Linear regression against **both** d-methamphetamine rotation and right hemisphere TH+ neuron depletion showed these results:

* = p < 0.05 for both regressions.
** = p < 0.01 for both regressions.
*** = p < 0.001 for both regressions.
**** = p < 0.0001 for both regressions.
☐ (blank cells) = p > 0.05 for one or both regressions.
\ = negatively-sloped linear regression lines (i.e. severely right hemisphere DA-depleted rats tended to have lower numbers, as in the graphs on page 42).
/ = positively-sloped linear regression lines (i.e. severely right hemisphere DA-depleted rats tended to have higher numbers, as in the graphs on page 47).

% TH+ Neuron Depletion vs. #(L)

$r^2 = 0.2161$
$p = 0.0001$
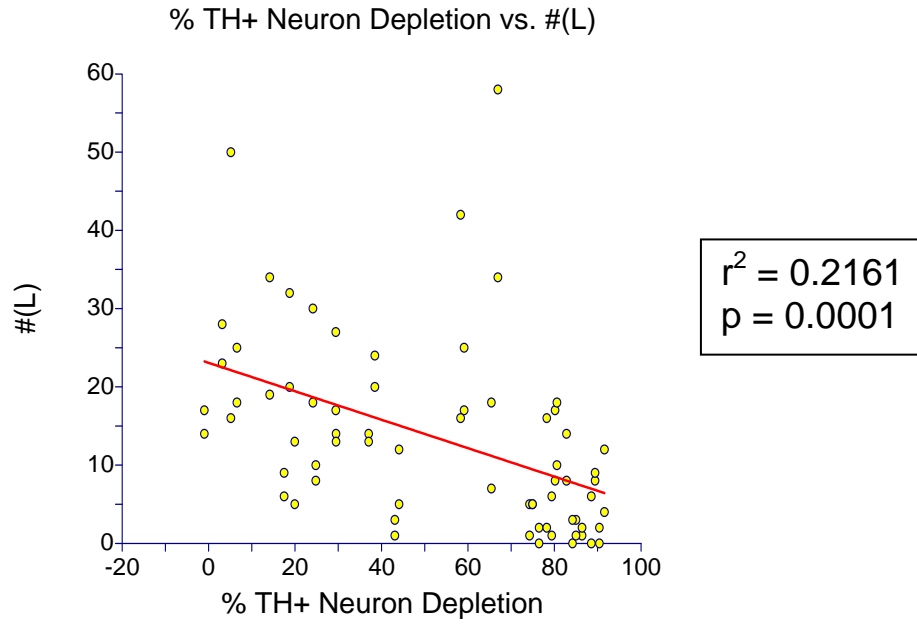
Figure 23. Linear regression of right hemisphere TH+ neuron depletion against number of simple sets with the left (contralateral-to-lesion) forepaw [#(L)].

Methamphetamine Rotation vs. #(L)

$r^2 = 0.1982$
$p = 0.0001$
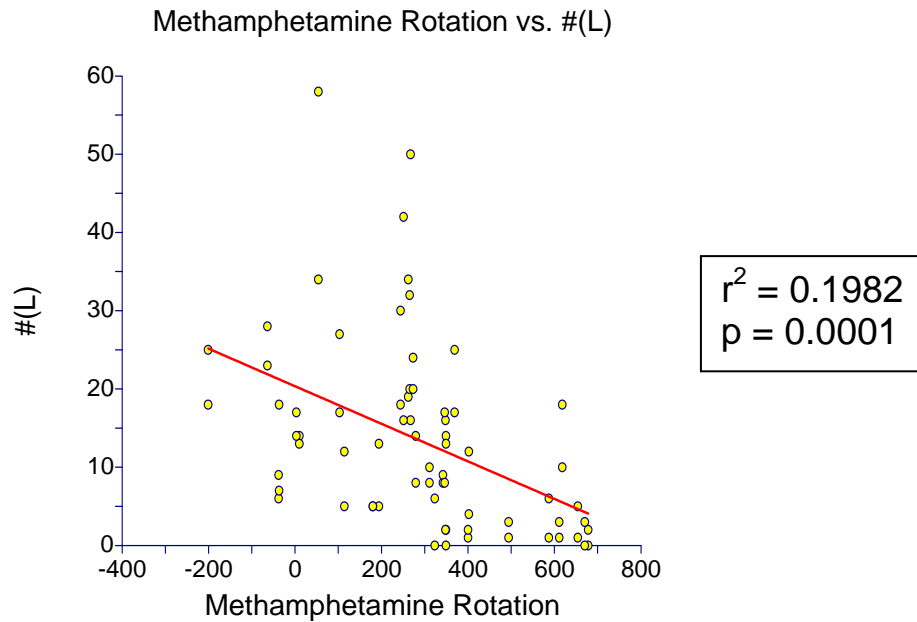
Figure 24. Linear regression of d-methamphetamine rotation against number of simple sets with the left (contralateral-to-lesion) forepaw [#(L)].
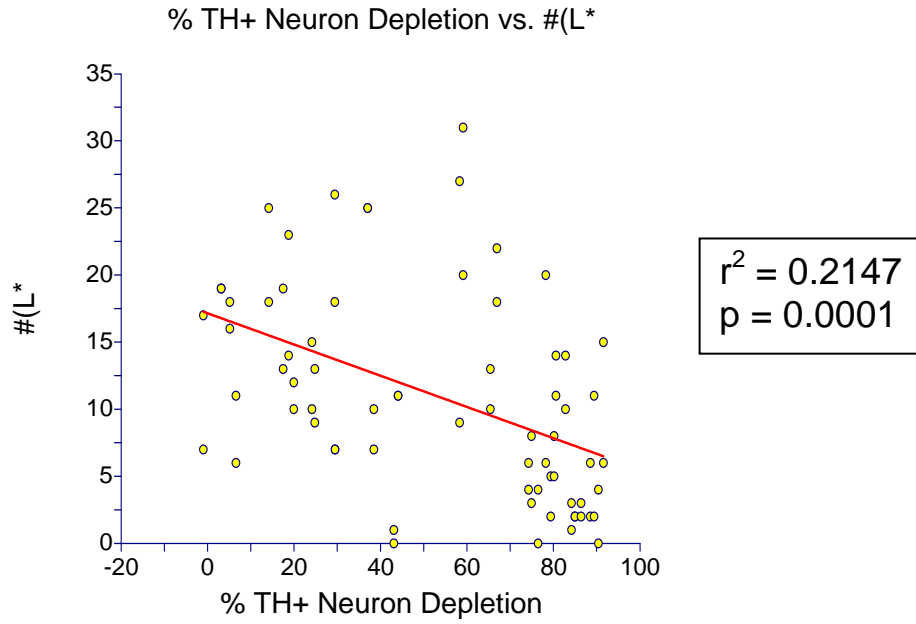
Figure 25. Linear regression of right hemisphere TH+ neuron depletion against number of complex sets beginning with a left forepaw touch [#(L*).

Figure 26. Linear regression of d-methamphetamine rotation against number of complex sets beginning with a left forepaw touch [#(L*).
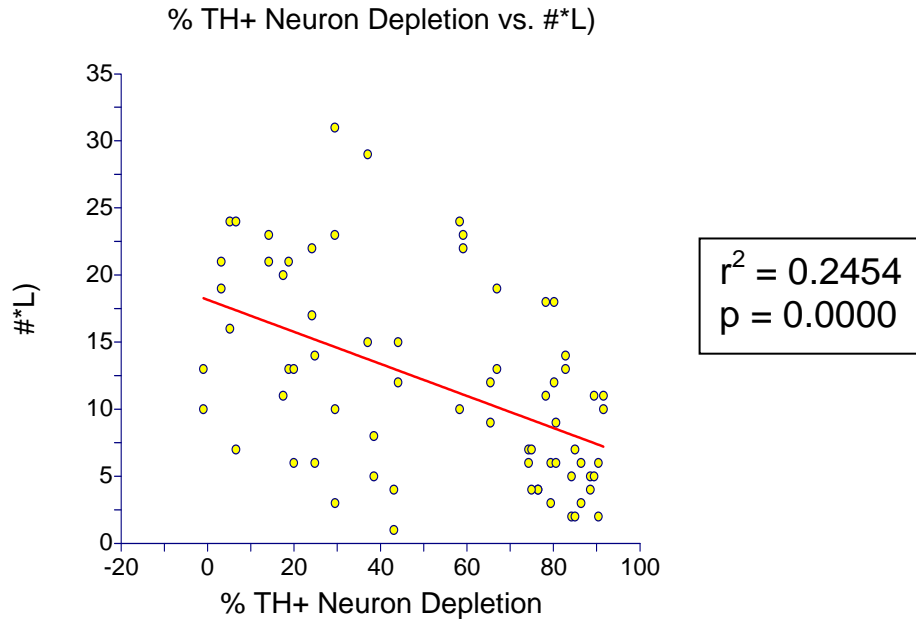
Figure 27. Linear regression of right hemisphere TH+ neuron depletion against number of complex sets in which the left forepaw is the last contacting the cylinder wall [#*L].
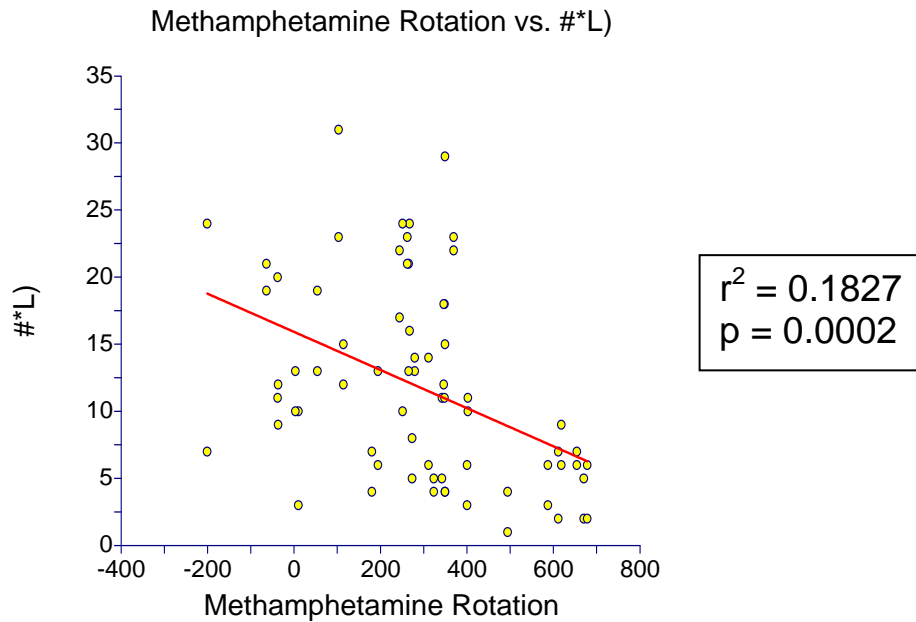
Figure 28. Linear regression of d-methamphetamine rotation against number of complex sets in which the left forepaw is the last contacting the cylinder wall [#*L].
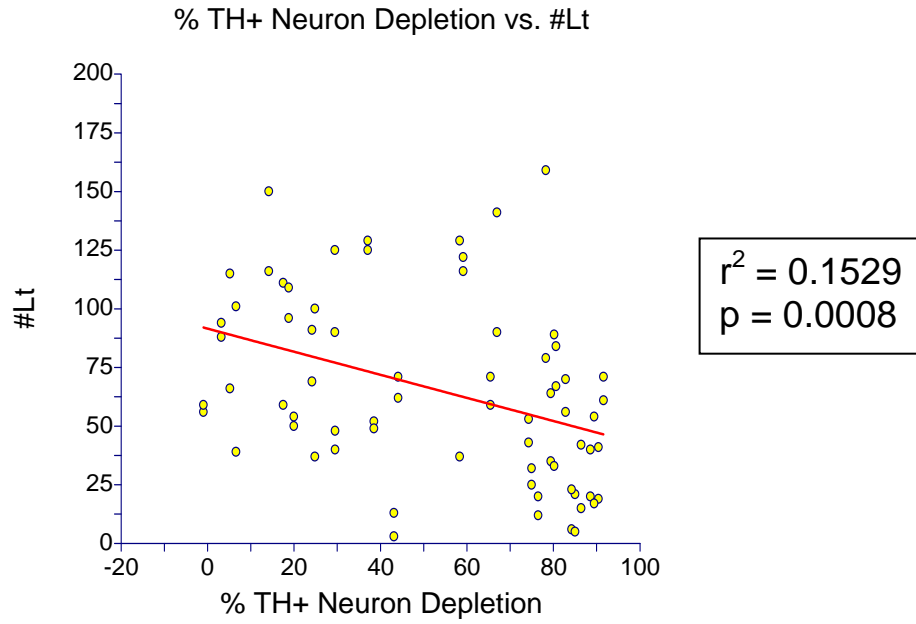
Figure 29. Linear regression of right hemisphere TH+ neuron depletion against number of touches with the left forepaw [#Lt].
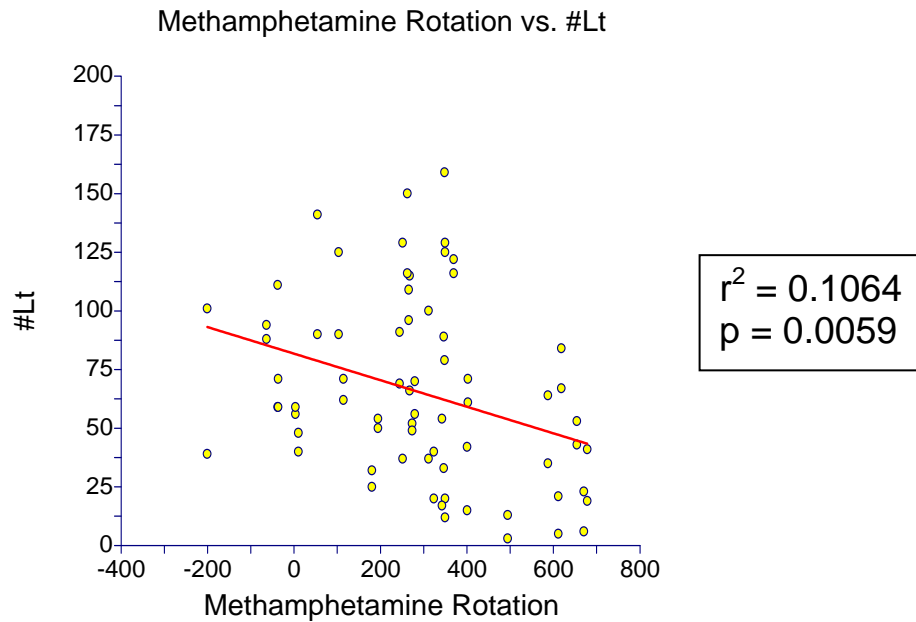
Figure 30. Linear regression of d-methamphetamine rotation against number of touches with the left forepaw [#Lt].
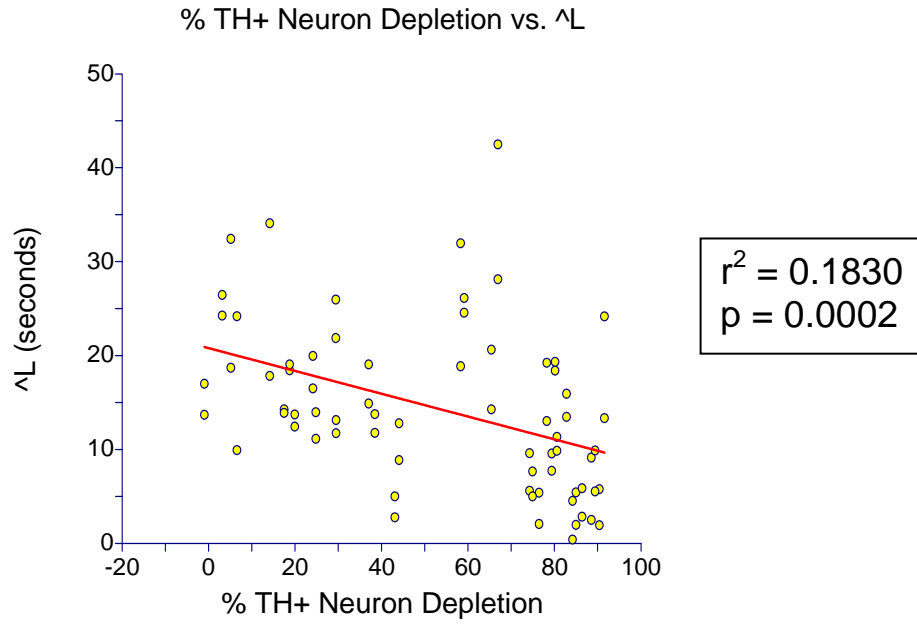
Figure 31. Linear regression of right hemisphere TH+ neuron depletion against total wall contact time with the left forepaw [^L].
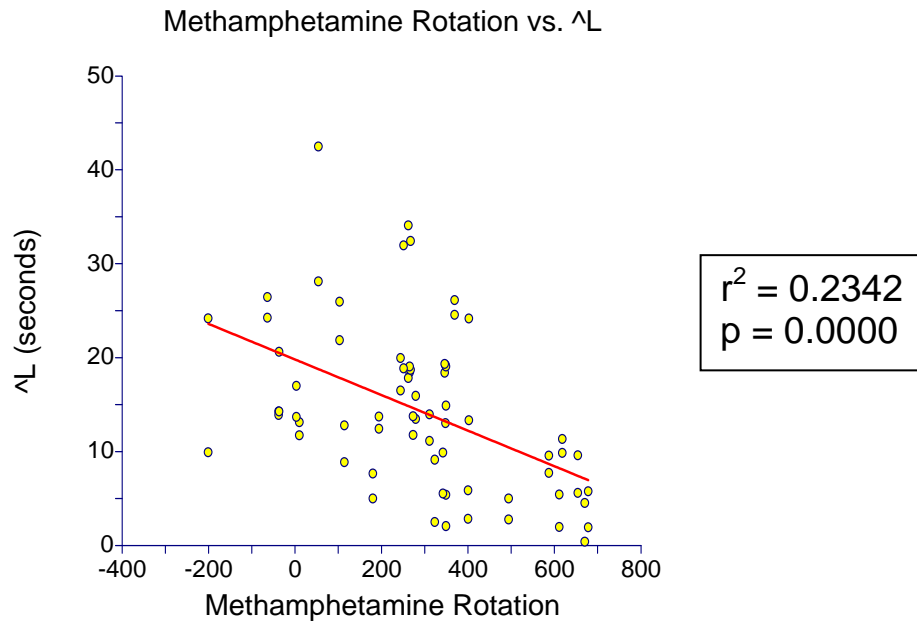
Figure 32. Linear regression of d-methamphetamine rotation against total wall contact time with the left forepaw [^L].
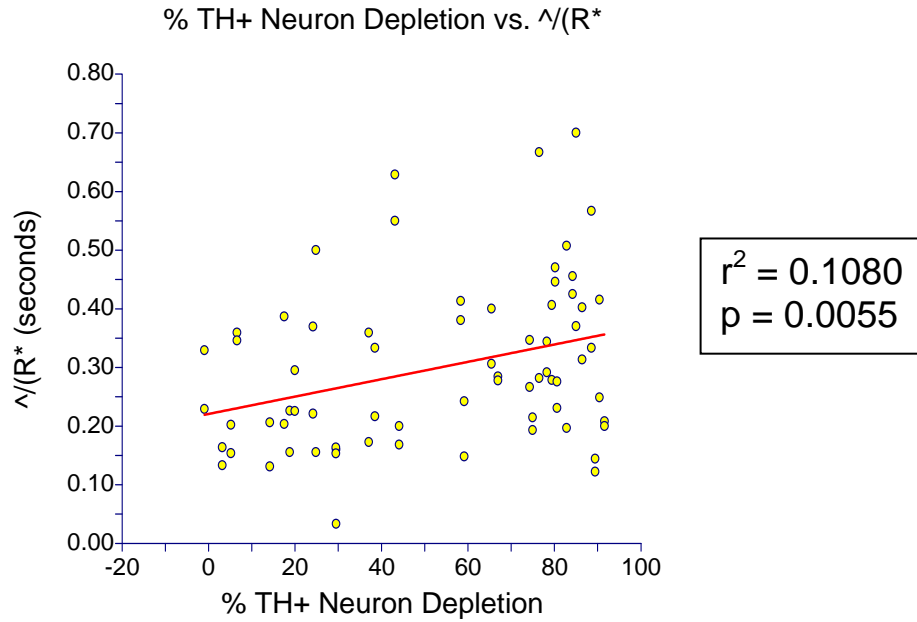
Figure 33. Linear regression of right hemisphere TH+ neuron depletion against average time of right (ipsilateral-to-lesion) forepaw initial touches of complex sets [^/(R*].
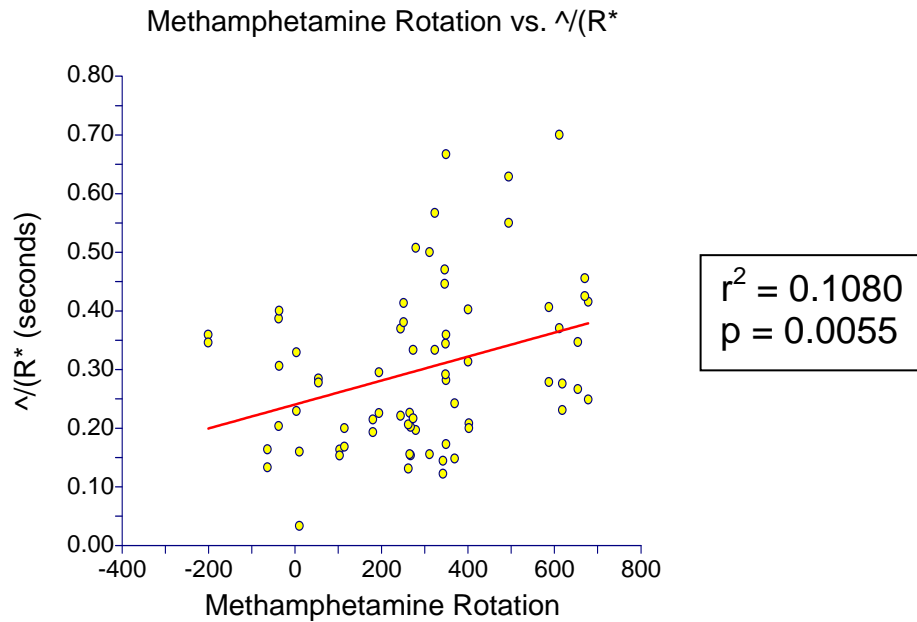
Figure 34. Linear regression of d-methamphetamine rotation against average time of right (ipsilateral-to-lesion) forepaw initial touches of complex sets [^/(R*].

Wall Contact Sequences

Severely DA-depleted rats tended to end complex sets with the left (contralateral-to-lesion) forepaw less often than more normal rats. They also tended to spend longer touching the cylinder wall with the right (ipsilateral-to-lesion) forepaw and less time with the left (contralateral-to-lesion) forepaw during various wall contact sequences than more normal rats. These observations are explained further in this section.

Count [#], time [^] and average time [^/] of various one- and two-movement wall contact sequences within complex sets were measured, and linear regression was performed for both d-methamphetamine rotation and right hemisphere TH+ neuron depletion against these sequences. Table 6 (page 50) shows only those sequences that were significant among the many sequences analyzed, whereas Table 10 and Table 12 in Appendix A (page 95 and 97, respectively) contain a list of all sequences analyzed. Behavior codes given in this section [in square brackets] correspond to those given in Table 6. (For a detailed explanation of these codes, refer to the "Codes" key under Table 6). The p-values given for each measure apply to linear regressions of *both* d-methamphetamine rotation and TH+ neuron depletion (e.g. linear regression of d-methamphetamine rotation against left forepaw contact time during a both-left sequence at the end of a complex set [^bL)] gave p= 0.0021, whereas linear regression of right hemisphere TH+ neuron depletion against the same measure [^bL)] gave p=0.0287; thus, [^bL)] is reported as significant at p<0.05).

The count of two movement sequences was significant: severely right hemisphere DA-depleted rats tended to begin complex sets with a left-both sequence [#(LB] (p<0.01;

see graphs on page 51) and end complex sets with a both-left sequence [#BL)] (p<0.01; see graphs on page 51) less often than more normal rats.

Time of only one movement sequence was significant: severely right hemisphere DA-depleted rats tended to spend less time with the left forepaw when ending complex sets with a both-left sequence compared to more normal rats [^bL)] (p<0.05).

Average sequence time analysis showed a general pattern of severely right hemisphere DA-depleted rats spending longer on right (ipsilateral-to-lesion) forepaw wall contact during certain sequences than more normal rats. This appears to be true of the following sequences: [^/bR] (p<0.05), [^/RB] (p<0.05), [^/Rb] (p<0.01), [^/RBL] (p<0.05), [^/Rbl] (p<0.01; see graphs on page 52), and [^/lbR] (p<0.05). On the other hand, the most severe hemiparkinson rats spent less time on average contacting the cylinder wall with the left (contralateral-to-lesion) forepaw during the initial contact time of a left-both-left sequence [^/Lbl] (p<0.01; see graphs on page 53).

**Table 6. Linear regression results of both d-methamphetamine rotation and right hemisphere TH+ neuron depletion against cylinder wall contact sequences.**

Count		Total Time		Average Time	
Codes	Trends	Codes	Trends	Codes	Trends
#BL)	*** \	^bL)	* \	^/bR	* /
#(LB	*** \			^/RB	* /
				^/Rb	** /
				^/RBL	* /
				^/Rbl	** /
				^/lbR	* /
				^/LRB	* \
				^/Lbl	** \

"Codes" Key:

\# = number of occurrences.
^ = time spent contacting the cylinder wall (applies to UPPER CASE letters only; lower case letters are shown solely for context).
^/ = average time spent contacting the cylinder wall (applies to UPPER CASE letters only; lower case letters are shown solely for context).
L = Left (contralateral-to-lesion) forepaw contacting the cylinder wall exclusively.
B = Both forepaws contacting the cylinder wall simultaneously.
R = Right (ipsilateral-to-lesion) forepaw contacting the cylinder wall exclusively.
) = ending of a set [e.g. "L)" means the left forepaw is the last touching the cylinder wall in a set].

"Trends" Key:

Linear regression against **both** d-methamphetamine rotation and right hemisphere TH+ neuron depletion showed these results:

* = $p < 0.05$ for both regressions.
** = $p < 0.01$ for both regressions.
*** = $p < 0.001$ for both regressions.
\ = negatively-sloped linear regression lines (i.e. severely right hemisphere DA-depleted rats tended to have lower numbers, as in the graphs on page 51).
/ = positively-sloped linear regression lines (i.e. severely right hemisphere DA-depleted rats tended to have higher numbers, as in the graphs on page 52).
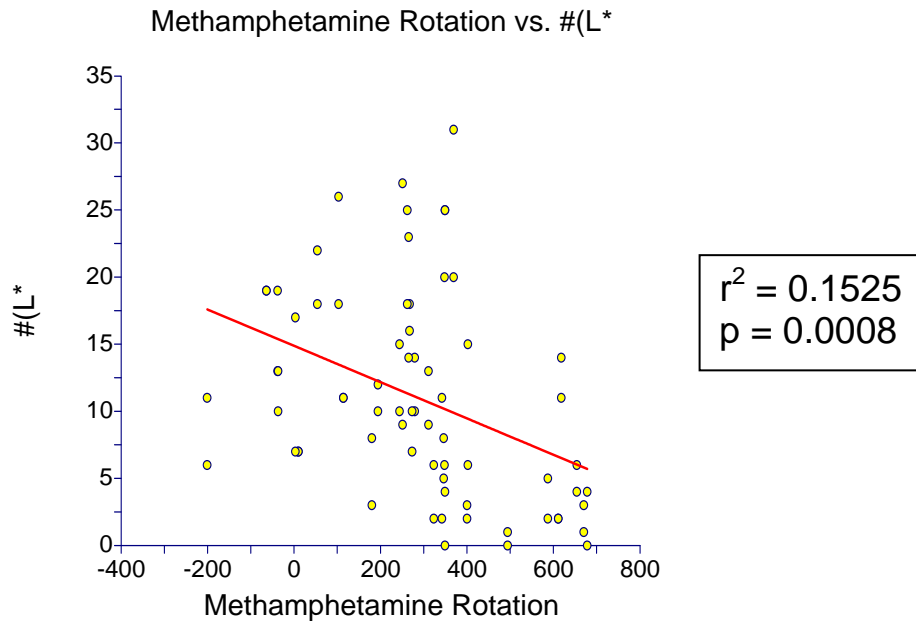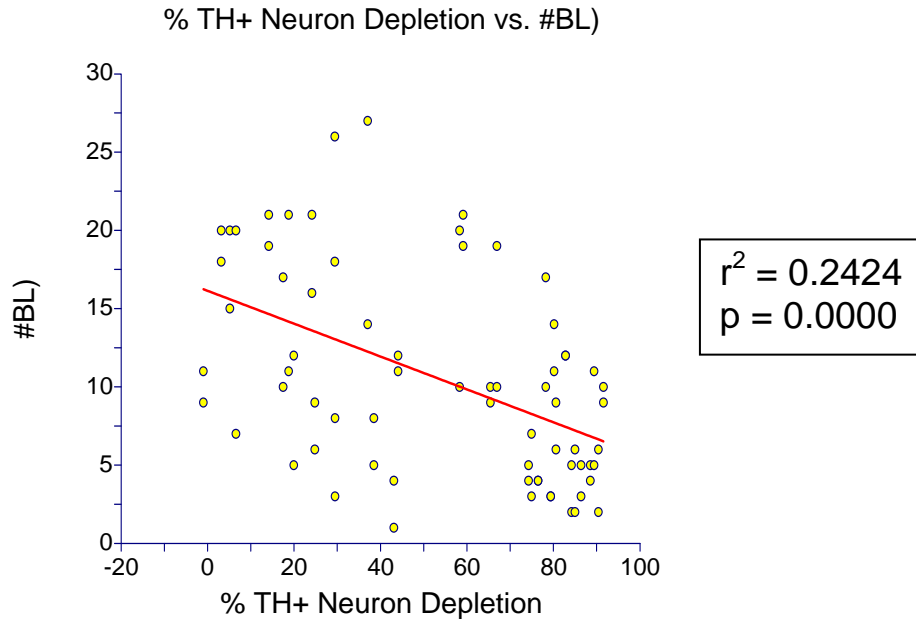
Figure 35. Linear regression of right hemisphere TH+ neuron depletion against count of complex sets ending in a Both-Left sequence [#BL)].
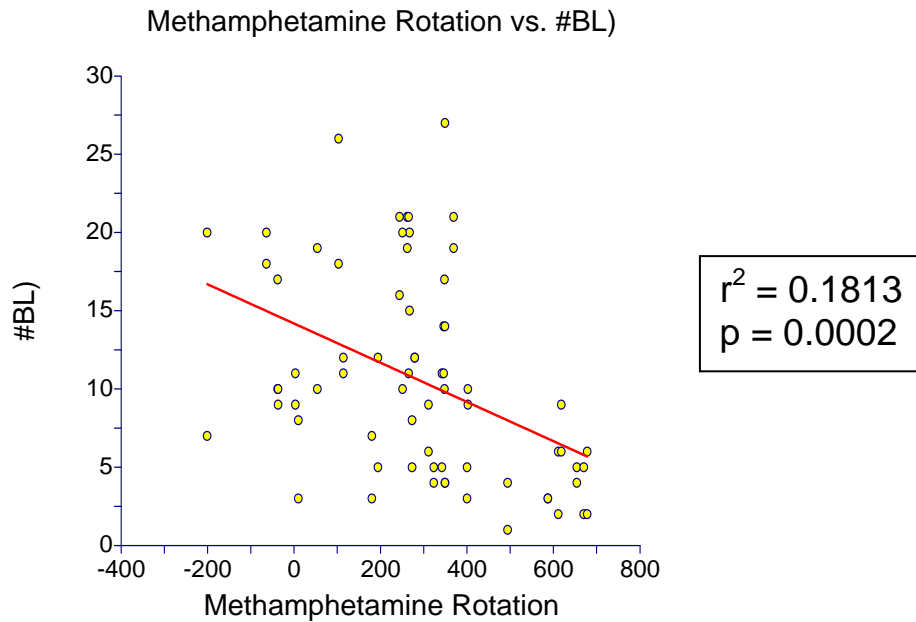
Figure 36. Linear regression of d-methamphetamine rotation against count of complex sets ending in a Both-Left sequence [#BL)].

% TH+ Neuron Depletion vs. ^/Rbl

$r^2 = 0.1214$
$p = 0.0031$
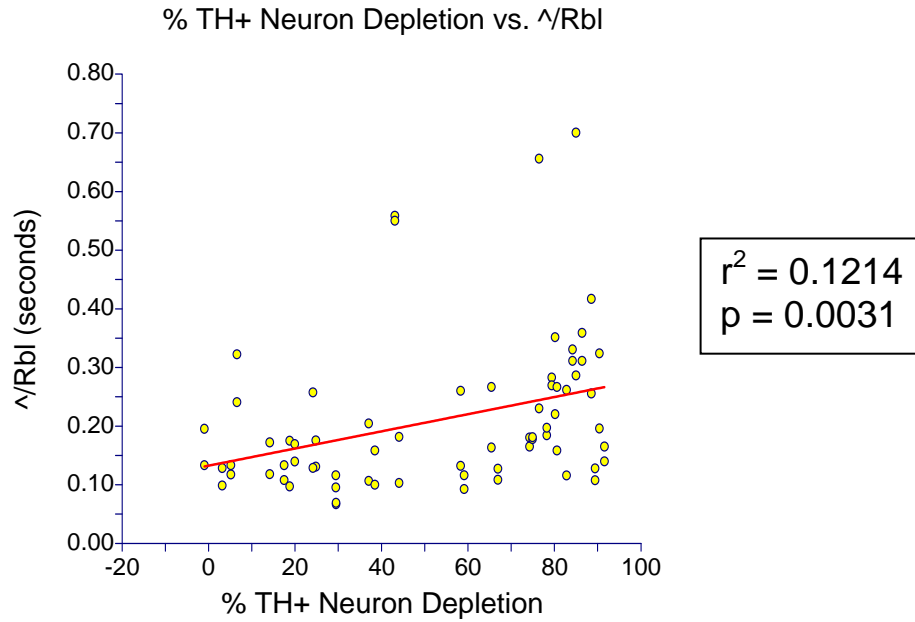
Figure 37. Linear regression of right hemisphere TH+ neuron depletion against average time spent contacting the cylinder wall exclusively with the __right__ (ipsilateral-to-lesion) forepaw during any __Right__-Both-Left sequence [^/Rbl].

Methamphetamine Rotation vs. ^/Rbl

$r^2 = 0.1561$
$p = 0.0007$
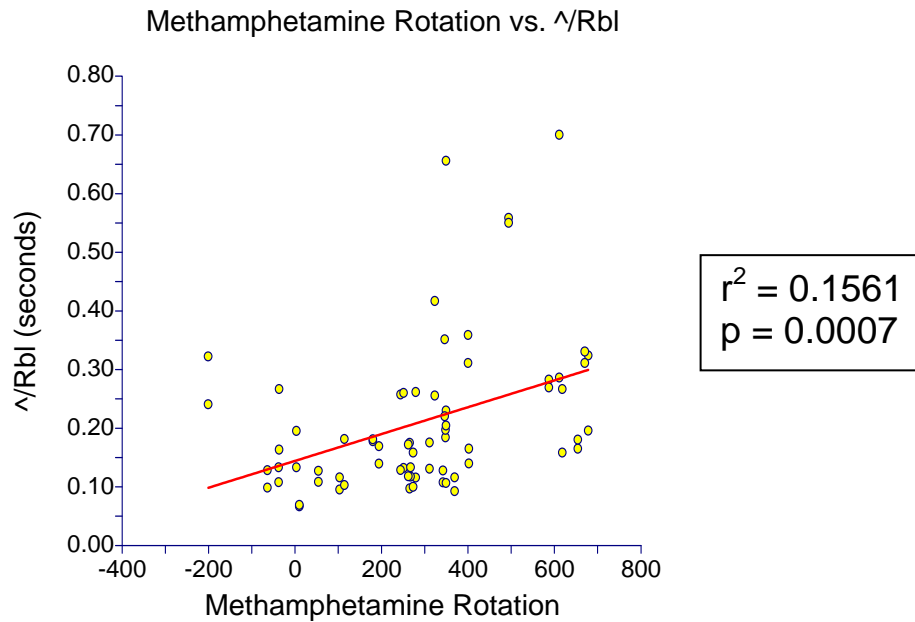
Figure 38. Linear regression of d-methamphetamine rotation against average time spent contacting the cylinder wall exclusively with the __right__ (ipsilateral-to-lesion) forepaw during any __Right__-Both-Left sequence [^/Rbl].

% TH+ Neuron Depletion vs. ^/Lbl

$r^2 = 0.1013$
$p = 0.0072$
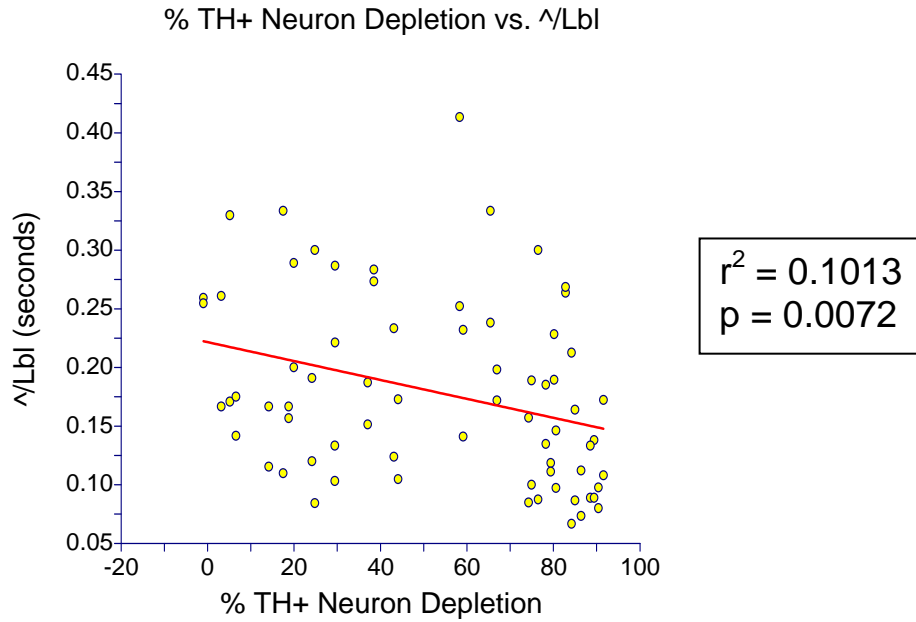
Figure 39. Linear regression of right hemisphere TH+ neuron depletion against average time spent contacting the cylinder wall exclusively with the <u>left</u> (contralateral-to-lesion) forepaw during the first portion of any <u>Left</u>-Both-Left sequence [^/Lbl].

Methamphetamine Rotation vs. ^/Lbl

$r^2 = 0.1510$
$p = 0.0009$
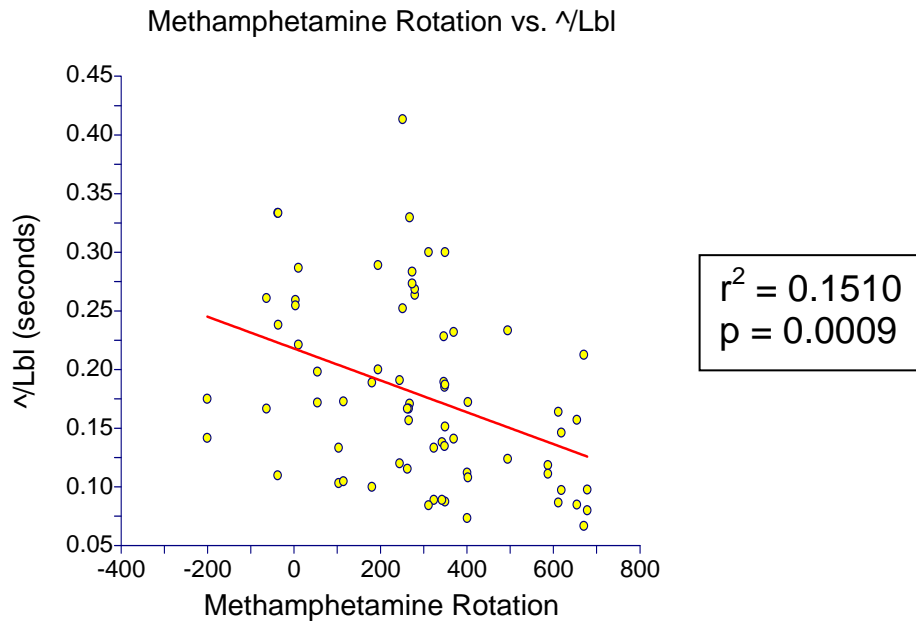
Figure 40. Linear regression of d-methamphetamine rotation against average time spent contacting the cylinder wall exclusively with the <u>left</u> (contralateral-to-lesion) forepaw during the first portion of any <u>Left</u>-Both-Left sequence [^/Lbl].

Right Verses Left Forelimb Use Asymmetries

Severely right hemisphere DA-depleted rats tended to make fewer cylinder wall touches with the left (contralateral-to-lesion) forepaw than more normal rats. When they did touch the cylinder wall with the left (contralateral-to-lesion) forepaw, they tended to leave it on the cylinder wall longer on average than more normal rats. These observations are explained further in this section.

Table 7 (page 57) shows results for linear regression of both d-methamphetamine rotation and right hemisphere TH+ neuron depletion against count asymmetry [%], total time asymmetry [%^], and average time asymmetry [%^/] of cylinder wall contact. (Behavior codes given in this section [in square brackets] correspond to those given in Table 7. For a detailed explanation of codes given [in square brackets] in this section, refer to the "Codes" key under Table 7). The p-values given for each measure apply to linear regressions of *both* d-methamphetamine rotation and TH+ neuron depletion (e.g. linear regression of d-methamphetamine rotation against left verses right forepaw use asymmetry for simple sets [%^(L)] gave p= 0.0003, whereas linear regression of right hemisphere TH+ neuron depletion against the same measure [%^(L)] gave p=0.0263; thus, [%^(L)] is reported as significant at p<0.05).

Right and left forepaw use for the first touch of any set are key components of the cylinder test's conventional forelimb use asymmetry score (Schallert et al., 2000; Schallert & Woodlee, 2005). These are listed in the first three rows of the "Count Asymmetry" portion of Table 7. Severely right hemisphere DA-depleted rats tended to make a higher percentage of the first touches of a set with the right (ipsilateral-to-lesion)

forepaw [%(R] (p<0.001) and a lower percentage of first touches of a set with the left (contralateral-to-lesion) forepaw [%(L] (p<0.01; see graphs on page 58), compared with more normal rats.

First touch of each set may be subdivided into two categories: 1) first touch of simple sets, and 2) first touch of complex sets. The results for both of these sub-categories showed the same trends as reported in the previous paragraph: severely right hemisphere DA-depleted rats tended to have more exclusive sets with the right forepaw [%(R)] (p<0.01) and fewer exclusive sets with the left forepaw [%(L)] (p<0.01; see graphs on page 59). Similarly, they tended to have a higher proportion of complex sets beginning with a right forepaw touch [%(R*] (p<0.001) and a lower proportion of complex sets beginning with the left forepaw [%(L*] (p<0.01; see graphs on page 60).

As expected from the patterns described in the preceding two paragraphs, severely right hemisphere DA-depleted rats showed a lower ratio of left forepaw touches to total touches [%Lt] (p<0.001) than more normal rats.

However, severely right hemisphere DA-depleted rats showed behavior that goes directly against the general pattern of avoiding left forepaw use: they tended to have a *higher* proportion of periods of left forepaw contact in the middle of complex sets [%*L*] (p<0.0001; see graphs on page 61] than more normal rats, and a lower proportion of right forepaw contact in the middle of complex sets [%*R*] (p<0.01). This behavior may account for the weaker significance of the ratio of non-initial left forepaw touches to total touches [%*Lt] (p<0.05) compared with the ratio of all left forepaw touches to total touches [%Lt] (p<0.001; see graphs on page 62).

Asymmetry in total time of cylinder wall contact generally followed the same patterns as count asymmetry, but with notable differences. Severely right hemisphere DA-depleted rats tended to be more asymmetric than more normal rats in the time they spent during the first touch of complex sets: in general, they spent more time on a first touch with the right forepaw [%^(R*] (p<0.001) and less time on a first touch with the with the left forepaw [%^(L*] (p<0.01) than more normal rats. This pattern seemed to hold true, albeit with a lower significance level, for simple sets with the right and left forepaw ([%^(R)] (p<0.05) and [%^(L)] (p<0.05), respectively): severely right hemisphere DA-depleted rats tended to spend more time on right forepaw touches and less time on left forepaw touches, compared to more normal rats.

Asymmetry in average time of cylinder wall contact showed interesting asymmetries: severely right hemisphere DA-depleted rats tended to spend *less* time, on average, for each left forepaw wall contact period than more normal rats [%^/L] (p<0.001). However, they spent comparatively *more* time than normal rats for each left forepaw touch on the cylinder wall [%^/Lt] (p<0.001; see graphs on page 64). This was also true of non-initial left forepaw touches [%^/*Lt] (p<0.01; see graphs on page 65).

Table 7. Linear regression results of both d-methamphetamine rotation and right hemisphere TH+ neuron depletion against cylinder wall contact asymmetries.

Count Asymmetry		Total Time Asymmetry		Average Time Asymmetry	
Codes	Trends	Codes	Trends	Codes	Trends
%(L	** \	%^(L	** \	%^/(L	
%(B		%^(B		%^/(B	
%(R	*** /	%^(R	** /	%^/(R	
%(L)	** \	%^(L)	* \	%^/(L)	
%(B)		%^(B)		%^/(B)	
%(R)	** /	%^(R)	* /	%^/(R)	
%(L*	** \	%^(L*	** \	%^/(L*	
%(B*		%^(B*		%^/(B*	
%(R*	*** /	%^(R*	*** /	%^/(R*	
%*L*	**** /	%^*L*		%^/*L*	
%*B*		%^*B*		%^/*B*	
%*R*	** \	%^*R*		%^/*R*	
%*L)		%^*L)		%^/*L)	
%*B)		%^*B)		%^/*B)	
%*R)	* /	%^*R)		%^/*R)	
%L	* \	%^L	*** \	%^/L	*** \
%B		%^B		%^/B	
%R		%^R		%^/R	
%Lt	*** \	%^Lt	* \	%^/Lt	*** /
%*Lt	* \	%^*Lt		%^/*Lt	** /

"Codes" Key:

% = percent of appropriate total [e.g. %Lt = #Lt/(#Lt+#Rt) and %L = #L/(#L+#B+#R)].

^ = time spent contacting the cylinder wall.

^/ = average time spent contacting the cylinder wall.

L = Left (contralateral-to-lesion) forepaw contacting the cylinder wall exclusively.

B = Both forepaws contacting the cylinder wall simultaneously.

R = Right (ipsilateral-to-lesion) forepaw contacting the cylinder wall exclusively.

t = touch [e.g. "Lt" means a left forepaw touch on the cylinder wall].

(= beginning of a set [e.g. "(L" means any simple or complex set beginning with a left forepaw touch; (L = (L)+(L*].

) = ending of a set [e.g. "L)" means the left forepaw is the last touching the cylinder wall in a set].

Shaded cells contain key components of conventional cylinder test measures.

* = a "wildcard"; signifies one or more distinct forepaw contacts during a set [e.g. "(L*" might represent "(LR)", "(LBLR)", etc.].

"Trends" Key:

Linear regression against **both** d-methamphetamine rotation and right hemisphere TH+ neuron depletion showed these results:

* = $p < 0.05$ for both regressions.

** = $p < 0.01$ for both regressions.

*** = $p < 0.001$ for both regressions.

**** = $p < 0.0001$ for both regressions.

☐ (blank cells) = $p > 0.05$ for one or both regressions.

\ = negatively-sloped linear regression lines (i.e. severely right hemisphere DA-depleted rats tended to have lower numbers, as in the graphs on page 58).

/ = positively-sloped linear regression lines (i.e. severely right hemisphere DA-depleted rats tended to have higher numbers, as in the graphs on page 61).
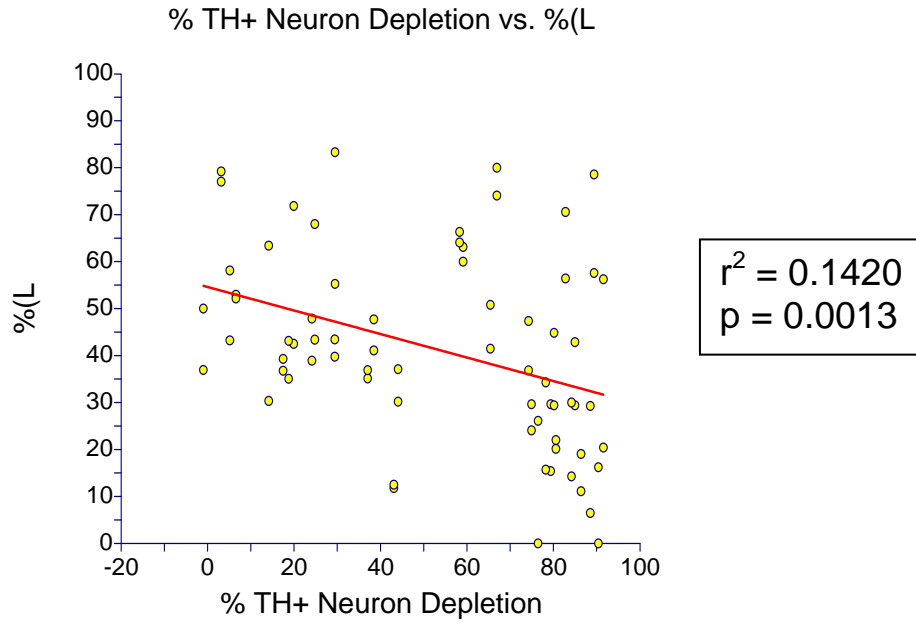
Figure 41. Linear regression of right hemisphere TH+ neuron depletion against the percentage of all sets that begin with an exclusive left forepaw touch [%(L].
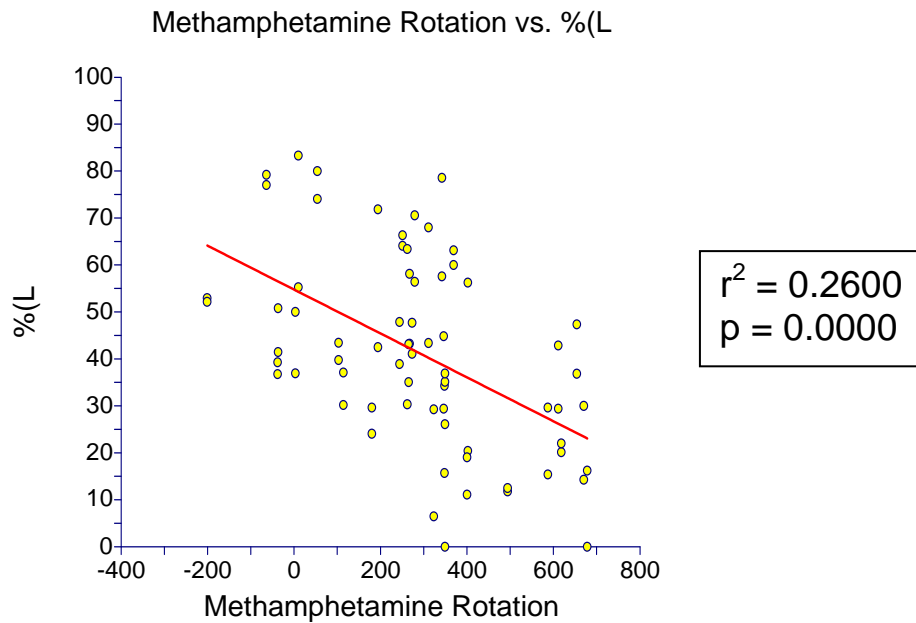
Figure 42. Linear regression of d-methamphetamine rotation against the percentage of all sets that begin with an exclusive left forepaw touch [%(L].
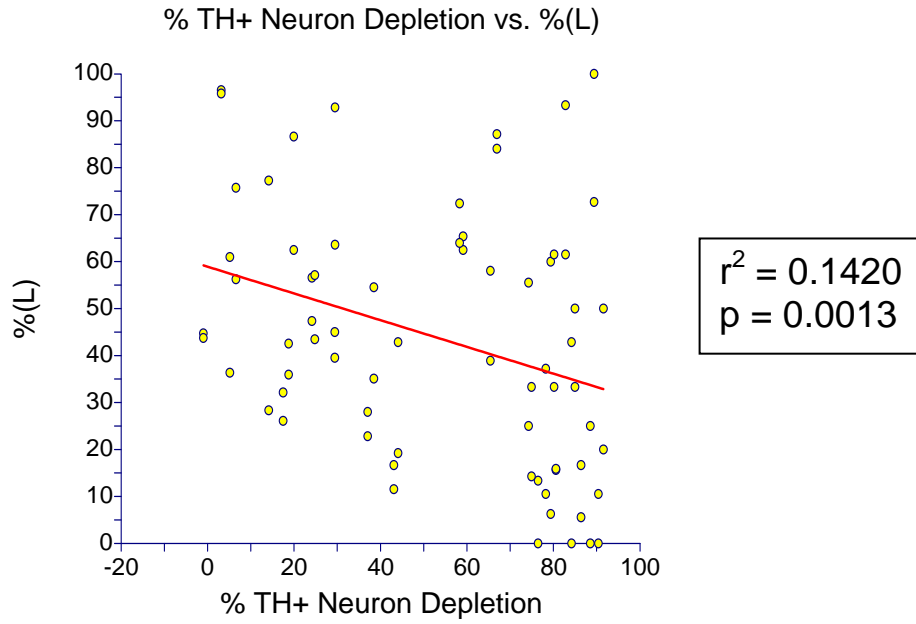
Figure 43. **Linear regression of right hemisphere TH+ neuron depletion against the percentage of all simple sets that are comprised of an exclusive left touch [%(L)].**
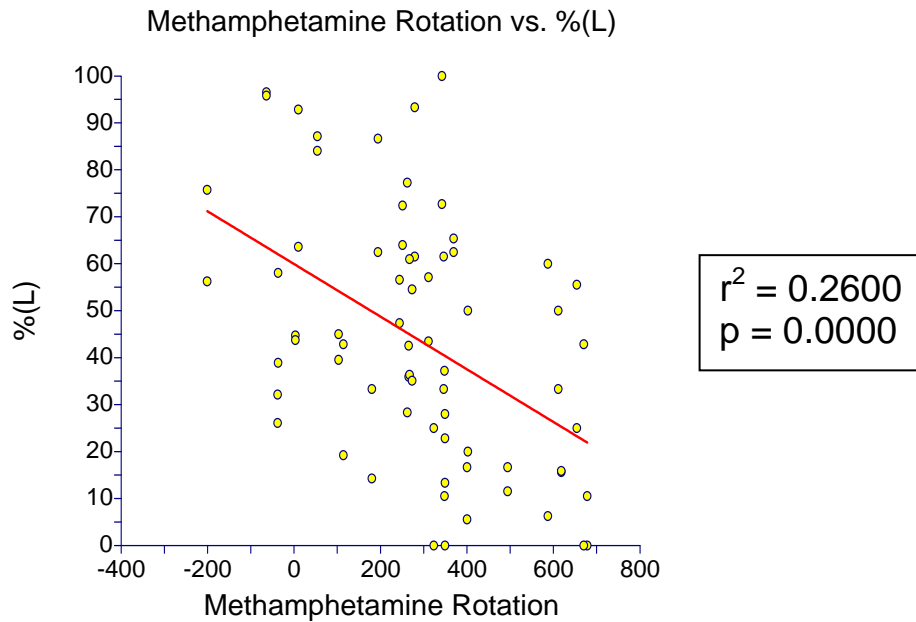
Figure 44. **Linear regression of d-methamphetamine rotation against the percentage of all simple sets that are comprised of an exclusive left touch [%(L)].**
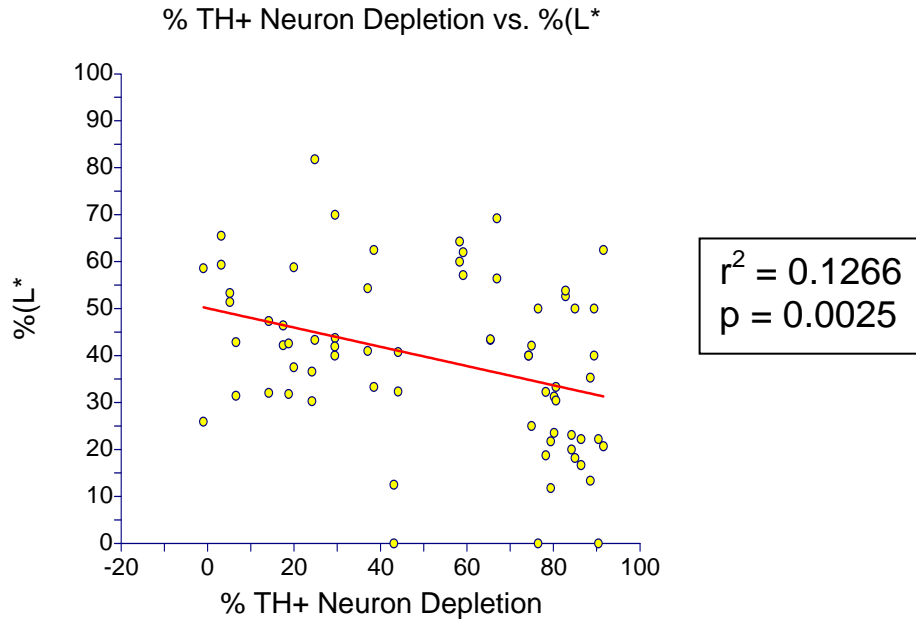
Figure 45. Linear regression of right hemisphere TH+ neuron depletion against the percentage of all complex sets that begin with an exclusive left touch [%(L*].
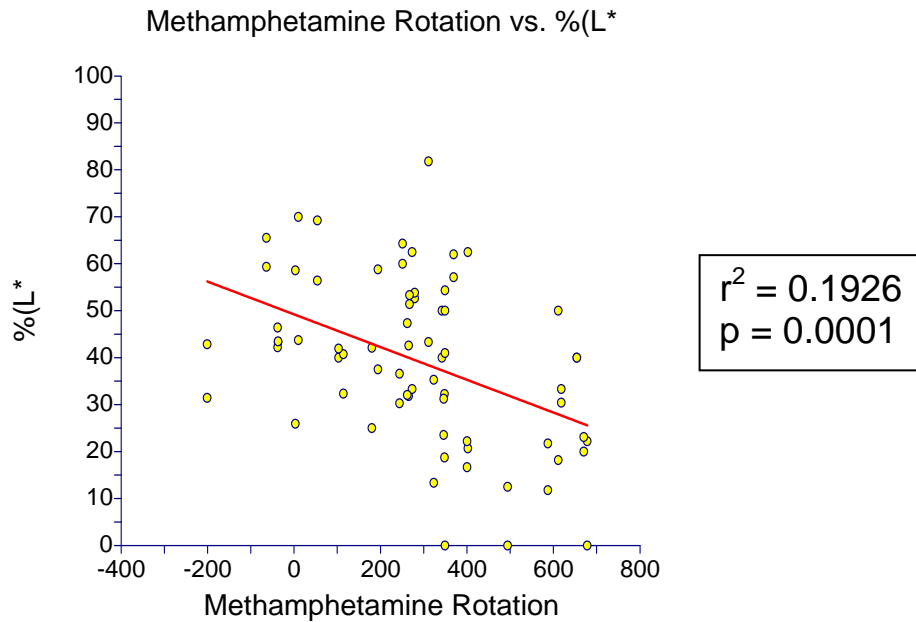
Figure 46. Linear regression of d-methamphetamine rotation against the percentage of all complex sets that begin with an exclusive left touch [%(L*].
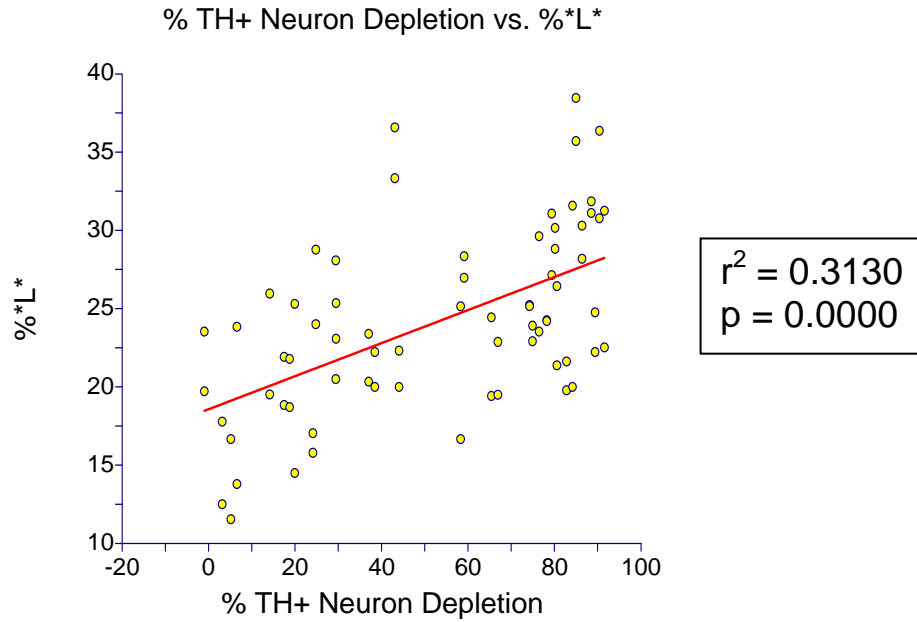
Figure 47. Linear regression of right hemisphere TH+ neuron depletion against percentage of middle-of-set cylinder wall contact periods comprised of exclusive left forepaw wall contact [%*L*].
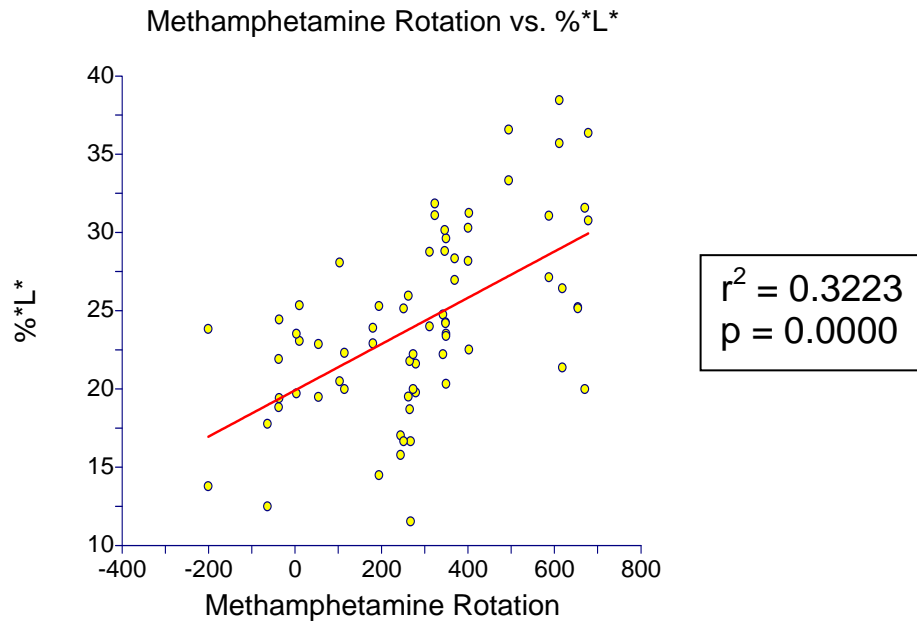
Figure 48. Linear regression of d-methamphetamine rotation against percentage of middle-of-set cylinder wall contact periods comprised of exclusive left forepaw wall contact [%*L*].
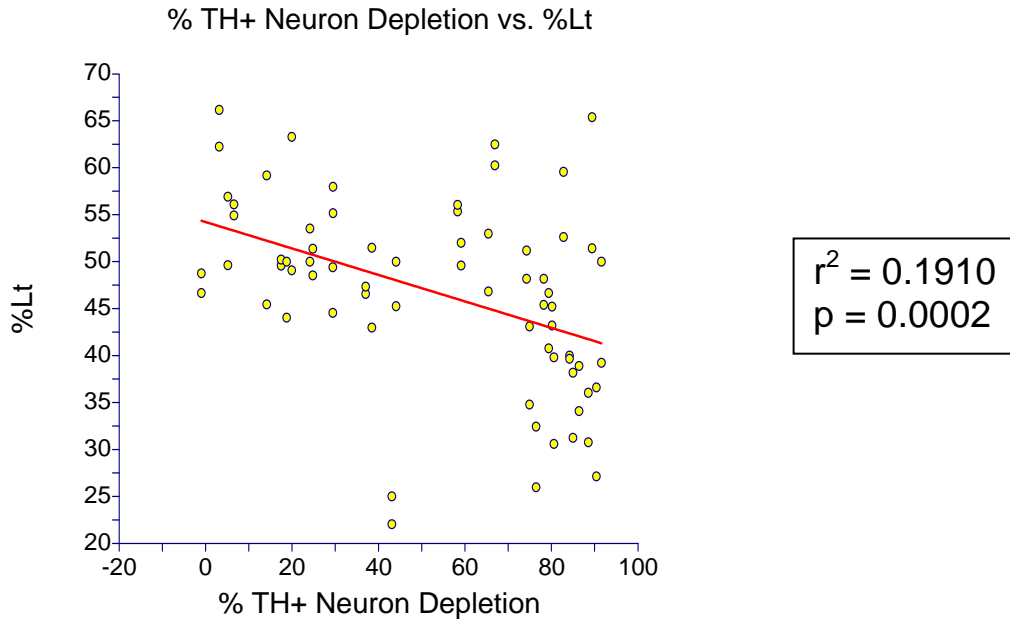
Figure 49. Linear regression of right hemisphere TH+ neuron depletion against percentage of all cylinder wall touches that are made with the left forepaw [%Lt].
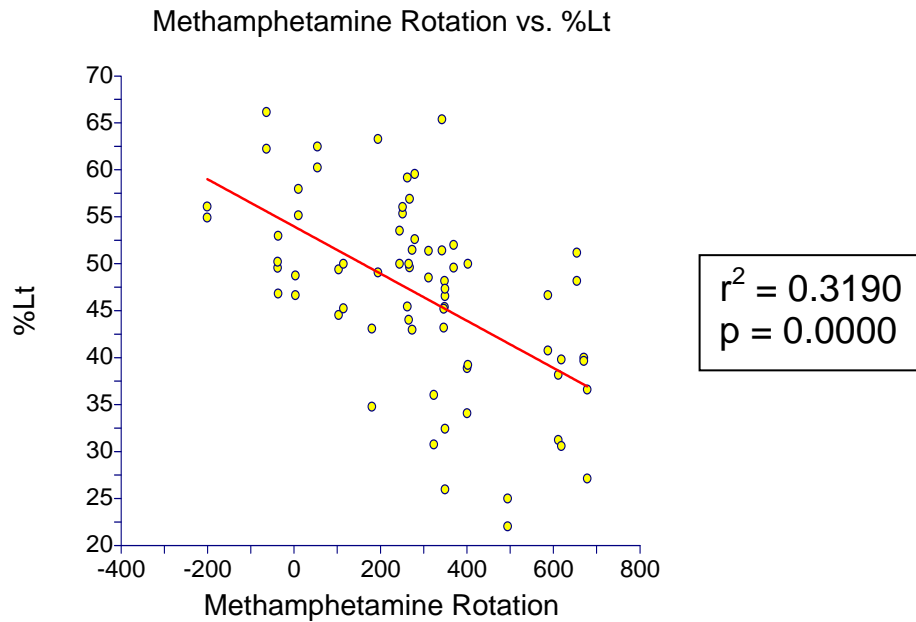
Figure 50. Linear regression of d-methamphetamine rotation against percentage of all cylinder wall touches that are made with the left forepaw [%Lt].

% TH+ Neuron Depletion vs. %^/L
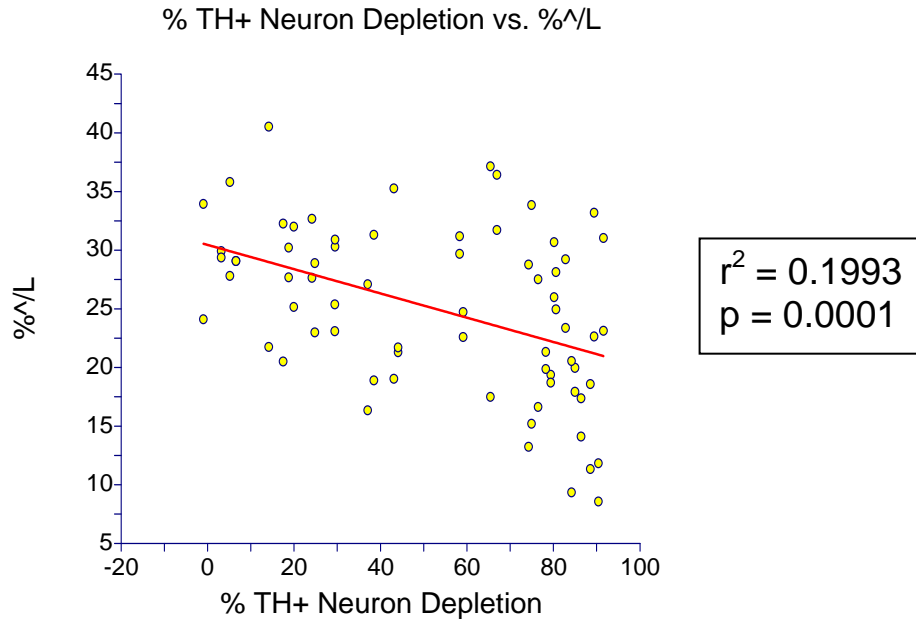
Figure 51. Linear regression of right hemisphere TH+ neuron depletion against asymmetry in average time of forepaw wall contact periods [%^/L].

Methamphetamine Rotation vs. %^/L
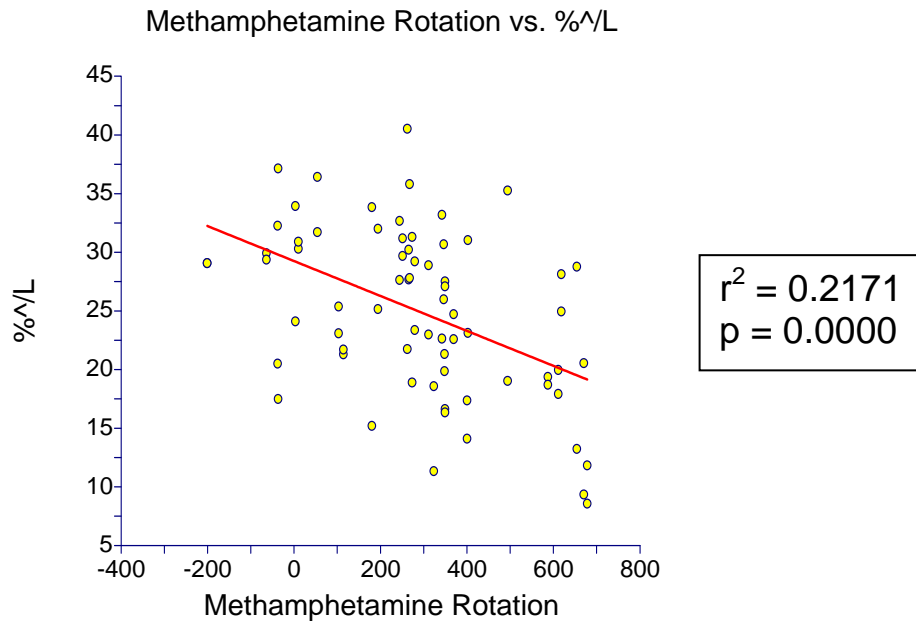
Figure 52. Linear regression of d-methamphetamine rotation against asymmetry in average time of forepaw wall contact periods [%^/L].
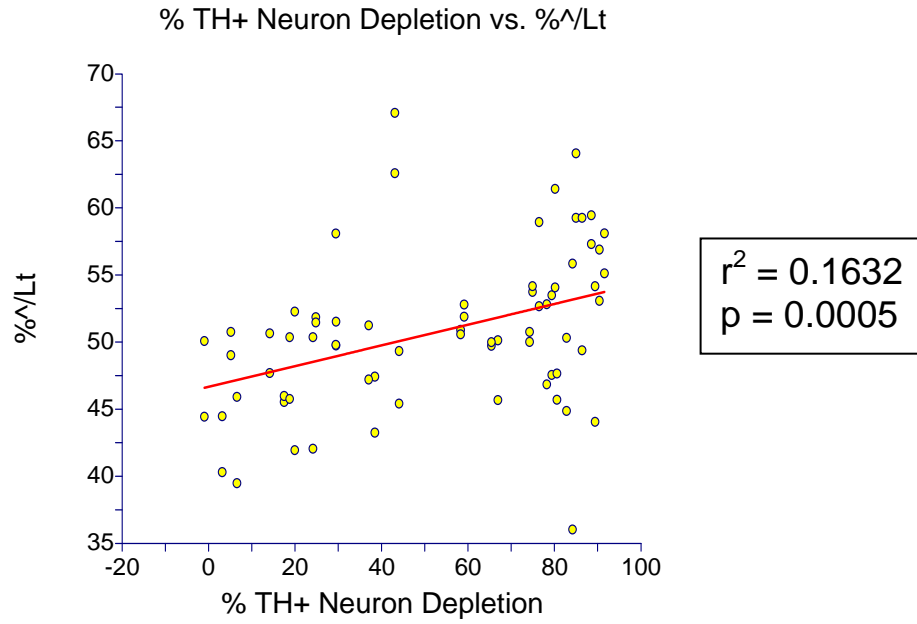
Figure 53. Linear regression of right hemisphere TH+ neuron depletion against asymmetry in average time of forepaw wall touches [%^/Lt].
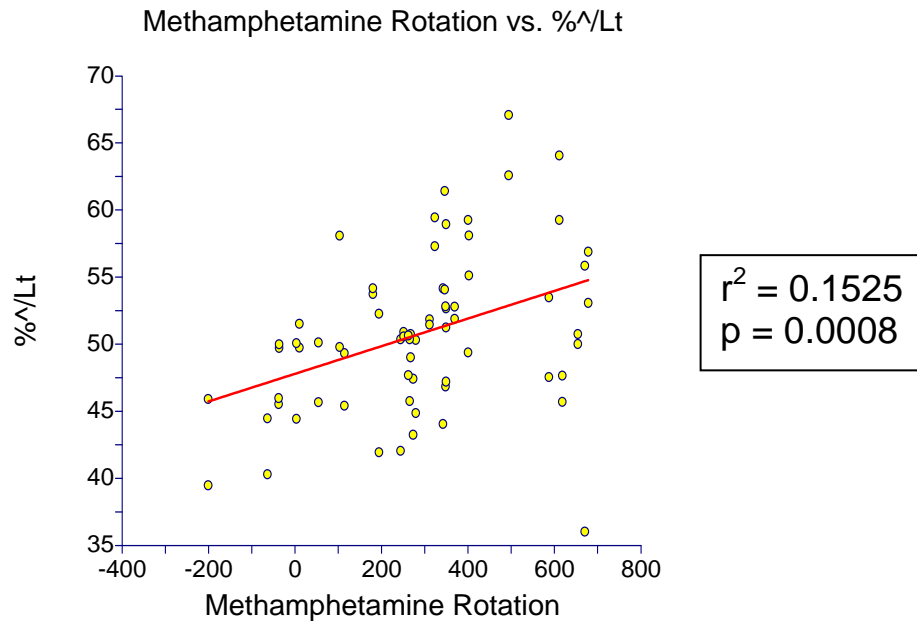
Figure 54. Linear regression of d-methamphetamine rotation against asymmetry in average time of forepaw wall touches [%^/Lt].

% TH+ Neuron Depletion vs. %^/*Lt

$r^2 = 0.1579$
$p = 0.0007$
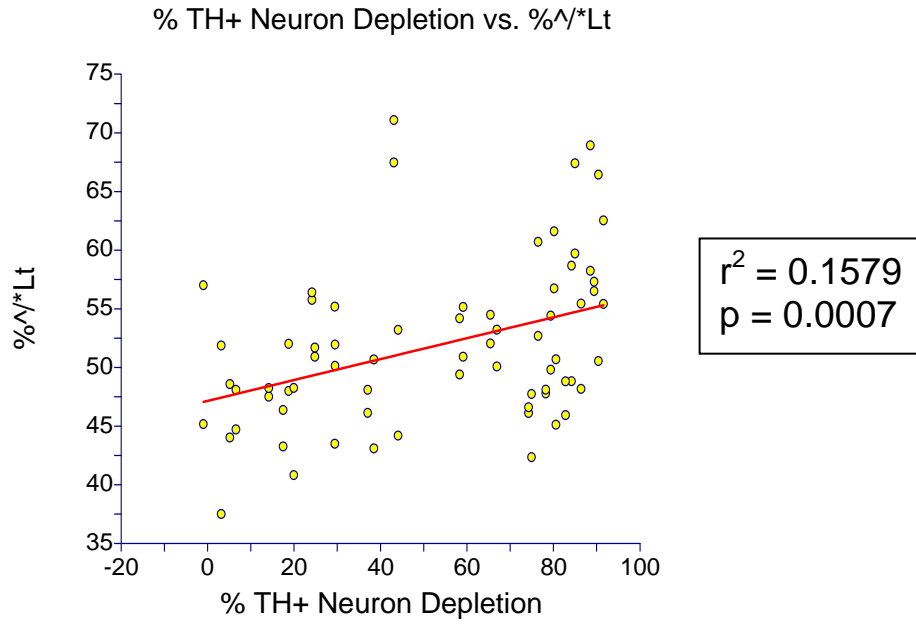
Figure 55. Linear regression of right hemisphere TH+ neuron depletion against asymmetry in average time of non-initial forepaw wall touches [%^/*Lt].

Methamphetamine Rotation vs. %^/*Lt

$r^2 = 0.1346$
$p = 0.0018$
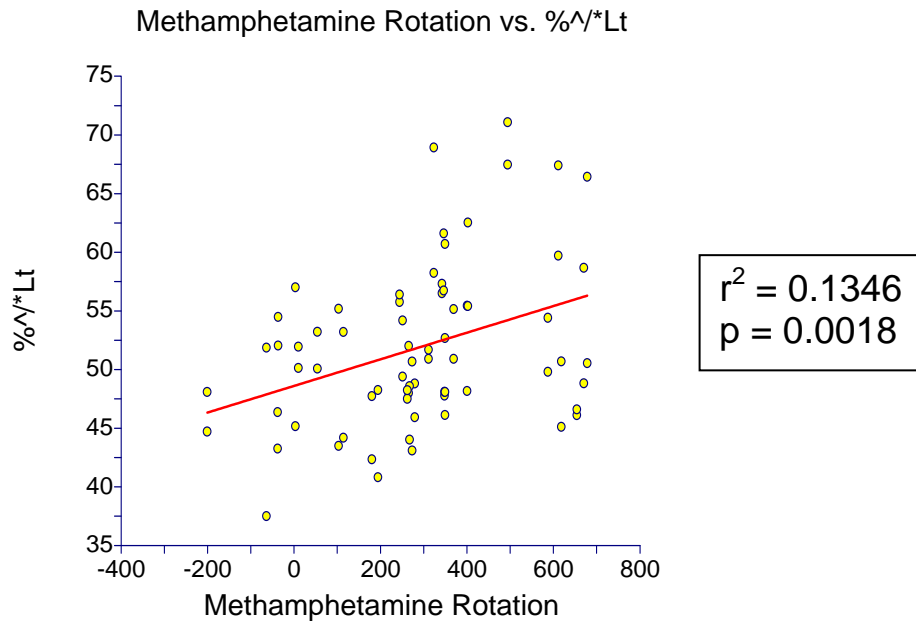
Figure 56. Linear regression of d-methamphetamine rotation against asymmetry in average time of non-initial forepaw wall touches [%^/*Lt].

Wall Contact Sequence Asymmetries

Severely right hemisphere DA-depleted rats tended to have a lower proportion of wall contact sequences involving left (contralateral-to-lesion) forepaw movement than more normal rats. In addition, when wall contact sequences involved contact with exclusively one forepaw, followed by placement with the other forepaw (while the first forepaw remained touching the cylinder wall), severely right hemisphere DA-depleted rats tended to be slower on average to place the left (contralateral-to-lesion) forepaw on the cylinder wall than the right (ipsilateral-to-lesion) forepaw. These observations are explained further in this section.

Linear regression was performed for both d-methamphetamine rotation and right hemisphere TH+ neuron depletion against count asymmetry [%], total time asymmetry [%^], and average time asymmetry [%^/] of many one- and two-movement wall contact sequences. Table 8 (page 69) shows only those sequence asymmetries that were significant among the many sequences analyzed, whereas Table 11 and Table 13 in Appendix A (page 96 and 98, respectively) list all sequences analyzed for asymmetries. Behavior codes given in this section [in square brackets] correspond to those given in Table 8. (For a detailed explanation of codes given [in square brackets] in this section, refer to the "Codes" key under Table 8). The p-values given for each measure apply to linear regressions of *both* d-methamphetamine rotation and TH+ neuron depletion (e.g. linear regression of d-methamphetamine rotation against [%^Rbl v Rbr] gave p= 0.0226, whereas linear regression of right hemisphere TH+ neuron depletion against the same

measure [%^Rbl v Rbr] gave p=0.0009; thus, [%^Rbl v Rbr] is reported as significant at p<0.05).

The "Count Asymmetry" column of Table 8 (page 69) contains a notable pattern: in all four measures, severely right hemisphere DA-depleted rats showed less initiation of movement by the left (contralateral-to-lesion) forepaw compared with the right (ipsilateral-to-lesion) forepaw. Most notable is the high occurrence of the Both-Left-Both wall contact pattern compared with Both-Right-Both [%BLB v BRB] (p<0.0001) in the behavior of the most severe hemiparkinson rats. The Both-Left verses Both-Right asymmetry [%BL v BR] (p<0.01; see graphs on page 70), as well as the Left-Both-Left verses Right-Both-Right asymmetry [%LBL v RBR] (p<0.01; see graphs on page 71) could be largely artifacts of the Both-Left-Both verses Both-Right-Both sequence asymmetry [%BLB v BRB] (p<0.0001; see graphs on page 72).

The "Total Time Asymmetry" column of Table 8 (page 69) is heavily influenced by "Count Asymmetry". The significance of the first nine rows in the "Total Time Asymmetry" column, [%^Bl v Br] (p<0.01), [%^lBl v rBr] (p<0.05), [%^RBL v RBR] (p<0.05), [%^Rbl v Rbr] (p<0.05), [%^rBl v rBr] (p<0.01), [%^BLB v BRB] (p<0.001), [%^Blb v Brb] (p<0.001), [%^bLb v bRb] (p<0.01), and [%^blB v brB] (p<0.01) can be explained in this way. The following three rows [%^BLR v BRL] (p<0.05), [%^Blr v Brl] (p<0.05), and [%^blR v brL] (p<0.05) are explainable by the fact that their "Count Asymmetry" counterpart, [%BLR v BRL], borders on significance. The last two rows of the "Total Time Asymmetry" column, [%^Lbl v Rbl] (p<0.01) and [%^Lbr v Rbl] (p<0.01), may be significant because they correspond to two highly significant measures

in the "Average Time Asymmetry" column, [%^/Lbl v Rbl] (p<0.0001) and [%^/Lb v Rb] (p<0.001).

Results shown in the "Average Time Asymmetry" column of Table 8 (page 69) are the most interesting. In every case, severely right hemisphere DA-depleted rats spent a higher percentage of time making wall contact sequences involving movement initiation with their left forepaw than wall contact sequences involving movement initiation with their right forepaw, compared to more normal rats. One of the most notable among these measures is the average time spent in a left forepaw wall contact that precedes a both forepaw wall contact, as opposed to the average time spent in a right forepaw wall contact that precedes a both forepaw wall contact [%^/Lb v Rb] (p<0.001; see graphs on page 73). Another measure that involves the same sequence is [%^/Lbl v Rbl] (p<0.0001; see graphs on page 74). Other measures that could illustrate the same phenomenon include the following: [%^/bL v bR] (p<0.05), [%^/LB v RB] (p<0.05), [%^/LBL v RBL] (p<0.01), [%^/Lbl v Rbr] (p<0.05), [%^/Rbl v RBL] (p<0.05), [%^/rbL v RBL] (p<0.01), [%^/lbR v rbL] (p<0.05), [%^/Lbr v Rbl] (p<0.01), [%^/blR v brL] (p<0.05), and [%^/bLb v bRb] (p<0.05).

Table 8. Linear regression results of both d-methamphetamine rotation and right hemisphere TH+ neuron depletion against wall contact sequence asymmetries.

Count Asymmetry			Total Time Asymmetry			Average Time Asymmetry		
Codes	Trends		Codes	Trends		Codes	Trends	
%BL v BR	**	/	%^Bl v Br	**	/	%^/bL v bR	*	\
%LBL v RBR	**	/	%^lBl v rBr	*	/	%^/LB v RB	*	\
%RBL v RBR	*	/	%^RBL v RBR	*	/	%^/Lb v Rb	***	\
%BLB v BRB	****	/	%^Rbl v Rbr	*	/	%^/LBL v RBL	**	\
			%^rBl v rBr	**	/	%^/Lbl v Rbl	****	\
			%^BLB v BRB	***	/	%^/Lbl v Rbr	*	\
			%^Blb v Brb	***	/	%^/Lbl v LBL	*	\
			%^bLb v bRb	**	/	%^/Lbr v LBR	*	\
			%^blB v brB	**	/	%^/Rbl v RBL	*	/
			%^BLR v BRL	*	/	%^/rbL v RBL	**	\
			%^Blr v Brl	*	/	%^/lbR v rbL	*	/
			%^blR v brL	*	/	%^/Lbr v Rbl	**	\
			%^Lbl v Rbl	**	\	%^/blR v brL	*	/
			%^Lbr v Rbl	**	\	%^/bLb v bRb	*	\

<div style="display:flex">

"Codes" Key:

% = percent, calculated as the first code divided by the sum of both codes [e.g. %BL v BR = #BL/(#BL+#BR)].

^ = time spent contacting the cylinder wall (applies to UPPER CASE letters only; lower case letters are shown solely for context).

^/ = average time spent contacting the cylinder wall (applies to UPPER CASE letters only; lower case letters are shown solely for context).

L = Left (contralateral-to-lesion) forepaw contacting the cylinder wall exclusively.

B = Both forepaws contacting the cylinder wall simultaneously.

R = Right (ipsilateral-to-lesion) forepaw contacting the cylinder wall exclusively.

v = "verses" [e.g. "%BL v BR" could be read "percent BL verses BR"].

"Trends" Key:

Linear regression against **both** d-methamphetamine rotation and right hemisphere TH+ neuron depletion showed these results:

* = p < 0.05 for both regressions.
** = p < 0.01 for both regressions.
*** = p < 0.001 for both regressions.
**** = p < 0.0001 for both regressions.

\ = negatively-sloped linear regression lines (i.e. severely right hemisphere DA-depleted rats tended to have <u>lower</u> numbers, as in the graphs on page 73).

/ = positively-sloped linear regression lines (i.e. severely right hemisphere DA-depleted rats tended to have <u>higher</u> numbers, as in the graphs on page 70).

</div>

% TH+ Neuron Depletion vs. %BL v BR

$r^2 = 0.1004$
$p = 0.0075$
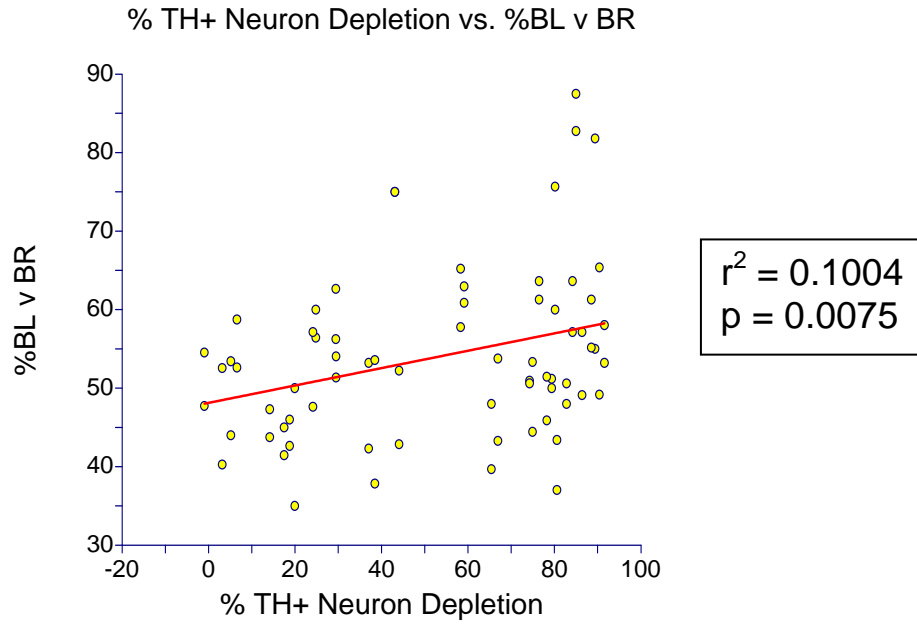
Figure 57. Linear regression of right hemisphere TH+ neuron depletion against percentage occurrence of a "Both-Left" sequence, as opposed to a "Both-Right" sequence [%BL v BR].

Methamphetamine Rotation vs. %BL v BR

$r^2 = 0.1087$
$p = 0.0053$
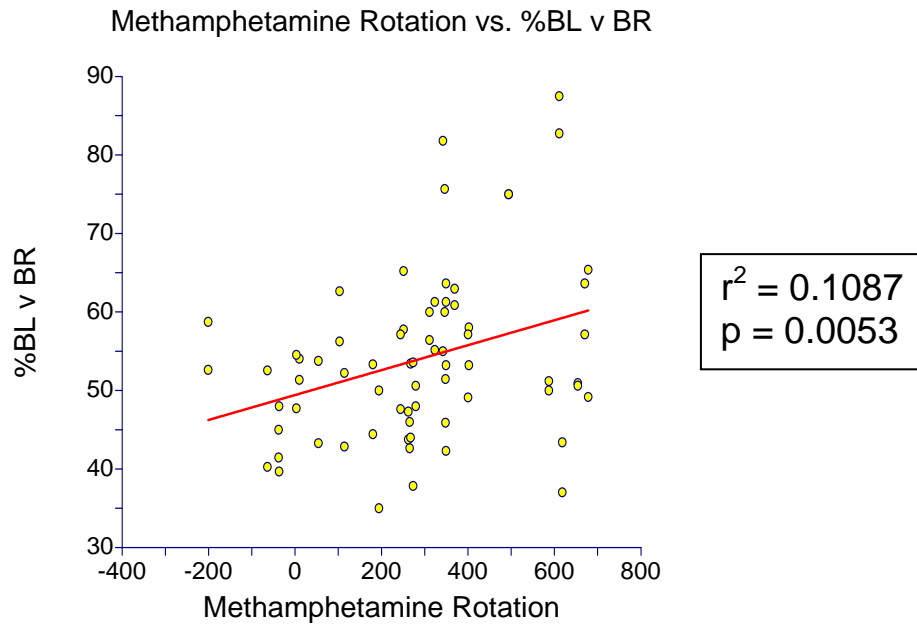
Figure 58. Lnear regression of d-methamphetamine rotation against percentage occurrence of a "Both-Left" sequence, as opposed to a "Both-Right" sequence [%BL v BR].

Figure 59. Linear regression of right hemisphere TH+ neuron depletion against percentage occurrence of a "Left-Both-Left" sequence, as opposed to a "Right-Both-Right" sequence [%LBL v RBR].

Figure 60. Linear regression of d-methamphetamine rotation against percentage occurrence of a "Left-Both-Left" sequence, as opposed to a "Right-Both-Right" sequence [%LBL v RBR].
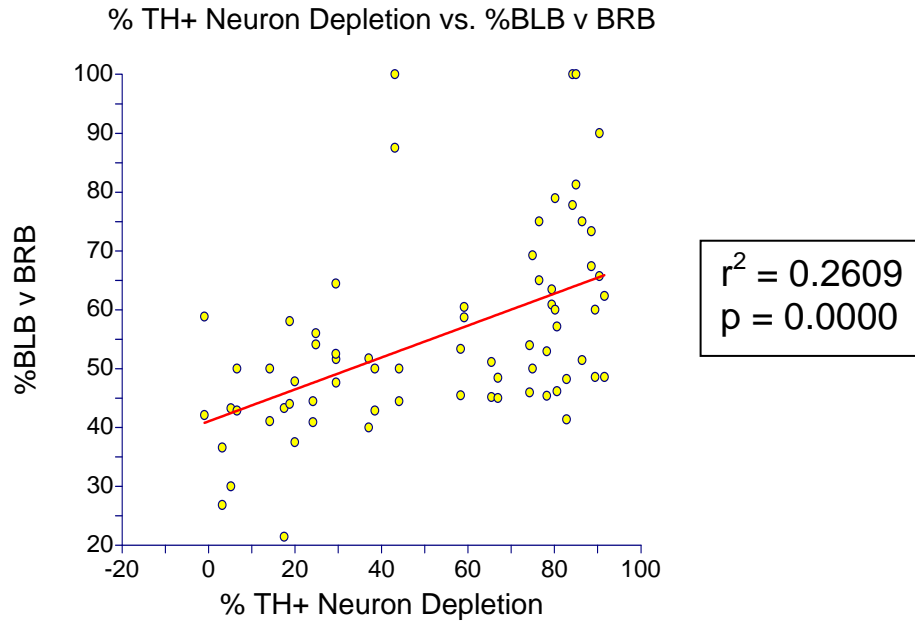
Figure 61. Linear regression of right hemisphere TH+ neuron depletion against percentage occurrence of a "Both-Left-Both" sequence, as opposed to a "Both-Right-Both" sequence [%BLB v BRB].

Figure 62. Linear regression of d-methamphetamine rotation against percentage occurrence of a "Both-Left-Both" sequence, as opposed to a "Both-Right-Both" sequence [%BLB v BRB].

% TH+ Neuron Depletion vs. %^/Lb v Rb

$r^2 = 0.1726$
$p = 0.0003$
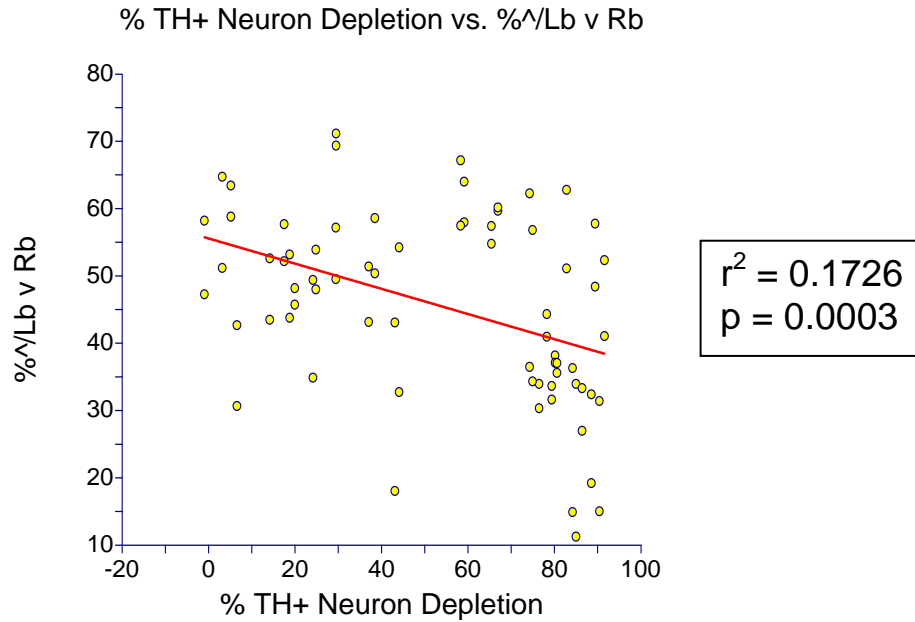
Figure 63. Linear regression of right hemisphere TH+ neuron depletion against asymmetry in average time spent contacting the cylinder wall with the <u>left</u> forepaw during a <u>Left</u>-Both sequence as opposed to time spent with the <u>right</u> forepaw during a <u>Right</u>-Both sequence [%^/Lb v Rb].

Methamphetamine Rotation vs. %^/Lb v Rb

$r^2 = 0.2726$
$p = 0.0000$
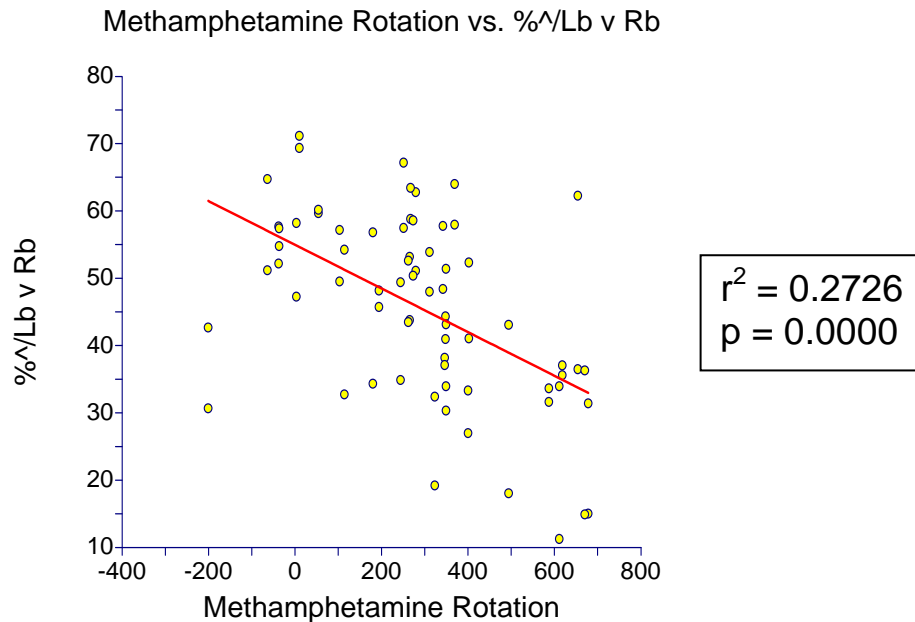
Figure 64. Linear regression of d-methamphetamine rotation against asymmetry in average time spent contacting the cylinder wall with the <u>left</u> forepaw during a <u>Left</u>-Both sequence as opposed to time spent with the <u>right</u> forepaw during a <u>Right</u>-Both sequence [%^/Lb v Rb].

% TH+ Neuron Depletion vs. %^/Lbl v Rbl

$r^2 = 0.1579$
$p = 0.0007$
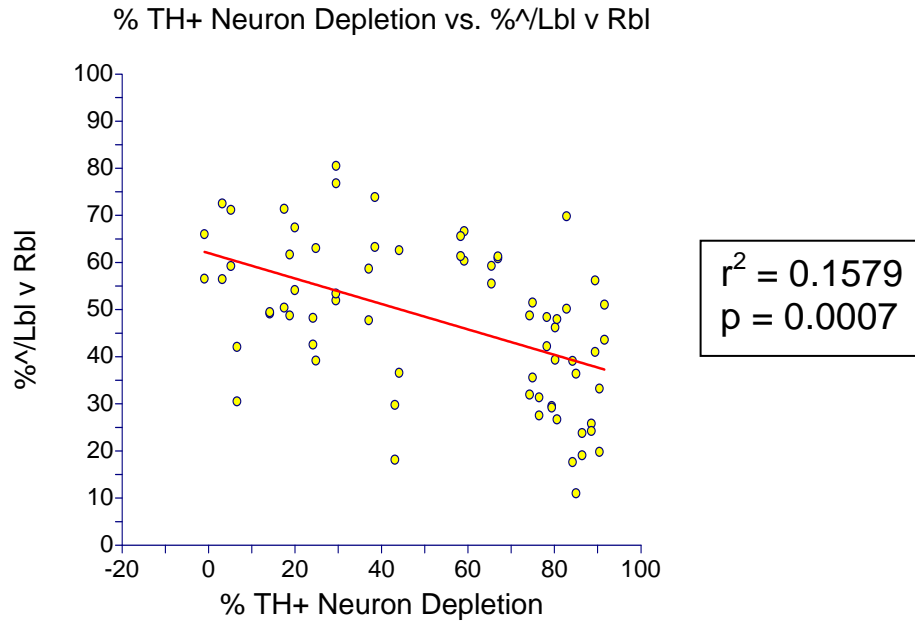
Figure 65. **Linear regression of right hemisphere TH+ neuron depletion against asymmetry in average time spent contacting exclusively with the <u>left</u> forepaw during the first portion of a <u>Left</u>-Both-Left sequence as opposed to time spent exclusively with the <u>right</u> forepaw during a <u>Right</u>-Both-Left sequence [%^/Lbl v Rbl].**

Methamphetamine Rotation vs. %^/Lbl v Rbl

$r^2 = 0.1346$
$p = 0.0018$
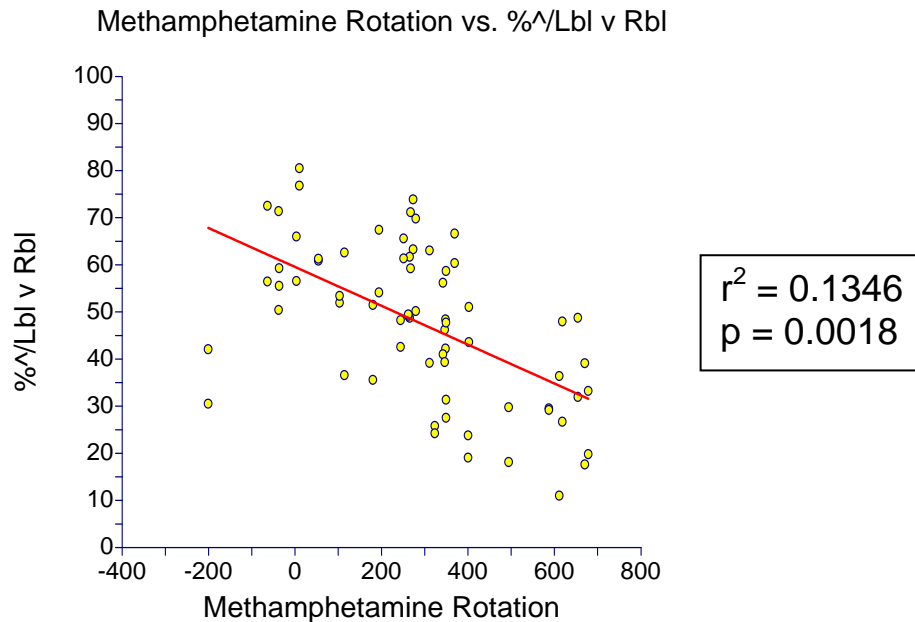
Figure 66. **Linear regression of d-methamphetamine rotation against asymmetry in average time spent contacting exclusively with the <u>left</u> forepaw during the first portion of a <u>Left</u>-Both-Left sequence as opposed to time spent exclusively with the <u>right</u> forepaw during a <u>Right</u>-Both-Left sequence [%^/Lbl v Rbl].**

Previously-used Cylinder Test Asymmetries

Severely right hemisphere DA-depleted rats tended to favor use of the ipsilateral-to-lesion forepaw as assessed by standard cylinder test asymmetry scoring methods (Schallert et al., 2000; Schallert & Woodlee, 2005), as assessed by lead-out paw during wall-stepping, and as assessed by forepaw used for weight shifting movements (Schallert & Woodlee, 2005). These observations are explained further in this section.

Right verses left forelimb use was measured as count [#] and count asymmetry [%] of various measures mentioned in cylinder test literature, plus a few related measures. These results are shown in Table 9 on page 77. (Behavior codes given in this section [in square brackets] correspond to those given in Table 9. For a detailed explanation of these codes, refer to the "Codes" key under Table 9). The p-values given for each measure apply to linear regressions of *both* d-methamphetamine rotation and TH+ neuron depletion (e.g. linear regression of d-methamphetamine rotation against the standard asymmetry score gave p= 0.0000, whereas linear regression of right hemisphere TH+ neuron depletion against this measure gave p=0.0022; thus, standard asymmetry score is reported as significant at p<0.01).

Key components of the standard asymmetry score (Schallert & Woodlee, 2005) are gray-shaded in the "Count" column of Table 9 (page 77). Use of the left and right forepaws to begin a set ([#(L) and [#(R), respectively) are the most influential among them. Use of both forepaws simultaneously to begin a set [#(B) is combined with "wall-stepping" [#WS] to give a score for "both" forepaw use in the formula given by Schallert and Woodlee (2005). "Wall-stepping" [#WS] is comprised of four sub-measures (right-

75

justified cells in Table 9): left touch-right touch stepping at the beginning [#(LtRt] and in the middle [#*LtRt] of complex sets; and right touch-left touch stepping at the beginning [#(RtLt] and in the middle [#*RtLt] of complex sets. These sub-measures in this analysis are mutually exclusive: any left or right forepaw touch was counted only once as part of a wall-stepping movement. In the "Count" column, three measures containing a left (contralateral-to-lesion) forepaw touch at the beginning of a set were significant: number of left forepaw touches at the beginning of any set [#(L] ($p<0.001$), number of left touch-right touch sequences at the beginning of complex sets [#(LtRt] ($p<0.001$), and number of repeated left simple sets [#(L)(L)] ($p<0.001$).

In the "Count Asymmetry" column of Table 9 (page 77), all asymmetry measures were significant: severely DA-depleted rats tended to be more asymmetric than less DA-depleted rats as measured by the standard asymmetry score ($p<0.01$; see graphs on page 78), which is calculated according to the following formula: $\{[\#(R] + \frac{1}{2}([\#(B] + [\#WS])\}$ divided by $\{[(R] + [(L] + [(B] + [WS]\} \times 100$ (Schallert & Woodlee, 2005); severely DA-depleted rats tended to step first with the right (ipsilateral-to-lesion) forepaw more often than the left (contralateral-to-lesion) forepaw during wall-stepping, both at the beginning of complex sets [%(LtRt] ($p<0.01$; see graphs on page 79) and in the middle of complex sets [%*LtRt] ($p<0.001$; see graphs on page 80), than less DA-depleted rats; severely DA-depleted rats tended to have a lower ratio of repeated left (contralateral-to-lesion) forepaw touch simple sets to repeated right (ipsilateral-to-lesion) forepaw touch simple sets [%(L)(L)] ($p<0.01$; see graphs on page 81) than less DA-depleted rats. The [%(L)(L)] asymmetry is referred to as "weight shifting movements" by Schallert and Woodlee (2005).

Table 9. Linear regression results of both d-methamphetamine rotation and right hemisphere TH+ neuron depletion against previously-used cylinder test asymmetry measures and a few related measures.

Count			Count Asymmetry		
Codes	Trends		Codes	Trends	
#(L	***	\	Standard Asymmetry Score	**	/
#(R					
#(B					
#WS					
#(LtRt	***	\	%(LtRt	**	\
#(RtLt					
#*LtRt			%*LtRt	***	\
#*RtLt					
#(L)(L)	***	\	%(L)(L)	**	\
#(R)(R)					

"Codes" Key:

= number of occurrences.
% = percent of appropriate total [e.g. %Lw = #Lw/(#Lw+#Rw)].
L = Left (contralateral-to-lesion) forepaw contacting the cylinder wall exclusively.
B = Both forepaws contacting the cylinder wall simultaneously.
R = Right (ipsilateral-to-lesion) forepaw contacting the cylinder wall exclusively.
WS = Wall-stepping: alternating touches with the right and left forepaw, or vice versa.
t = touch [e.g. "Lt" means a left forepaw touch on the cylinder wall].
(= beginning of a set [e.g. "(L" means any simple or complex set beginning with a left forepaw touch].
) = ending of a set [e.g. "L)" means the left forepaw is the last touching the cylinder wall in a set].
Shaded cells contain key components of conventional cylinder test measures.
* = a "wildcard"; signifies one or more distinct forepaw contacts during a set [e.g. "*Lt" means a left forepaw touch preceded by any number of contiguous left or right touches: "RtLt", "(LtRtLtRtLt", etc.].

"Trends" Key:

Linear regression against **both** d-methamphetamine rotation and right hemisphere TH+ neuron depletion showed these results:

** = p < 0.01 for both regressions.
*** = p < 0.001 for both regressions.
☐ (blank cells) = p > 0.05 for one or both regressions.
\ = negatively-sloped linear regression lines (i.e. severely right hemisphere DA-depleted rats tended to have lower numbers, as in the graphs on page 78).
/ = positively-sloped linear regression lines (i.e. severely right hemisphere DA-depleted rats tended to have higher numbers, as in the graphs on page 79).
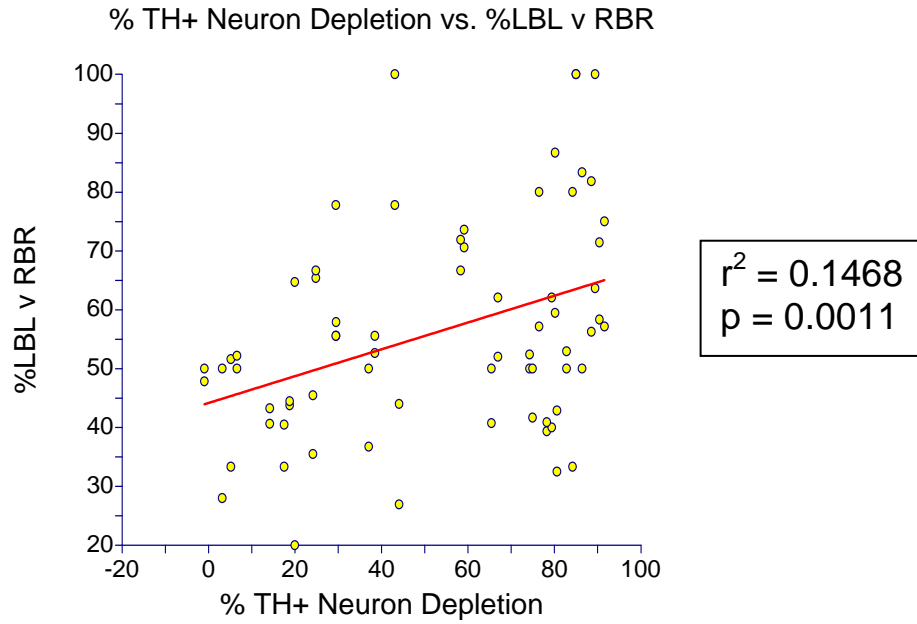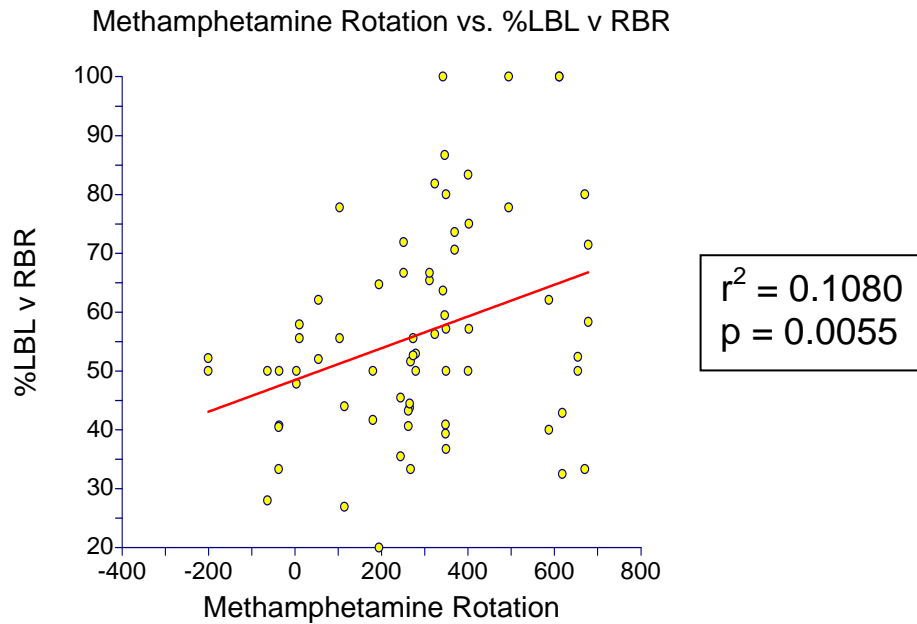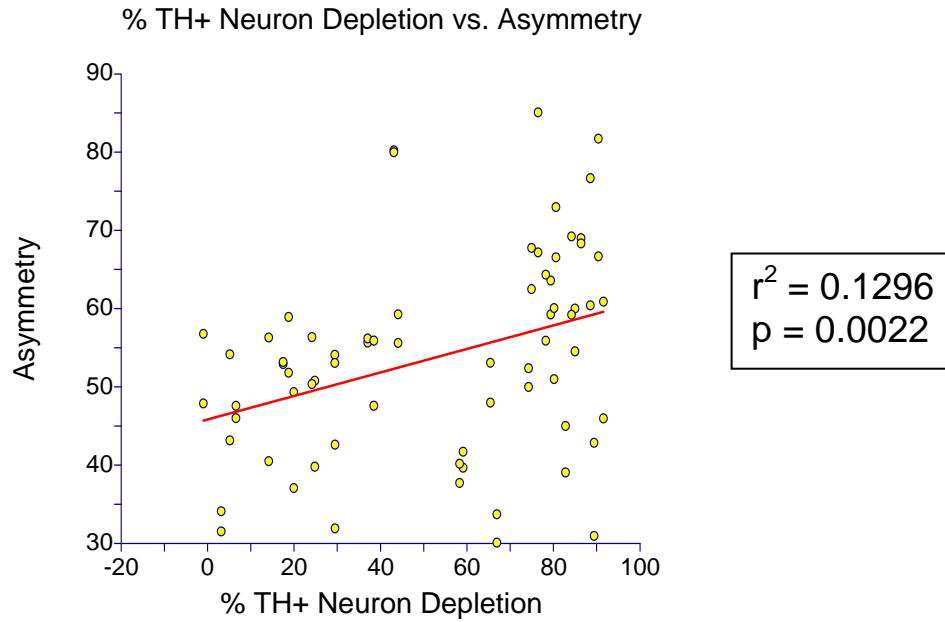
Figure 67. Linear regression of right hemisphere TH+ neuron depletion against the standard cylinder test asymmetry score (Schallert & Woodlee, 2005).
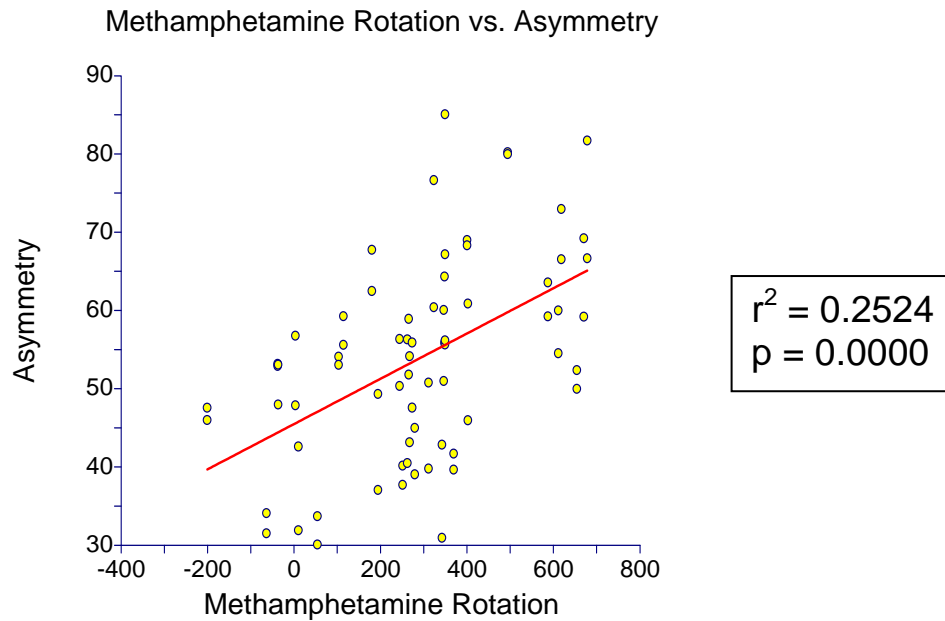
Figure 68. Linear regression of d-methamphetamine rotation against the standard cylinder test asymmetry score (Schallert & Woodlee, 2005).
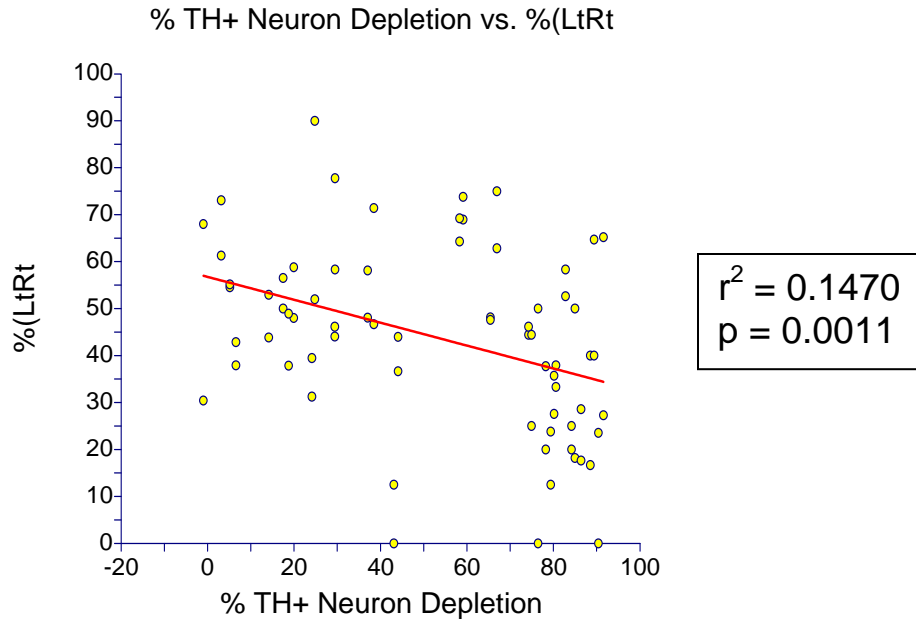
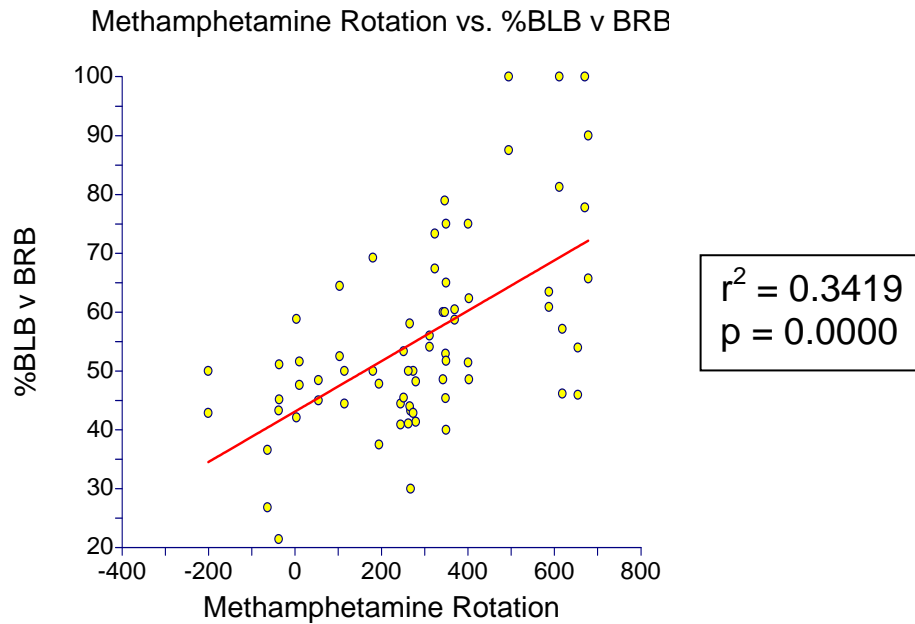**Figure 69. Linear regression of right hemisphere TH+ neuron depletion against percentage occurrence of a "Left touch-Right touch" sequence [%(LtRt], as opposed to a "Right touch-Left touch" sequence, at the beginning of complex sets.**
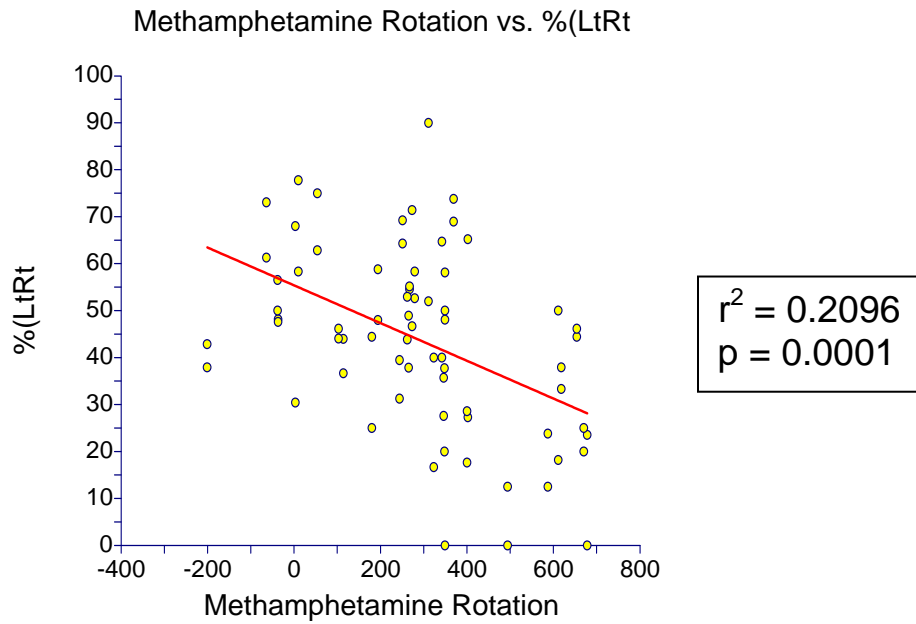
Figure 70. Linear regression of d-methamphetamine rotation against percentage occurrence of a "Left touch-Right touch" sequence [%(LtRt], as opposed to a "Right touch-Left touch" sequence, at the beginning of complex sets.
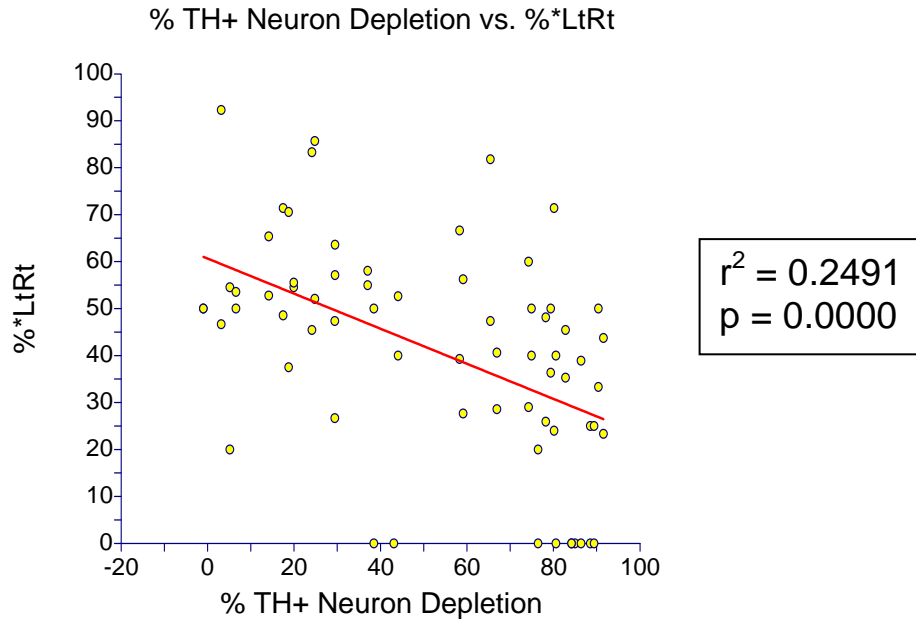
Figure 71. Linear regression of right hemisphere TH+ neuron depletion against percentage occurrence of a "Left touch-Right touch" sequence [%*LtRt], as opposed to a "Right touch-Left touch" sequence, in the middle of complex sets.
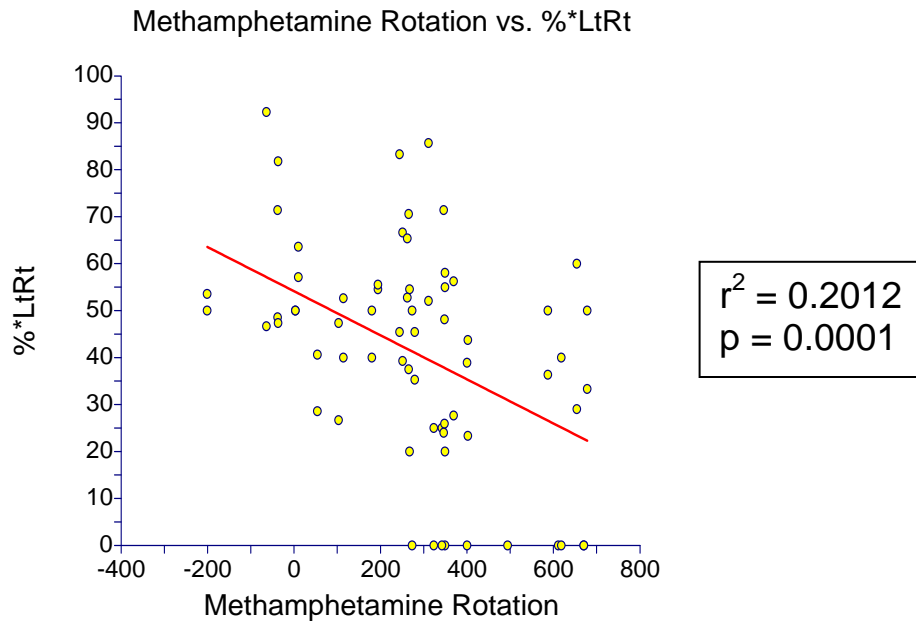
Figure 72. Linear regression of d-methamphetamine rotation against percentage occurrence of a "Left touch-Right touch" sequence [%*LtRt], as opposed to a "Right touch-Left touch" sequence, in the middle of complex sets.

% TH+ Neuron Depletion vs. %(L)(L)

$r^2 = 0.1122$
$p = 0.0046$
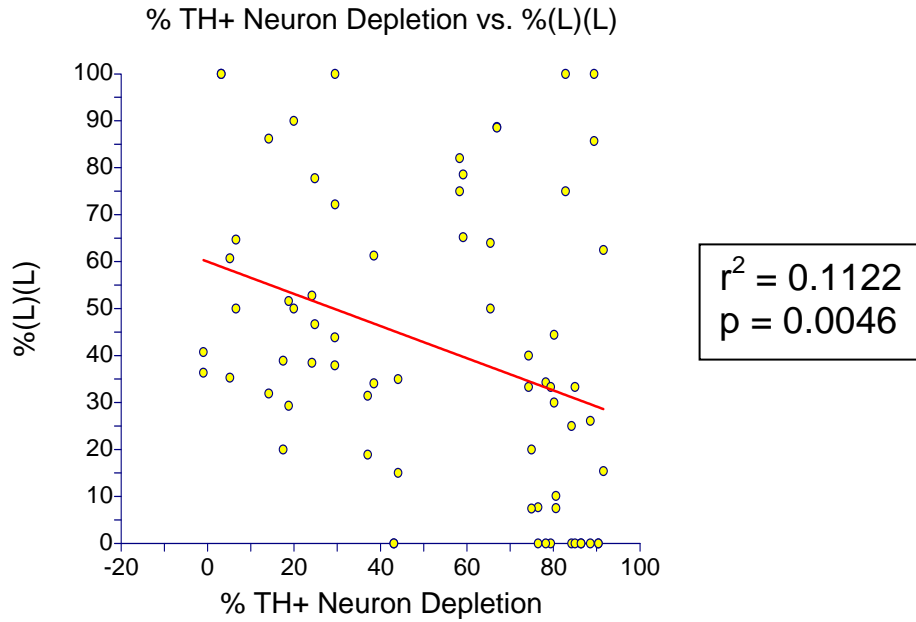
Figure 73. Linear regression of right hemisphere TH+ neuron depletion against percentage of repeated occurrence of left-touch simple sets [%(L)(L)], as opposed to right-touch simple sets. Referred to as "weight shifting movements" by Schallert and Woodlee (2005).

Methamphetamine Rotation vs. %(L)(L)

$r^2 = 0.2496$
$p = 0.0000$
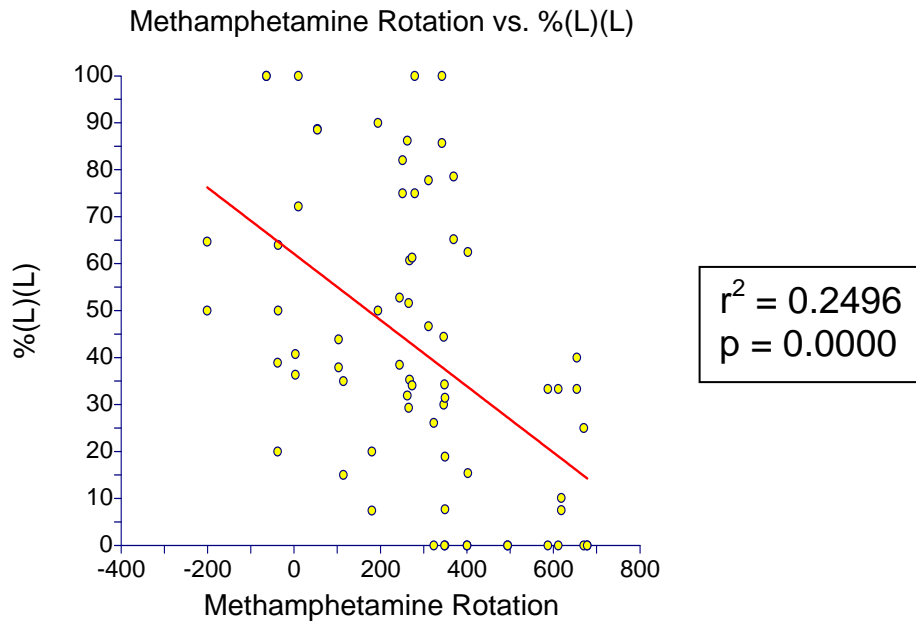
Figure 74. Linear regression of d-methamphetamine rotation against percentage of repeated occurrence of left-touch simple sets [%(L)(L)], as opposed to right-touch simple sets. Referred to as "weight shifting movements" by Schallert and Woodlee (2005).

DISCUSSION

Previous Use of the Cylinder Test

The cylinder test has been used to assess forelimb use in several animal models of disease, including Huntington's Disease (McBride et al., 2004), Parkinson's Disease (Lundblad et al., 2002; Shi et al., 2004), spinal cord injury (Jin, Fischer, Tessler, & Houle, 2002) and various stroke models (Karhunen et al., 2003; Schallert (2006); Windle et al., 2006).

The measures most commonly used to assess forelimb use asymmetry in the cylinder test are described by Schallert et al. (2000) and by Schallert and Woodlee (2005). These include the first forepaw to contact the cylinder wall during a rear and the first forepaw to contact the wall after both forepaws are removed from the wall during a rear. "Wall-stepping", defined as "rapidly alternating steps along the cylinder wall" is also used.

Other measures have been used to supplement the most commonly-used cylinder measures. For example, asymmetry in forelimb use for landing after a rear has been used (Schallert et al., 2000), as well as asymmetry in forelimb use for weight-shifting movements during exploration (Schallert & Woodlee, 2005). Forelimb contact time with the cylinder wall has also been measured (Baskin, Dietrich, & Green, 2003). Measures appropriate for specific disease models have been introduced, such as forelimb-sliding after focal ischemic infarcts (Shanina, Schallert, Witte, & Redecker, 2006).

82

No cylinder test measures that are specific to hemiparkinson rats have yet been proposed. Severely DA-depleted hemiparkinson rats have been shown to prefer use of their ipsilateral-to-lesion forepaw when first supporting their weight against the cylinder wall during a rear and upon landing after a rear (Schallert et al., 2000); however, other patterns and timing of forepaw contact with the cylinder wall have not been studied in hemiparkinson rat models.

Purpose and Limitations of this Thesis

This thesis explores possibilities for hemiparkinson-specific measures that may improve sensitivity of the cylinder test to detect unilateral DA depletion. It does not investigate *all* possibilities, nor assess all measures previously used for hemiparkinson rats, such as forepaw use asymmetry in landing after rears. It addresses the question, "how do rats of various nigrostriatal lesion sizes differ from each other and from normal rats in forepaw placement behavior on the cylinder wall?"

The results reported herein are given for the purpose of hypothesis generation rather than hypothesis testing, for several reasons. First, only female Long-Evans rats were used in this experiment, and their behavior may be different from male rats'. Also, because the neurotoxin MPP+ was used to achieve unilateral nigrostriatal lesions, further testing is required to determine whether rats that have been given other lesions to dopaminergic pathways (using 6-OHDA, for example) behave in a similar way to MPP+ lesioned rats in the cylinder test. Hypothesis testing would presumably require larger

sample sizes and would be aided by a cylinder system that could collect extensive forelimb placement data quickly and efficiently, as described below.

For the cylinder test to be most useful in assessing functional recovery in unilateral dopamine depletion rat models, a complete comparison of hemiparkinson rat behavior (male *and* female) with behavior of normal rats should be made. Any behavior of hemiparkinson rats that proves different from normal rat behavior in the cylinder test could be useful as an outcome measure for hemiparkinson rats.

I started this project with the idea to find some pattern of difference between the cylinder behavior of rats with a large DA lesion size compared to a small DA lesion size. By measuring DA depletion using histological stains and comparing these results with behavioral outcomes, I hoped to determine how well the cylinder test can detect unilateral DA depletion. When I infused MPP+ into the right hemisphere nigrostriatal bundle of a group of female rats, I observed a high variation in functional deficits between animals. Whereas for hypothesis-testing purposes this variation might be less desirable, I found that it was useful in assessing differences in cylinder behavior among these rats.

I wondered if additional measures might be combined with conventional cylinder test measures to create a composite measure of unilateral DA depletion that would be more sensitive than any single measure.

For new behavioral measures in the cylinder test to be reliable, they must consistently correlate with known biochemical markers of DA depletion. Tyrosine hydroxylase (TH) immunostaining and amphetamine-induced rotation testing – performed long enough after nigrostriatal lesions to avoid contraversive rotation (Robinson et al., 1994) – are both commonly-used ways to assess degree of unilateral

dopamine depletion in hemiparkinson rats. By comparing both TH+ neuron counts and amphetamine rotation results with various patterns of forelimb use in hemiparkinson rats of varied lesion sizes, I hoped to be conservative and accurate in my conclusions regarding which cylinder test behavioral measures are most useful.

Documenting Cylinder Behavior

Videotaping each rat for five minutes in the cylinder test from a ventral perspective gives a good indication of forelimb use on the cylinder wall during spontaneous exploration (Gharbawie, Whishaw, & Whishaw, 2004). Comprehensive real-time scoring of rats' forelimb use is unrealistic in the cylinder test as currently designed, because rats often make several touches on the cylinder wall per second. Frame-by-frame video analysis, although rather time-consuming, allowed me to make a complete record of five minutes of wall touches for each rat, which proved useful in determining patterns of forelimb use that may be unique to hemiparkinson rats.

My strategy was to record a temporally accurate representation of rats' forepaw placements on the cylinder wall. With this documentation in place for each rat, the data were analyzed for patterns that might give insight into hemiparkinson rat forelimb use over a range of dopamine depletion.

The formulas I used in Microsoft Excel to count both frequency and duration of wall contact patterns came a few at a time. I began with more basic measures, such as first touch of complex sets compared to simple sets, and gradually expanded to other measures, including a multitude of wall contact sequences. (For a list of all wall contact

sequences analyzed, see Appendix A on page 95). I soon saw the need to create an unambiguous symbolic representation of wall contact behavior, and developed a system of behavioral codes [given in square brackets throughout this thesis].

As I laboriously recorded forelimb wall contacts using frame-by-frame video analysis, I often wondered what automated system might collect data more efficiently. The best idea I dreamed up was a cylinder wall covered with a pressure-sensitive pad. A pressure-sensitive pad could also be placed on the floor. Each pad would be able to detect a wide range of pressure – from a slight paw touch to a push-off or landing force – and would send data about pressure, time, and location of each touch to a computer for analysis. Whether pressure is measured with a pressure-sensitive pad or some other way, I predict that it will prove valuable in assessing hemiparkinson rat deficits and compensatory behaviors, similar to the work of Muir & Whishaw (1999) in analyzing ground reaction forces in locomoting hemiparkinson rats.

That much of a "super-cylinder" setup seems achievable. But to achieve the most efficient analysis, and avoid frame-by-frame video analysis entirely, this high-tech cylinder setup would also need to reliably detect the difference between right and left forepaw contact. I am still wondering how to accomplish this.

Is it possible to engineer an efficient high-tech cylinder system? I think so. I certainly advise any who might take up the cylinder test research torch to invest their time developing one rather than spending dozens of tedious hours analyzing cylinder videos frame-by-frame as I did for this thesis!

Would a more high-tech cylinder system be practical for research use? The answer to this question will depend on the needs and creativity of researchers. The

results of this thesis serve as evidence that the behavior of rats in the cylinder test is worth studying in more detail. From my current vantage-point, a high-tech cylinder setup is a much more practical and efficient tool than time-consuming frame-by-frame video methods.

Many questions that cannot be determined efficiently by frame-by-frame video analysis could be quickly answered by a pressure-sensitive cylinder, including pressure exerted by the ipsilateral-to-lesion verses contralateral-to-lesion forepaw on the cylinder wall during various contact patterns on the cylinder wall, spontaneous turning behavior during cylinder exploration, spatial patterns of exploring the wall (including ipsilateral or contralateral bias in lateral exploration), how behavior changes during multiple cylinder sessions, and how different stimuli in the environment (smells or sounds, for example) affect behavior during the test.

An important issue that would need investigation with this new cylinder setup, however, is whether rats explore a non-transparent cylinder in the same way as a transparent one. Rats are likely to be more active in the darker environment of a non-transparent cylinder, and this factor may improve the cylinder test, particularly for less-active rat breeds (Schallert & Woodlee, 2005).

What Are the Best Asymmetry Measures?

The results of this thesis offer an expanded view of hemiparkinson rat forelimb use asymmetry in the cylinder test by closely examining forepaw placement asymmetries and by examining contact time asymmetries. A "super-cylinder" setup could more

efficiently and accurately measure the asymmetries in forepaw placement and time proposed in this thesis, as well as placement location and pressure, which are not addressed in this thesis. Optimal analysis of forelimb use asymmetry in the cylinder test would likely combine the best measures from all four of these components.

Trial-to-trial variability appears to be a significant factor standing in the way of using current cylinder test measures (Schallert & Woodlee, 2005) to accurately estimate degree of dopamine depletion in female MPP+ hemiparkinson rats. Variability in female rats may be more than in male rats, because during the high-estrogen time of the female menstrual cycle, striatal dopamine release is enhanced (Becker, 1999).

The problem of trial-to-trial reliability may be mitigated by combining outcome measures of distinguishing behaviors that correlate closely with DA asymmetry and have large sample sizes from trial to trial.

The "first touch" component of the conventional asymmetry score [%(L], described as "the first forelimb to contact the wall with weight support" (Karhunen et al., 2003), is relatively reliable because it combines two good outcome measures: 1) asymmetry in exclusive touches with the contralateral-to-lesion forepaw only verses ipsilateral-to-lesion forepaw only [%(L)], and 2) asymmetry in first touch of a complex set [%(L*], each of which occurs very commonly during a cylinder session. I found both of these component measures to be highly correlated with TH+ neuron count and d-methamphetamine rotation; however, for any given cylinder session, the component measures may be more variable than the combined first-touch measure [%(L], because sample size is smaller. The combined sample size is large enough to minimize trial-to-trial variability.

From my analysis, the most reliable single measures with the largest sample size, in addition to those listed in the previous paragraph, may be the following: 1) percentage of total touches that are made with the contralateral-to-lesion forepaw [%Lt], 2) asymmetry in average time per touch [%^/Lt], and 3) asymmetry in average time of contralateral-to-lesion forepaw wall contact periods [%^/L]. Other useful measures (but perhaps less reliable due to smaller sample sizes) include [%*L*] and [%BRB v BLB].

Combining Asymmetry Measures

Combining multiple asymmetry measures from a single cylinder session into one composite score may be accomplished in several ways:

One way to combine measures is to sum multiple raw count measures together into ipsilateral, contralateral, and both forepaw use, then calculate a single asymmetry score. The standard cylinder measure given by Schallert and Woodlee (2005) uses this method (e.g. "both" forepaw use = [#(B] + [#LtRt] + [#RtLt]; see graphs on page 78). This method gives weight to each component measure according to sample size, and thus limits the influence of measures with high trial-to-trial variability due to small sample sizes.

Another way of combining measures is to average asymmetry percentages (e.g. Asymmetry = average of [%Lt] and [%^/Lt]; see graphs on page 91). This method gives equal weight to each measure included. To change this, each measure could be weighted according to sample size and power to detect asymmetries.

A third way of combining measures is to convert significant asymmetry percentages to standard z-scores, then take an average of these standard z-scores for each cylinder session (see graphs on page 92). Measures that have a "both" component can be given a single asymmetry score by using the following formula: [(ipsi + ½ both) divided by (ipsi + contra + both)] X 100. Then the regression slopes for all measures to be combined must be made to be all positive or all negative using the formula [100%-asymmetry scores] for measures that have the wrong slope. This method can effectively compare animals within a study; however, it does not facilitate comparison across studies. An average z-score of zero obtained by this method does not mean that a rat has zero asymmetry, but only that the rat's scores fell in the middle of those collected in the study.

For each of the methods described above, combining the results of multiple cylinder sessions may produce more accurate results; however, if recovery occurs during the time span of repeated testing, combining the scores of multiple testing sessions may not be appropriate.

Perhaps the best ways to combine measures from multiple cylinder sessions in group comparison experiments include repeated-measures multiple-variable analysis of variance (rMANOVA) and mixed-effects regression models (Gueorguieva & Krystal, 2004).
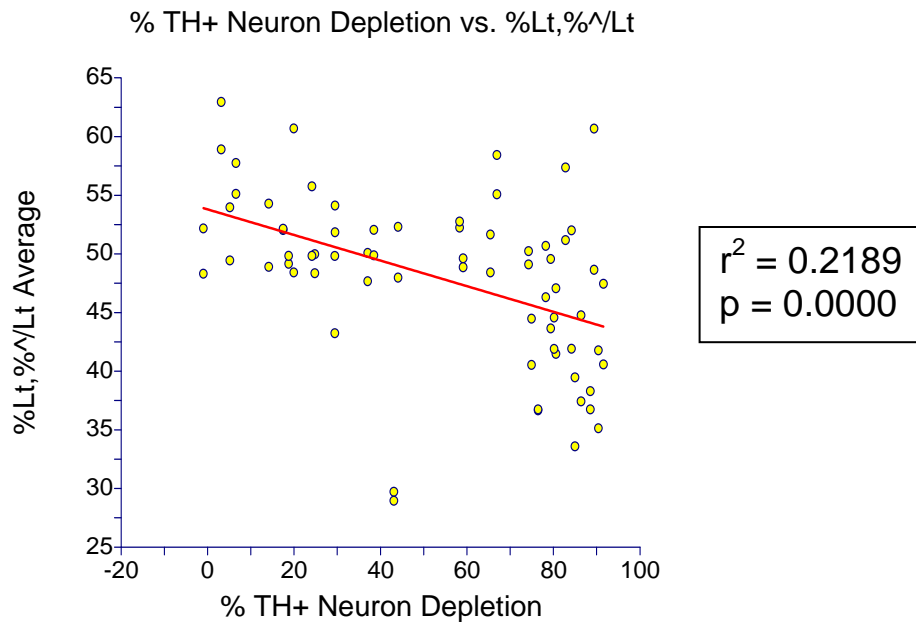
Figure 75. Linear regression of right hemisphere TH+ neuron depletion against the average of two measures: 1) asymmetry in cylinder wall touches [%Lt], and 2) asymmetry in average time of cylinder wall touches [%^/Lt].
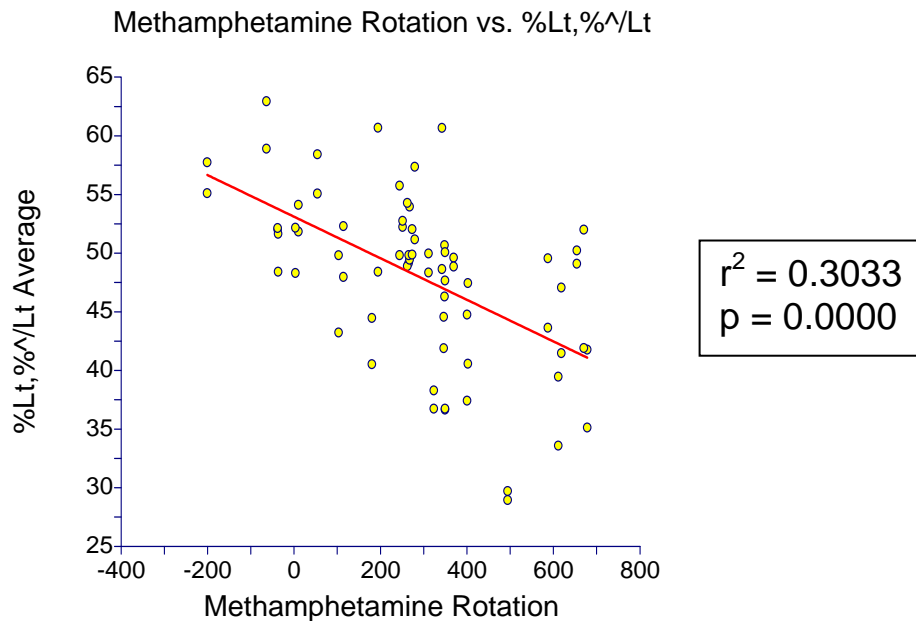
Figure 76. Linear regression of d-methamphetamine rotation against the average of two measures: 1) asymmetry in cylinder wall touches [%Lt], and 2) asymmetry in average time of cylinder wall touches [%^/Lt].
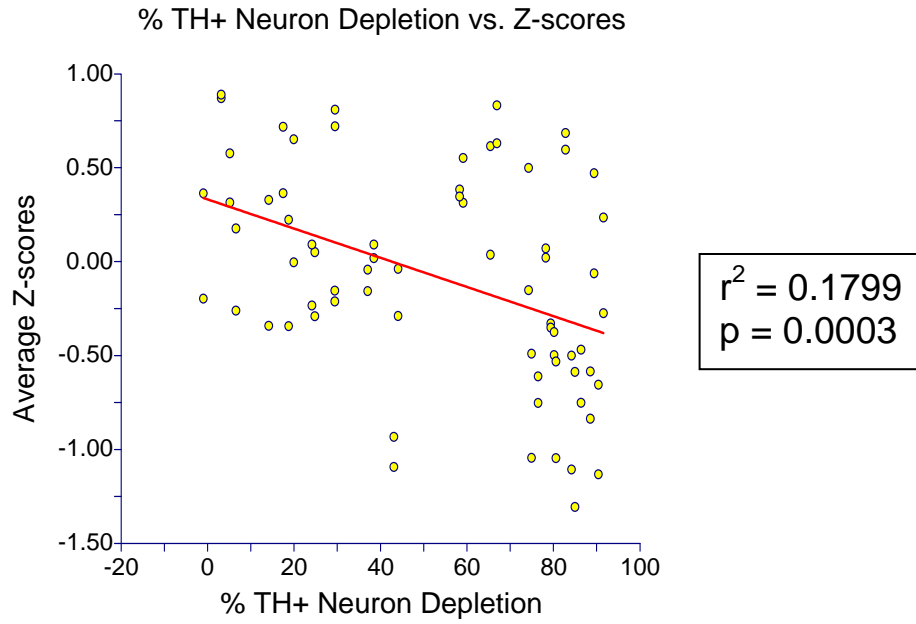
Figure 77. Linear regression of right hemisphere TH+ neuron depletion against the average Z-scores of all significant asymmetry measures given in this thesis.
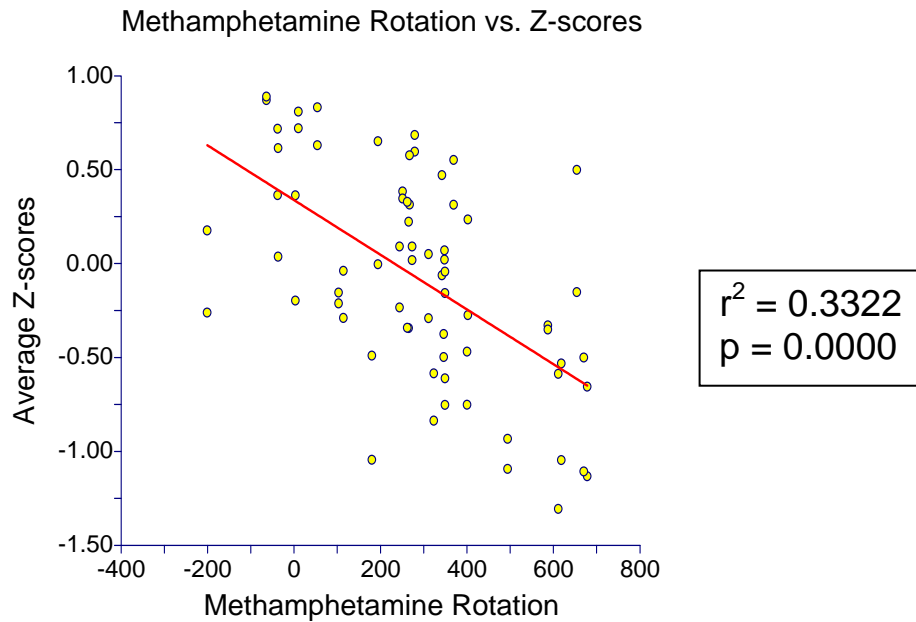
Figure 78. Linear regression of d-methamphetamine rotation against the average Z-scores of all significant asymmetry measures given in this thesis.

Hemiparkinson Rat Motor Impairments

Miklyaeva, Martens, & Whishaw (1995) give a detailed analysis of hemiparkinson rat movements and postural support in which they propose that "the most likely explanation of their underlying deficit is an inability to use the bad limbs to apply forces that will move the body." This thesis does not explain the behavior of hemiparkinson rats well enough to determine to what extent this statement is true. However, the count and time elements of the forepaw-wall contact patterns I measured certainly support the hypothesis of Miklyaeva et al. Evidence that supports their hypothesis includes the fact that hemiparkinson rats tend to leave the contralateral-to-lesion forepaw in place longer than the ipsilateral-to-lesion paw, as seen in the [%BLB vs BRB], [%*L*], and [%^/Lt] asymmetries, and tend to make fewer total touches with the contralateral-to-lesion paw, as seen in the [%Lt] and [%*Lt] asymmetries.

These same results also support the hypothesis that hemiparkinson rats have difficulty initiating independent movements with the contralateral-to-lesion forelimb at certain times, similar to human Parkinson's patients having difficulty initiating movements or "freezing" during particular tasks, as well as the hypothesis that hemiparkinson rats display bradykinesia in the contralateral-to-lesion forepaw.

I predict that a pressure-sensitive cylinder setup would be useful in determining to what extent hemiparkinson rats display bradykinesia, have difficulty initiating movement, and show inability to use the contralateral-to-lesion forepaw "to apply forces that will move the body".

CONCLUSION

As for any scientific experiment, it is easy to conclude that more research is required. I recommend that future research include development of a cylinder setup that can quickly and efficiently measure forelimb wall and floor contact components of location, time, and pressure of touches simultaneously while reliably distinguishing between right and left forepaw contact.

The question of whether or not hemiparkinson rats' "underlying deficit is an inability to use the bad limbs to apply forces that will move the body" (Miklyaeva, Martens, & Whishaw, 1995) remains unanswered, but could be answered by comparing behavior of hemiparkinson rats in a cylinder setup that accurately measures pressure exerted on the wall and floor during forelimb use in the cylinder.

My data support the hypothesis that hemiparkinson rats display "inability to use the bad limbs to apply forces that will move the body", the hypothesis that hemiparkinson rats have difficulty initiating movement with the contralateral-to-lesion forelimb, and the hypothesis that hemiparkinson rats display bradykinesia in the contralateral-to-lesion forelimb. By combining new measures of forelimb wall placement asymmetry with measures of contact time asymmetry, the cylinder test may be more sensitive to detect hemiparkinson rat motor impairments resulting from unilateral DA depletion.

Although this thesis expands knowledge of hemiparkinson rat forelimb use in the cylinder test, many important questions remain unanswered. But my portion of this relay is over; I officially pass on the torch to those who will continue the investigation.

Table 10. One-movement wall contact sequences counted and timed.

Count	TIME	Ave Time	Time	Ave Time
#BL	^BL	^/BL	^Bl	^/Bl
#BL)			^bL; ^bL)	^/bL; ^/bL)
#LB	^LB	^/LB	^Lb	^/Lb
#(LB			^lB	^/lB
#LR	^LR	^/LR	^Lr	^/Lr
#(LR			^lR	^/lR
#RL	^RL	^/RL	^Rl	^/Rl
#(RL			^rL	^/rL
#BR	^BR	^/BR	^Br	^/Br
#BR)			^bR; ^bR)	^/bR; ^/bR)
#RB	^RB	^/RB	^Rb	^/Rb
#(RB			^rB	^/rB

Table 10 and Table 12 Codes Key:

\# = number of occurrences.
^ = time spent contacting the cylinder wall (applies to UPPER CASE letters only; lower case letters are
    shown solely for context).
^/ = average time spent contacting the cylinder wall (applies to UPPER CASE letters only; lower case
    letters are shown solely for context).
L = Left (contralateral-to-lesion) forepaw contacting the cylinder wall exclusively.
B = Both forepaws contacting the cylinder wall simultaneously.
R = Right (ipsilateral-to-lesion) forepaw contacting the cylinder wall exclusively.
(= beginning of a set [e.g. "(L" means the left forepaw is the first touching the cylinder wall in a set].
) = ending of a set [e.g. "L)" means the left forepaw is the last touching the cylinder wall in a set].

Table 11. One-movement wall contact sequences analyzed for asymmetries.

Group	% Count	% TIME	% Ave TIME	% Time	% Ave Time	% Ave Time
BL)	%BL) v BR)			%^bL) v rL)		%^/bL) v rL)
BL	%BL v BR	%^BL v BR	%^/BL v BR	%^Bl v Rl	%^/Bl v bL	%^/Bl v Br
				%^bL v rL		%^/bL v bR
				%^Bl v Br		%^/Bl v Rl
				%^bL v bR		%^/bL v rL
LB	%LB v RB	%^LB v RB	%^/LB v RB	%^Lb v Lr	%^/Lb v lB	%^/Lb v Lr
	%(LB v (RB			%^lB v lR		%^/lB v lR
				%^Lb v Rb		%^/Lb v Rb
				%^lB v rB		%^/lB v rB
LR	%LR v RL	%^LR v RL	%^/LR v RL	%^Lr v Br	%^/Lr v lR	%^/Lr v Br
	%(LR v (RL			%^lR v bR		%^/lR v bR
RL				%^Rl v Rb	%^/Rl v rL	%^/Rl v Rb
				%^rL v rB		%^/rL v rB
BR					%^/Br v bR	
RB					%^/Rb v rB	

Table 11 and Table 13 Codes Key:

% = percent, calculated as the first code divided by the sum of both codes [e.g. %BL v BR = #BL/(#/BL+#BR)].

^ = time spent contacting the cylinder wall (applies to UPPER CASE letters only; lower case letters are shown solely for context).

^/ = average time spent contacting the cylinder wall (applies to UPPER CASE letters only; lower case letters are shown solely for context).

L = Left (contralateral-to-lesion) forepaw contacting the cylinder wall exclusively.

B = Both forepaws contacting the cylinder wall simultaneously.

R = Right (ipsilateral-to-lesion) forepaw contacting the cylinder wall exclusively.

(= beginning of a set [e.g. "(L" means the left forepaw is the first touching the cylinder wall in a set].

) = ending of a set [e.g. "L)" means the left forepaw is the last touching the cylinder wall in a set].

v = "verses" [e.g. "%BL v BR" could be read "percent BL verses BR"].

Table 12. Two-movement wall contact sequences counted and timed.

Count	TIME	Ave Time	Time	Ave Time
#LBL	^LBL	^/LBL	^Lbl	^/Lbl
			^lBl	^/lBl
			^lbL	^/lbL
#LBR	^LBR	^/LBR	^Lbr	^/Lbr
			^lBr	^/lBr
			^lbR	^/lbR
#LRL	^LRL	^/LRL	^Lrl	^/Lrl
			^lRl	^/lRl
			^lrL	^/lrL
#LRB	^LRB	^/LRB	^Lrb	^/Lrb
			^lRb	^/lRb
			^lrB	^/lrB
#RBL	^RBL	^/RBL	^Rbl	^/Rbl
			^rBl	^/rBl
			^rbL	^/rbL
#RBR	^RBR	^/RBR	^Rbr	^/Rbr
			^rBr	^/rBr
			^rbR	^/rbR
#BLB	^BLB	^/BLB	^Blb	^/Blb
			^bLb	^/bLb
			^blB	^/blB
#BLR	^BLR	^/BLR	^Blr	^/Blr
			^bLr	^/bLr
			^blR	^/blR
#BRL	^BRL	^/BRL	^Brl	^/Brl
			^bRl	^/bRl
			^brL	^/brL
#BRB	^BRB	^/BRB	^Brb	^/Brb
			^bRb	^/bRb
			^brB	^/brB
#RLB	^RLB	^/RLB	^Rlb	^/Rlb
			^rLb	^/rLb
			^rlB	^/rlB
#RLR	^RLR	^/RLR	^Rlr	^/Rlr
			^rLr	^/rLr
			^rlR	^/rlR

See Codes Key on page 95.

Table 13. Two-movement wall contact sequences analyzed for asymmetries.

Group	% Count	% TIME	% Ave TIME	% Time	% Ave Time	% Ave Time
LBL	%LBL v RBR	%^LBL v RBR	%^/LBL v RBR	%^Lbl v Rbl	%^/Lbl v Rbl	%^/Lbl v LBL
	%LBL v LBR	%^LBL v LBR	%^/LBL v LBR	%^lBl v rBl	%^/lBl v rBl	%^/lBl v LBL
	%LBL v RBL	%^LBL v RBL	%^/LBL v RBL	%^lbL v rbL	%^/lbL v rbL	%^/lbL v LBL
				%^Lbl v Lbr	%^/Lbl v Lbr	
				%^lBl v lBr	%^/lBl v lBr	
				%^lbL v lbR	%^/lbL v lbR	
LBR	%LBR v RBR	%^LBR v RBR	%^/LBR v RBR	%^Lbr v Rbr	%^/Lbr v Rbr	%^/Lbr v LBR
	%LBR v RBL	%^LBR v RBL	%^/LBR v RBL	%^lBr v rBr	%^/lBr v rBr	%^/lBr v LBR
				%^lbR v rbR	%^/lbR v rbR	%^/lbR v LBR
				%^Lbr v Rbl	%^/Lbr v Rbl	
				%^lBr v rBl	%^/lBr v rBl	
				%^lbR v rbL	%^/lbR v rbL	
LRL	%LRL v RLR	%^LRL v RLR	%^/LRL v RLR	%^Lrl v Rlr	%^/Lrl v Rlr	%^/Lrl v LRL
				%^lRl v rLr	%^/lRl v rLr	%^/lRl v LRL
				%^lrL v rlR	%^/lrL v rlR	%^/lrL v LRL
LRB	%LRB v RLB	%^LRB v RLB	%^/LRB v RLB	%^Lrb v Rlb	%^/Lrb v Rlb	%^/Lrb v LRB
				%^lRb v rLb	%^/lRb v rLb	%^/lRb v LRB
				%^lrB v rlB	%^/lrB v rlB	%^/lrB v LRB
RBL	%RBL v RBR	%^RBL v RBR	%^/RBL v RBR	%^Rbl v Rbr	%^/Rbl v Rbr	%^/Rbl v RBL
				%^rBl v rBr	%^/rBl v rBr	%^/rBl v RBL
				%^rbL v rbR	%^/rbL v rbR	%^/rbL v RBL
LBL				%^Lbl v Rbr	%^/Lbl v Rbr	%^/Rbr v RBR
				%^lBl v rBr	%^/lBl v rBr	%^/rBr v RBR
				%^lbL v rbR	%^/lbL v rbR	%^/rbR v RBR
BLB	%BLB v BRB	%^BLB v BRB	%^/BLB v BRB	%^Blb v Brb	%^/Blb v Brb	%^/Blb v BLB
				%^bLb v bRb	%^/bLb v bRb	%^/bLb v BLB
				%^blB v brB	%^/blB v brB	%^/blB v BLB
BLR	%BLR v BRL	%^BLR v BRL	%^/BLR v BRL	%^Blr v Brl	%^/Blr v Brl	%^/Blr v BLR
				%^bLr v bRl	%^/bLr v bRl	%^/bLr v BLR
				%^blR v brL	%^/blR v brL	%^/blR v BLR
BRL						%^/Brl v BRL
						%^/bRl v BRL
						%^/brL v BRL
BRB						%^/Brb v BRB
						%^/bRb v BRB
						%^/brB v BRB
RLB						%^/Rlb v RLB
						%^/rLb v RLB
						%^/rlB v RLB
RLR						%^/Rlr v RLR
						%^/rLr v RLR
						%^/rlR v RLR

See Codes Key on page 96.

REFERENCES

Ballard, P. A., Tetrud, J. W., & Langston, J. W. (1985). Permanent human parkinsonism due to 1-methyl-4-phenyl-1,2,3,6-tetrahydropyridine (MPTP): seven cases. *Neurology, 35*(7), 949-956.

Baskin, Y. K., Dietrich, W. D., & Green, E. J. (2003). Two effective behavioral tasks for evaluating sensorimotor dysfunction following traumatic brain injury in mice. *J Neurosci Methods, 129*(1), 87-93.

Becker, JB (1999). Gender differences in dopaminergic function in striatum and nucleus accumbens. *Pharmacol Biochem Behav 64*(4), 803-812.

Betarbet, R., Sherer, T. B., & Greenamyre, J. T. (2005). Ubiquitin-proteasome system and Parkinson's diseases. *Exp Neurol, 191 Suppl 1*, S17-27.

Betarbet, R., Sherer, T. B., MacKenzie, G., Garcia-Osuna, M., Panov, A. V., & Greenamyre, J. T. (2000). Chronic systemic pesticide exposure reproduces features of Parkinson's disease. *Nat Neurosci, 3*(12), 1301-1306.

Bourn, W. M., Chin, L., & Picchioni, A. L. (1972). Enhancement of audiogenic seizure by 6-hydroxydopamine. *J Pharm Pharmacol, 24*(11), 913-914.

Bove, J., Prou, D., Perier, C., & Przedborski, S. (2005). Toxin-induced models of Parkinson's disease. *NeuroRx, 2*(3), 484-494.

Braak, H., Del Tredici, K., Rub, U., de Vos, R. A., Jansen Steur, E. N., & Braak, E. (2003). Staging of brain pathology related to sporadic Parkinson's disease. *Neurobiol Aging, 24*(2), 197-211.

Brooks, A. I., Chadwick, C. A., Gelbard, H. A., Cory-Slechta, D. A., & Federoff, H. J. (1999). Paraquat elicited neurobehavioral syndrome caused by dopaminergic neuron loss. *Brain Res, 823*(1-2), 1-10.

Dauer, W., Kholodilov, N., Vila, M., Trillat, A. C., Goodchild, R., Larsen, K. E., et al. (2002). Resistance of alpha -synuclein null mice to the parkinsonian neurotoxin MPTP. *Proc Natl Acad Sci U S A, 99*(22), 14524-14529.

Davis, G. C., Williams, A. C., Markey, S. P., Ebert, M. H., Caine, E. D., Reichert, C. M., et al. (1979). Chronic Parkinsonism secondary to intravenous injection of meperidine analogues. *Psychiatry Res, 1*(3), 249-254.

Feany, M. B., & Bender, W. W. (2000). A Drosophila model of Parkinson's disease. *Nature, 404*(6776), 394-398.

Fearnley, J. M., & Lees, A. J. (1991). Ageing and Parkinson's disease: substantia nigra regional selectivity. *Brain, 114 (Pt 5)*, 2283-2301.

Fiskum, G., Starkov, A., Polster, B. M., & Chinopoulos, C. (2003). Mitochondrial mechanisms of neural cell death and neuroprotective interventions in Parkinson's disease. *Ann N Y Acad Sci, 991*, 111-119.

Forno, L. S., Langston, J. W., DeLanney, L. E., & Irwin, I. (1988). An electron microscopic study of MPTP-induced inclusion bodies in an old monkey. *Brain Res, 448*(1), 150-157.

Gasser, T. (2001). Genetics of Parkinson's disease. *J Neurol, 248*(10), 833-840.

German, D. C., & Manaye, K. F. (1993). Midbrain dopaminergic neurons (nuclei A8, A9, and A10): three-dimensional reconstruction in the rat. *J Comp Neurol, 331*(3), 297-309.

Gharbawie, O. A., Whishaw, P. A., & Whishaw, I. Q. (2004). The topography of three-dimensional exploration: a new quantification of vertical and horizontal exploration, postural support, and exploratory bouts in the cylinder test. *Behav Brain Res, 151*(1-2), 125-135.

Gueorguieva R., & Krystal J. H. (2004). Move over ANOVA: progress in analyzing repeated-measures data and its reflection in papers published in the Archives of General Psychiatry. *Arch Gen Psychiatry. 61*(3), 310-7.

Hornykiewicz, O. (2001). Parkinson Disease. *Encyclopedia of Life Sciences*, John Wiley & Sons, Ltd.

Huang, Y., Cheung, L., Rowe, D., & Halliday, G. (2004). Genetic contributions to Parkinson's disease. *Brain Res Brain Res Rev, 46*(1), 44-70.

Jeon, B. S., Jackson-Lewis, V., & Burke, R. E. (1995). 6-Hydroxydopamine lesion of the rat substantia nigra: time course and morphology of cell death. *Neurodegeneration, 4*(2), 131-137.

Jin, Y., Fischer, I., Tessler, A., & Houle, J.D. (2002). Transplants of fibroblasts genetically modified to express BDNF promote axonal regeneration from supraspinal neurons following chronic spinal cord injury. *Exp Neurol, 177(1),* 265-275.

Karhunen, H., Virtanen, T., Schallert, T., Sivenius, J., & Jolkkonen, J. (2003). Forelimb use after focal cerebral ischemia in rats treated with an alpha 2-adrenoceptor antagonist. *Pharmacol Biochem Behav, 74*(3), 663-669.

Kowall, N. W., Hantraye, P., Brouillet, E., Beal, M. F., McKee, A. C., & Ferrante, R. J. (2000). MPTP induces alpha-synuclein aggregation in the substantia nigra of baboons. *Neuroreport, 11*(1), 211-213.

Lane, E.L., Cheetham, S.C., & Jenner, P. (2006) Does contraversive circling in the 6-OHDA-lesioned rat indicate an ability to induce motor complications as well as therapeutic effects in Parkinson's disease? *Exp Neurol, 197*(2), 284-290

Langston, J. W., Ballard, P., Tetrud, J. W., & Irwin, I. (1983). Chronic Parkinsonism in humans due to a product of meperidine-analog synthesis. *Science, 219*(4587), 979-980.

Lundblad M., Andersson M., Winkler C., Kirik D., Wierup N., & Cenci M.A. (2002), Pharmacological validation of behavioural measures of akinesia and dyskinesia in a rat model of Parkinson's disease. *Eur J Neurosci, 15(1),* 120-132.

Luthman, J., Fredriksson, A., Sundstrom, E., Jonsson, G., & Archer, T. (1989). Selective lesion of central dopamine or noradrenaline neuron systems in the neonatal rat: motor behavior and monoamine alterations at adult stage. *Behav Brain Res, 33*(3), 267-277.

Manning-Bog, A. B., McCormack, A. L., Li, J., Uversky, V. N., Fink, A. L., & Di Monte, D. A. (2002). The herbicide paraquat causes up-regulation and aggregation of alpha-synuclein in mice: paraquat and alpha-synuclein. *J Biol Chem, 277*(3), 1641-1644.

Marder, K., Tang, M. X., Mejia, H., Alfaro, B., Cote, L., Louis, E., et al. (1996). Risk of Parkinson's disease among first-degree relatives: A community-based study. *Neurology, 47*(1), 155-160.

Marsden, C. D. (1994). Problems with long-term levodopa therapy for Parkinson's disease. *Clin Neuropharmacol, 17 Suppl 2*, S32-44.

Martin, J. B. (2002). The integration of neurology, psychiatry, and neuroscience in the 21st century. *Am J Psychiatry, 159*(5), 695-704.

McBride, J.L., Behrstock, S.P., Chen, E.Y., Jakel, R.J., Siegel, I., Svendsen, C.N., et al. (2004). Human neural stem cell transplants improve motor function in a rat model of Huntington's disease. *J Comp Neurol, 475(2),* 211-219.

McCormack, A. L., Thiruchelvam, M., Manning-Bog, A. B., Thiffault, C., Langston, J. W., Cory-Slechta, D. A., et al. (2002). Environmental risk factors and Parkinson's disease: selective degeneration of nigral dopaminergic neurons caused by the herbicide paraquat. *Neurobiol Dis, 10*(2), 119-127.

McNaught, K. S., & Olanow, C. W. (2006). Protein aggregation in the pathogenesis of familial and sporadic Parkinson's disease. *Neurobiol Aging, 27*(4), 530-545.

McNaught, K. S., Perl, D. P., Brownell, A. L., & Olanow, C. W. (2004). Systemic exposure to proteasome inhibitors causes a progressive model of Parkinson's disease. *Ann Neurol, 56*(1), 149-162.

Miklyaeva, E.I., Martens, D.J., & Whishaw, I.Q. (1995) Impairments and compensatory adjustments in spontaneous movement after unilateral dopamine depletion in rats, *Brain Res* 681, 23-40.

Muir, G.D., & Whishaw I.Q. (1999) Ground reaction forces in locomoting hemi-parkinsonian rats: a definitive test for impairments and compensations. *Exp Brain Res 126*(3), 307-314.

Nicklas, W. J., Youngster, S. K., Kindt, M. V., & Heikkila, R. E. (1987). MPTP, MPP+ and mitochondrial function. *Life Sci, 40*(8), 721-729.

Parkinson, J. (2002). An essay on the shaking palsy. 1817. *J Neuropsychiatry Clin Neurosci, 14*(2), 223-236; discussion 222.

Peng, J., Mao, X. O., Stevenson, F. F., Hsu, M., & Andersen, J. K. (2004). The herbicide paraquat induces dopaminergic nigral apoptosis through sustained activation of the JNK pathway. *J Biol Chem, 279*(31), 32626-32632.

Pinna, A., Pontis, S., & Morelli, M. (2006). Expression of dyskinetic movements and turning behaviour in subchronic l-DOPA 6-hydroxydopamine-treated rats is influenced by the testing environment. *Behav Brain Res, 171*(1), 175–178.

Prensa, L., & Parent, A. (2001). The nigrostriatal pathway in the rat: A single-axon study of the relationship between dorsal and ventral tier nigral neurons and the striosome/matrix striatal compartments. *J Neurosci. 21*(18), 7247-7260.

Priyadarshi, A., Khuder, S. A., Schaub, E. A., & Priyadarshi, S. S. (2001). Environmental risk factors and Parkinson's disease: a metaanalysis. *Environ Res, 86*(2), 122-127.

Przedborski, S., & Ischiropoulos, H. (2005). Reactive oxygen and nitrogen species: weapons of neuronal destruction in models of Parkinson's disease. *Antioxid Redox Signal, 7*(5-6), 685-693.

Przedborski, S., Jackson-Lewis, V., Naini, A.B., Jakowec, M., Petzinger, G., Miller, R., et al. (2001). The parkinsonian toxin 1-methyl-4-phenyl-1,2,3,6-tetrahydropyridine (MPTP): a technical review of its utility and safety. *J Neurochem,* 76(5), 1265-1274.

Ransom, B. R., Kunis, D. M., Irwin, I., & Langston, J. W. (1987). Astrocytes convert the parkinsonism inducing neurotoxin, MPTP, to its active metabolite, MPP+. *Neurosci Lett, 75*(3), 323-328.

Rasband, W.S. (1997-2006). ImageJ. http://rsb.info.nih.gov/ij/ National Institutes of Health, Bethesda, Maryland, USA.

Robinson, T.E., Noordhoorn, M., Chan, E.M., Mocsary, Z., Camp, D.M., & Whishaw, I.Q. (1994). Relationship between asymmetries in striatal dopamine release and the direction of amphetamine-induced rotation during the first week following a unilateral 6-OHDA lesion of the substantia nigra. *Synapse, 17*(1), 16-25.

Sachs, C., & Jonsson, G. (1975). Mechanisms of action of 6-hydroxydopamine. *Biochem Pharmacol, 24*(1), 1-8.

Schallert T., Fleming S. M., Leasure J. L., Tillerson, J. L., & Bland S. T. (2000). CNS plasticity and assessment of forelimb sensorimotor outcome in unilateral rat models of stroke, cortical ablation, parkinsonism and spinal cord injury. *Neuropharmacology 39,* 777– 787.

Schallert, T., & Woodlee, M.T. (2005). Orienting and placing. In I. Q. Whishaw and B. Kolb (Eds.), *The behavior of the laboratory rat: a handbook with tests*. Oxford: Oxford University Press.

Schallert, T. (2006). Behavioral tests for preclinical intervention assessment. *NeuroRX, 3*(10), 497–504.

Schober, A. (2004). Classic toxin-induced animal models of Parkinson's disease: 6-OHDA and MPTP. *Cell Tissue Res, 318*(1), 215-224.

Schuler, F., & Casida, J. E. (2001). Functional coupling of PSST and ND1 subunits in NADH:ubiquinone oxidoreductase established by photoaffinity labeling. *Biochim Biophys Acta, 1506*(1), 79-87.

Shanina, E.V., Schallert, T., Witte, O.W., & Redecker, C. (2006). Behavioral recovery from unilateral photothrombotic infarcts of the forelimb sensorimotor cortex in rats: role of the contralateral cortex. *Neuroscience 139*(4), 1495-1506.

Sherman, M. Y., & Goldberg, A. L. (2001). Cellular defenses against unfolded proteins: a cell biologist thinks about neurodegenerative diseases. *Neuron, 29*(1), 15-32.

Shi L.H., Woodward D.J., Luo F., Anstrom K., Schallert T., & Chang J.Y. (2004). High-frequency stimulation of the subthalamic nucleus reverses limb-use asymmetry in rats with unilateral 6-hydroxydopamine lesions. *Brain Res, 1013*(1), 98-106.

Shimohama, S., Sawada, H., Kitamura, Y., & Taniguchi, T. (2003). Disease model: Parkinson's disease. *Trends Mol Med, 9*(8), 360-365.

Shimoji, M., Zhang, L., Mandir, A. S., Dawson, V. L., & Dawson, T. M. (2005). Absence of inclusion body formation in the MPTP mouse model of Parkinson's disease. *Brain Res Mol Brain Res, 134*(1), 103-108.

Song, D. D., Shults, C. W., Sisk, A., Rockenstein, E., & Masliah, E. (2004). Enhanced substantia nigra mitochondrial pathology in human alpha-synuclein transgenic mice after treatment with MPTP. *Exp Neurol, 186*(2), 158-172.

Tanner, C. M., Ottman, R., Goldman, S. M., Ellenberg, J., Chan, P., Mayeux, R., et al. (1999). Parkinson disease in twins: an etiologic study. *Jama, 281*(4), 341-346.

Ungerstedt, U. (1968). 6-Hydroxy-dopamine induced degeneration of central monoamine neurons. *Eur J Pharmacol, 5*(1), 107-110.

Ungerstedt, U. (1971). Adipsia and aphagia after 6-hydroxydopamine induced degeneration of the nigro-striatal dopamine system. *Acta Physiol Scand Suppl, 367,* 95-122.

Wakabayashi, K., & Takahashi, H. (1997). Neuropathology of autonomic nervous system in Parkinson's disease. *Eur Neurol, 38 Suppl 2*, 2-7.

Windle, V., Szymanska, A., Granter-Button, S., White, C., Buist, R., Peeling, J., et al. (2006). An analysis of four different methods of producing focal cerebral ischemia with endothelin-1 in the rat. *Exp Neurol, 201(2)*, 324-34.

Wright, J. M., Wall, R. A., Perry, T. L., & Paty, D. W. (1984). Chronic parkinsonism secondary to intranasal administration of a product of meperidine-analogue synthesis. *N Engl J Med, 310*(5), 325.

Zhu, C., Vourc'h, P., Fernagut, P. O., Fleming, S. M., Lacan, S., Dicarlo, C. D., et al. (2004). Variable effects of chronic subcutaneous administration of rotenone on striatal histology. *J Comp Neurol, 478*(4), 418-426.